Recent Developments on 3D Sensors

Cinzia Da Via, The University of Manchester, UK

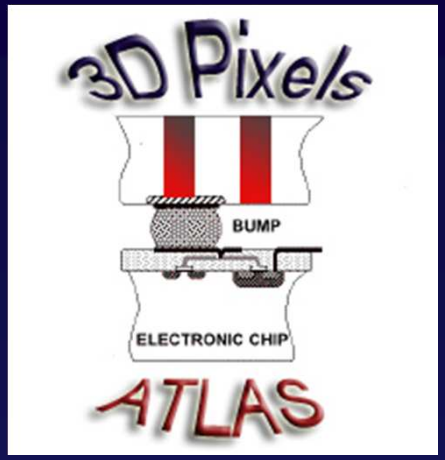

- Introduction
- 3D silicon technology: fabrication
- Properties and Applications
- Industrialization and future
- Summary and outlook

MEMS and 3D sensors

Micro-Electro-Mechanical Systems, or MEMS, is a technology that in its most general form can be defined as miniaturized mechanical and electro-mechanical elements (i.e., devices and structures) that are made using the techniques of micro-fabrication, developed in the '70ies was first commercialized in the '80ies

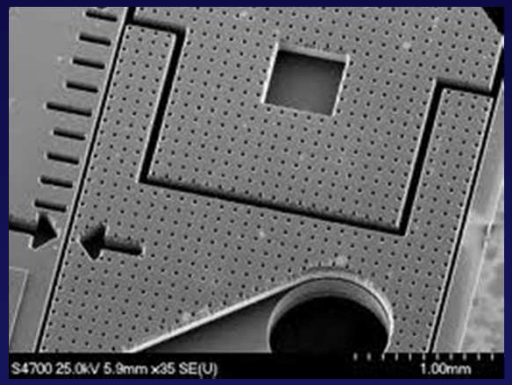

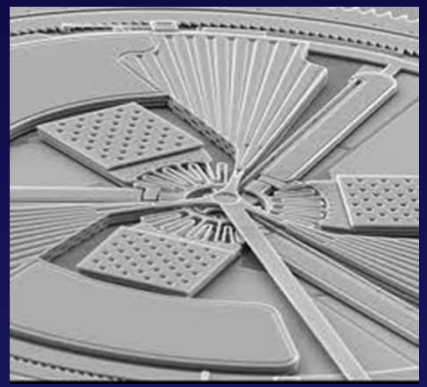

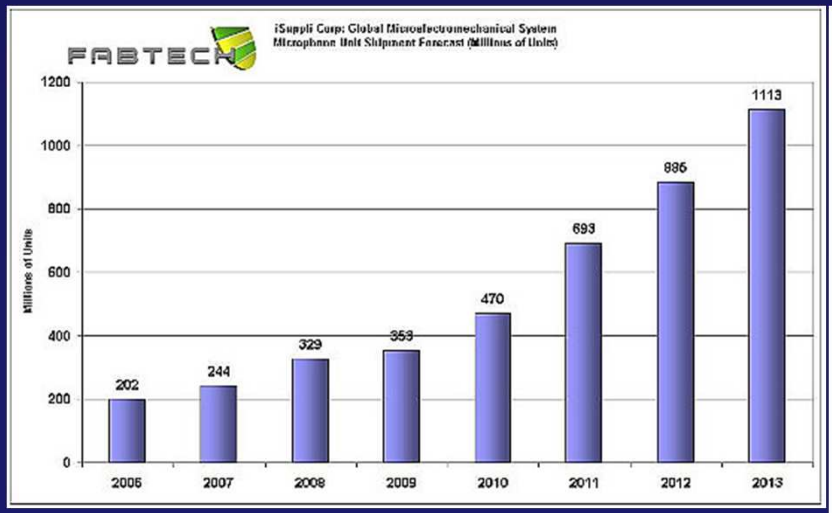

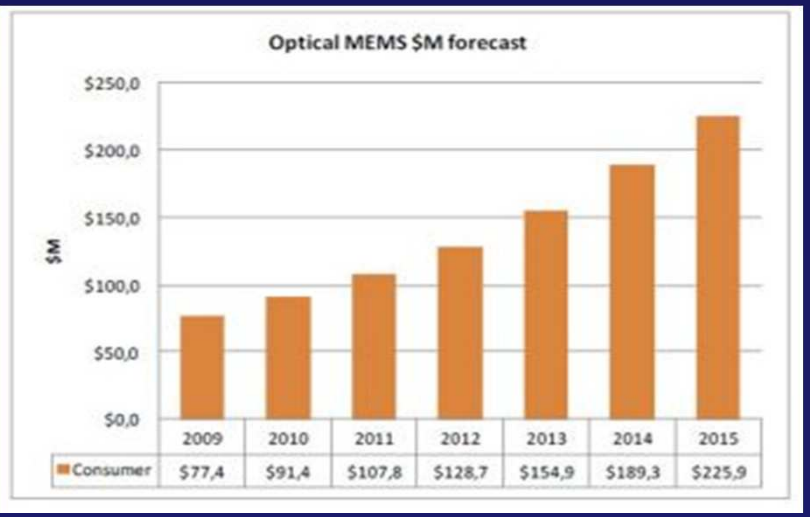

3D Silicon sensors

MANCHESTER 1824

Centre for Integrated Systems

Stanford Nanofabrication Facility

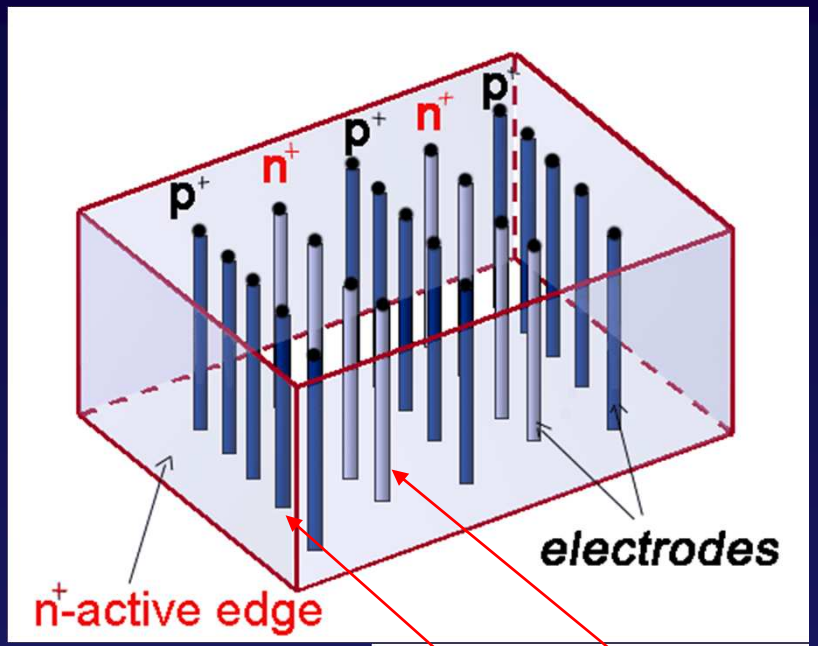

1. NIMA 395 (1997) 328 →

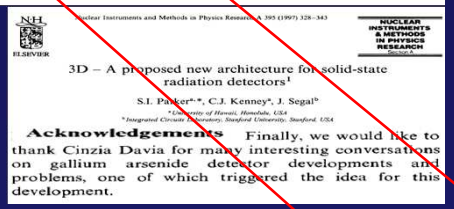

3D – A proposed new architecture for solid-state radiation detectors[1]

S.I. Parker*, C.J. Kenney, J. Segal

Acknowledgements Finally, we would like to thank Cinzia Davia for many interesting conversations on gallium arsenide detector developments and problems, one of which triggered the idea for this development.

2. IEEE Trans Nucl Sci 46 (1999) 1224
3. IEEE Trans Nucl Sci 48 (2001) 189
4. IEEE Trans Nucl Sci 48 (2001) 1629
5. IEEE Trans Nucl Sci 48 (2001) 2405
6. Proc. SPIE 4784 (2002)365
7. CERN Courier, Vol 43, Jan 2003, pp 23-26
8. NIM A 509 (2003) 86-91
9. NIMA 524 (2004) 236-244
10. NIM A 549 (2005) 122
11. NIM A 560 (2006) 127
12. NIM A 565 (2006) 272
13. IEEE TNS 53 (2006) 1676

3D silicon detectors were proposed in 1995 by S. Parker, and active edges in 1997 by C. Kenney.

Combine traditional VLSI processing and MEMS (Micro Electro Mechanical Systems) technology.

Electrodes are processed inside the detector bulk instead of being implanted on the Wafer's surface.

The edge is an electrode! Dead volume at the Edge < 5 microns! Essential for

Planar silicon sensors basic working principle

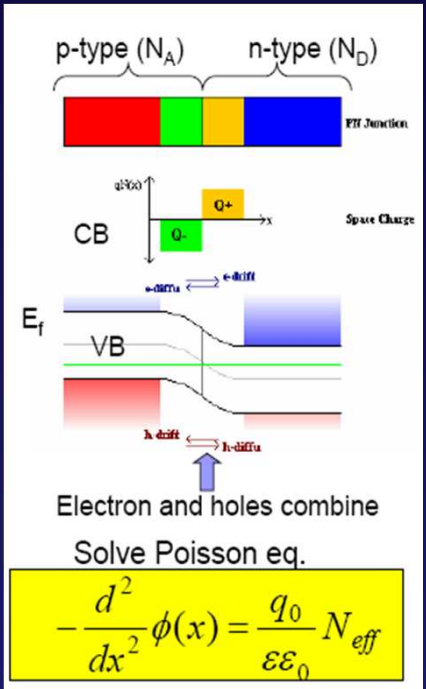

- Reversed biased p-n junction to establish region with no mobile carriers
- Increase external reverse bias Increase E field ⇒ e^- and h^+ drift to electrodes
- Increase depletion region size
- Reduce capacitance $\varepsilon\varepsilon_0 A/dW$
- Small current flow
- Requires an external readout electronics
- Segmentation allows spatial resolution (strips, pixels, single and double-sided s = pitch/sqr 12)

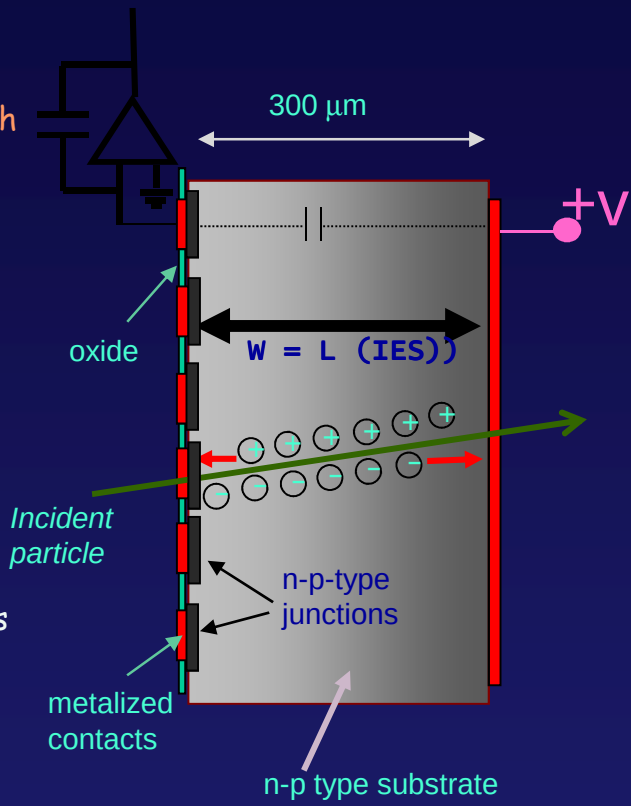

Substrate normally:

- n-type p-type
- 4 kΩ-cm FZ
- Doping of ~10^{12} cm^{-3}
- [O] ~10^{15} cm^{-3}
- [C] ~10^{15} cm^{-3}
- 300µm thick
- Orientation <111>

$$V_{FD} = \frac{(W)^2 \times e \times |N_{eff}|}{2\varepsilon_0\varepsilon_{Si}}$$

$$|N_{eff}| = |N_D - N_A|$$

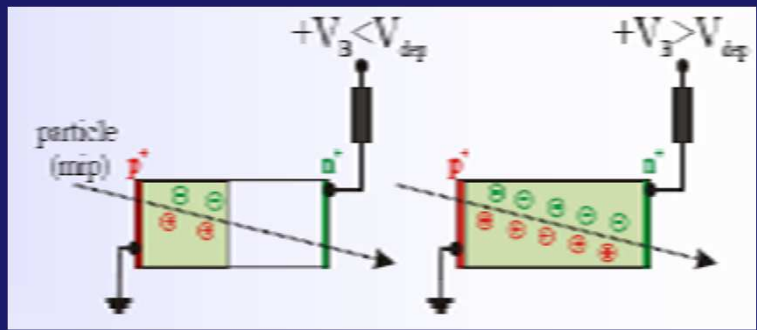

Signal formation: Ramo's Theorem

from V. Radeka

MANCHESTER 1824

S. Ramo, Proc. IRE **27 (1939) 584**
From H Spieler, lecture notes (99),

The induced current on electrode A is $i_A = q\, v_x \frac{\partial V_{q1}}{dx}$

where *Vq1 is the "weighting potential" that describes the coupling of a* charge at any position to electrode A.

After trapping:

$$S = Q(x) = Qo(x)e^{-x/\mu E\tau}$$

$$\mu E\tau = v\tau = \lambda \text{ effective drift length}$$

After integrating between 0 and inter electrode spacing L:

$$S = Q(x) = Qo(x)\frac{\lambda}{L}[1 - e^{-L/\lambda}] \propto \lambda/L$$

Note that the electric field and the weighting field are distinctly different.
· The electric field determines the charge trajectory and velocity
· The weighting field depends only on geometry and determines how charge motion couples to a specific electrode.
· Only in 2-electrode configurations are the electric field and the weighting field of the same form.

Weight depends on pitch to thickness ratio

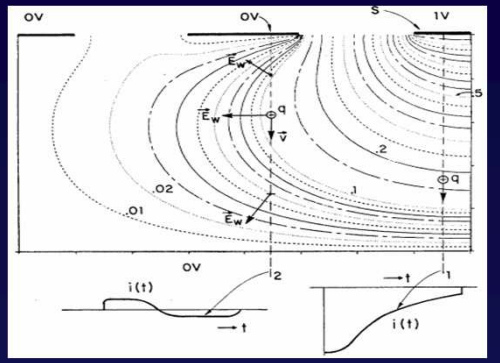

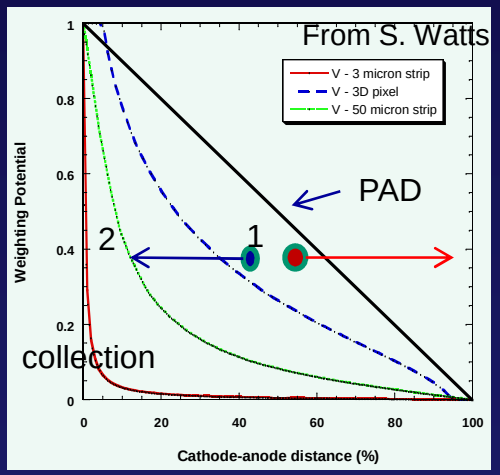

Signal contribution

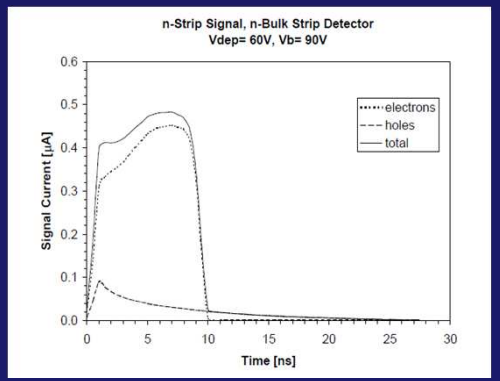

3D versus planar detectors (not to scale)

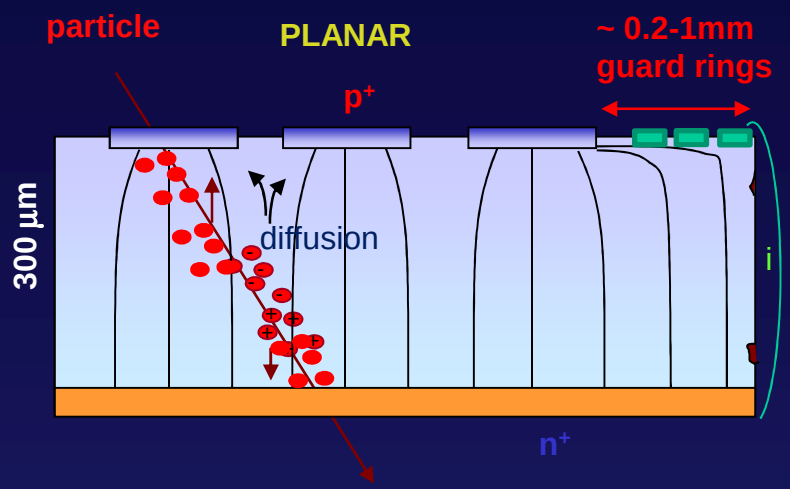

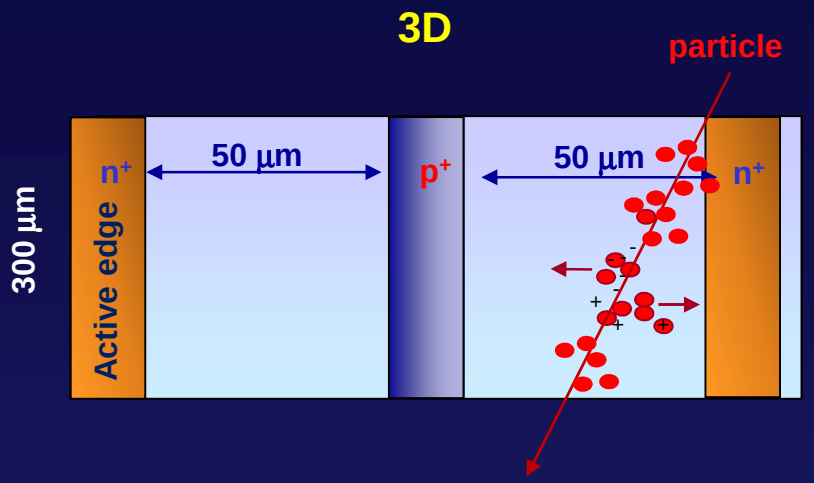

	3D	planar
❖DEPLETION VOLTAGES	< 10 V	70 V
❖After irradiation	180 V	1000V
❖Power dissipation	goes with V	goes with V
❖EDGE SENSITIVITY	< 5 µm	500 µm
❖CHARGE 1 MIP (300 mm)	24000e-	24000e-
❖CAPA CITANCE	30-50f	~20fF
❖COLLECTION DISTANCE	50 µm	300 µm
❖SPEED	1-2ns	10-20 ns

3D has Lower charge sharing probability

MEDICI simulation of a 3D structure

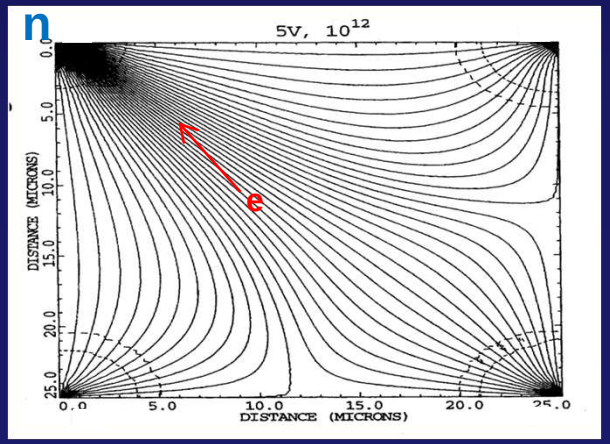

Drift lines parallel to the surface

3D charge sharing: Energy resolution

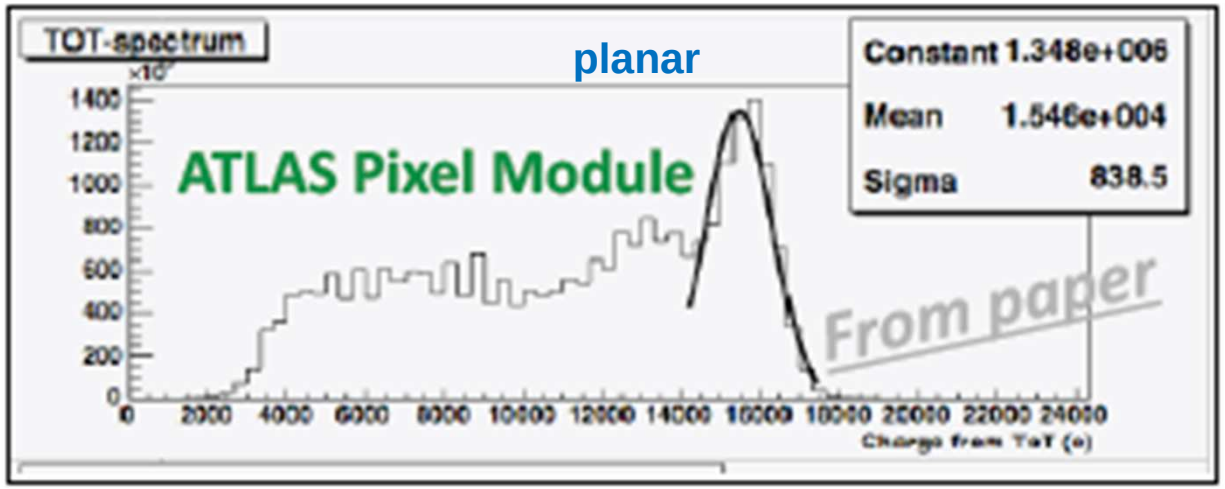

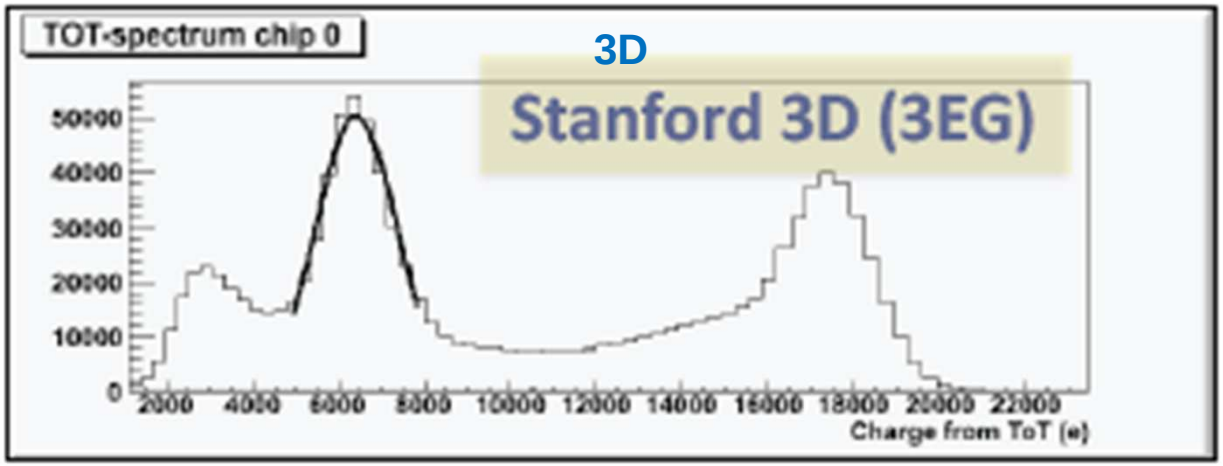

Measurements Performed using the ATLAS FE-I3 Readout chip and the TurboDaq system (developed in Bonn)

Measurements by
A. La Rosa CERN
B. Now UniGe!

^{241}Am

Type	Energy	Percentage
Alpha (α)	5.485 MeV	84.5 %
Alpha (α)	5.443 MeV	13.0 %
Beta (β)	52 keV	Unknown
Gamma (γ)	59.5 keV	35.9 %
Gamma (γ)	26.3 keV	2.4 %
Gamma (γ)	13.9 keV	42 %

Speed

3D Tests with 0.13 μm CMOS Amplifier chip
(A Kok, S. Parker, C. Da Viá, P. Jarron,
M. Depeisse, G. Anelli), fabricated at Stanford
By J. Hasi, C. Kenney

MANCHESTER 1824

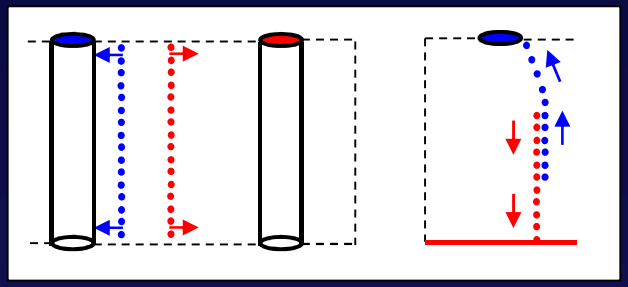

- Short collection distance
- High average e-field at low V_{bias}
- Parallel charge collection

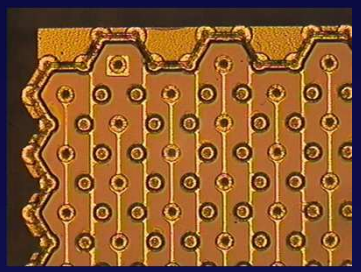

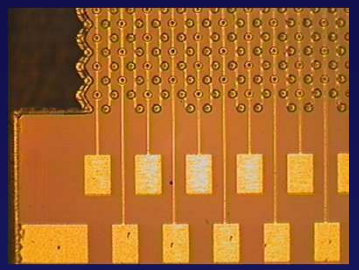

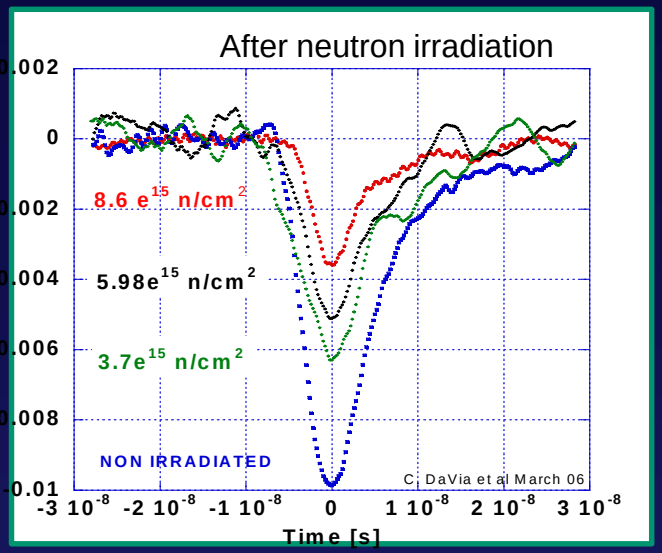

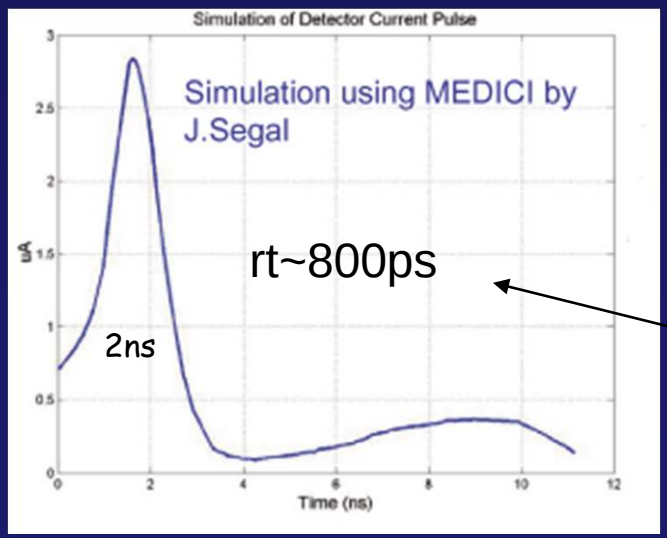

Raw oscilloscope trace

3D signal simulation

3D Inter-electrode spacing = 50 μm

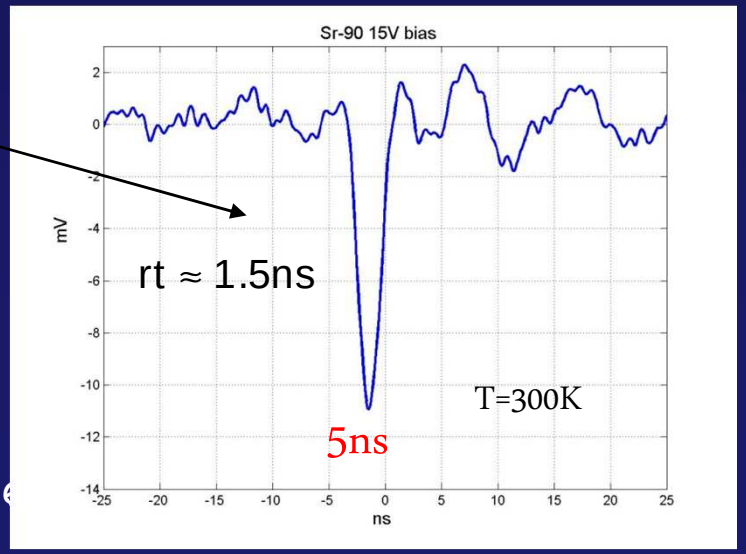

3D with different electrode configuration

MANCHESTER 1824

Financial support:
STFC-UK for the FP420 project
DOE, USA for ATLAS Upgrade

Design and fabrication by:
J. Hasi, Manchester
C. Kenney, MBC at CIS-Stanford

Thickness <210 μm>
p-type substrate 12kΩcm

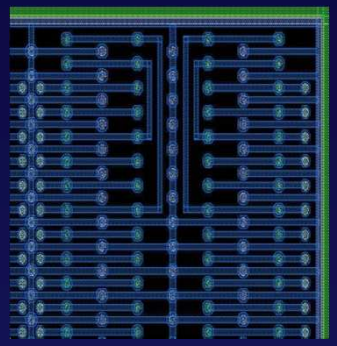

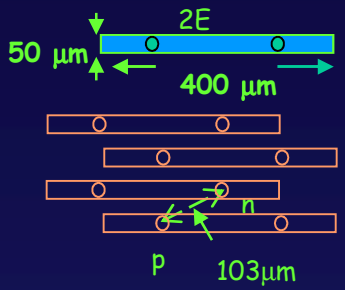

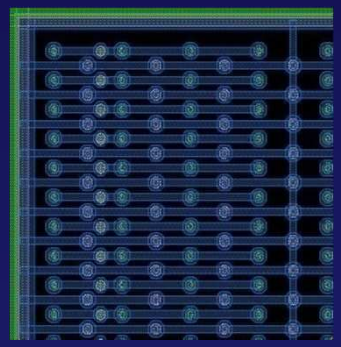

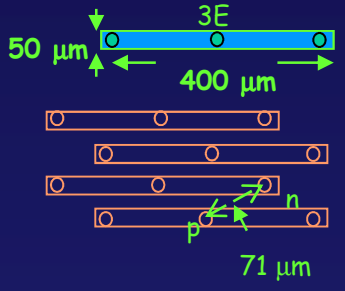

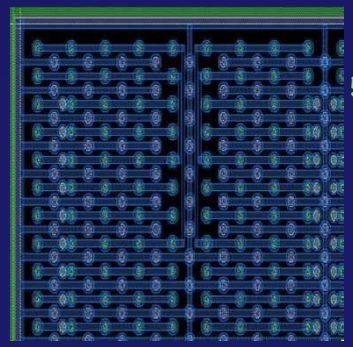

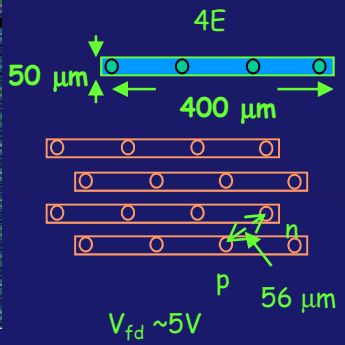

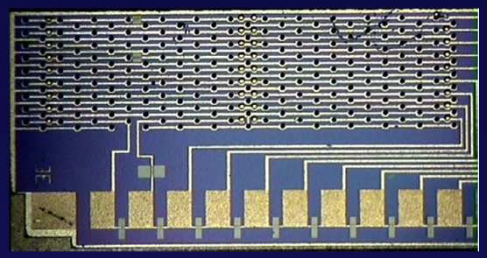

Baby-3E

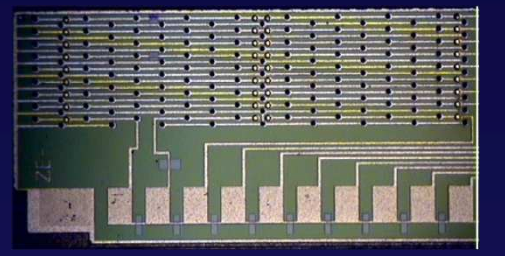

Baby-2E

FE-I3ATLAS pixel chip
7.2 x 8 mm^2
2880 pixels

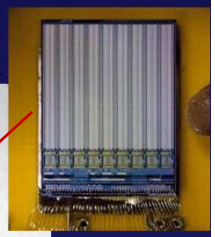

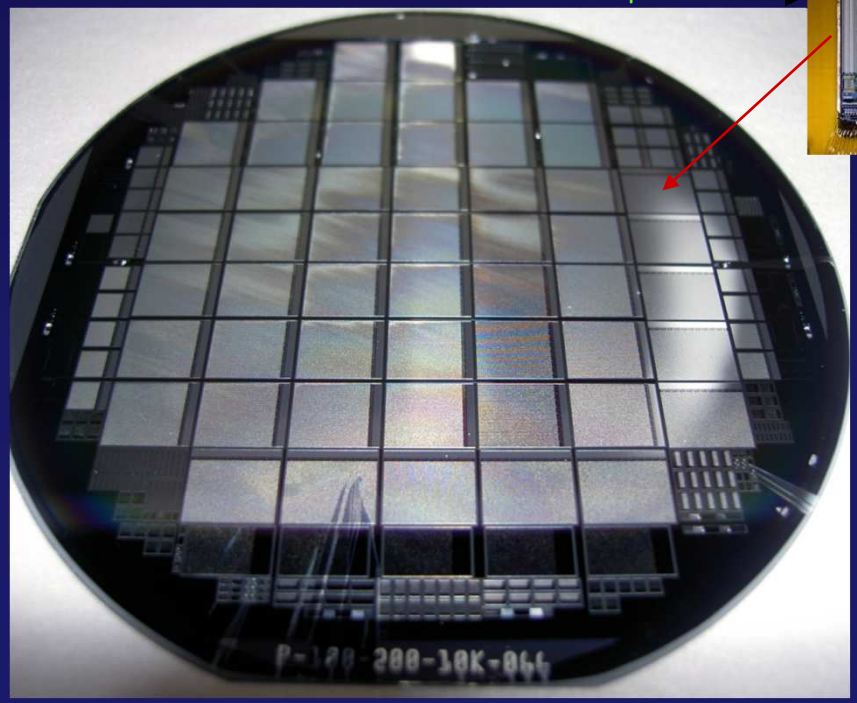

Atlas chip picture from Bekerle Vertex03

Fabrication at Stanford by C. Kenney and J. Hasi

3D micro-fabrication

MANCHESTER 1824

1- etching the electrodes

2-filling them with dopants

Aspect ratio: D:d = 11:1

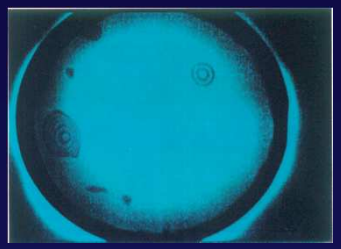

WAFER BONDING
(mechanical stability)
Si-OH + HO-Si -> Si-O-Si + H_2O

Step 1-3
oxidize and
fusion bond
wafer

Step 4-6 pattern
and etch p^+ window
contacts

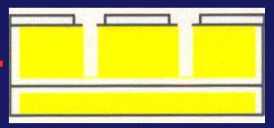

Step 7-8 etch
p^+ electrodes

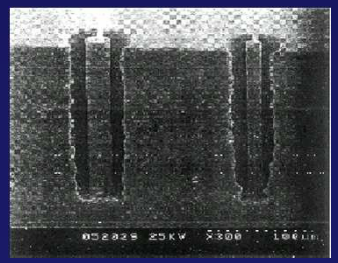

DEEP REACTIVE
ION ETCHING (STS)
(electrodes definition)
Bosh process
SiF_4 (gas) +C_4F_8 (teflon)

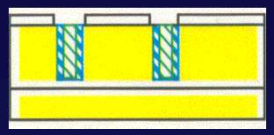

Step 9-13 dope
and fill p^+
electrodes

Step 14-17 etch
n^+ window
contacts and
electrodes

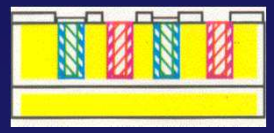

Step 18-23 dope
and fill n^+
electrodes

Step 24-25
deposit and
pattern Aluminum

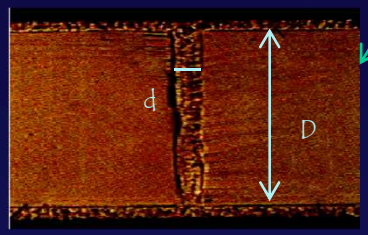

LOW PRESSURE
CHEMICAL VAPOR
DEPOSITION
(Electrodes filling with
conformal doped polysilicon
SiH4 at ~620C)
$2P_2O_5$ +5 Si-> 4P + 5 SiO_2
$2B_2O_3$ +3Si -> 4 B +3 SiO_2

Both electrodes appear on both surfaces

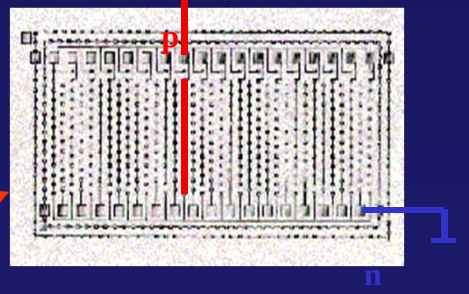

METAL DEPOSITION
Shorting electrodes of the same type
with Al for strip electronics readout
or deposit metal for bump-bonding

Cinzia Da Via, Uni. Manchester. Status 3D, UniGE , 2nd November 2011

Aspect ratio

M. Puech. ALCATEL

11:1 1997

24:1 2009

Today

40-60:1

110:1!!!

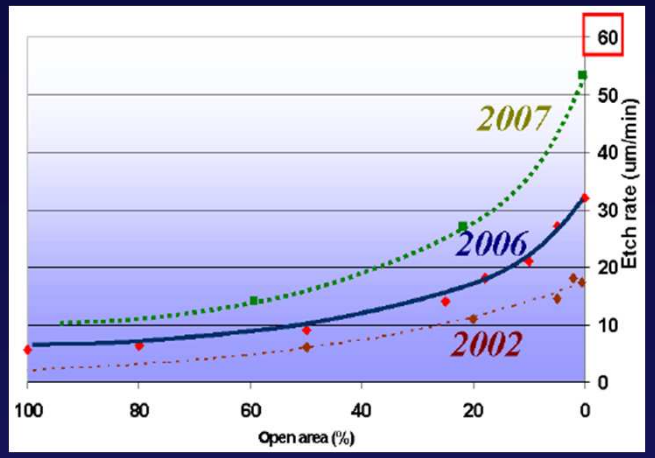

Etching rate depends on exposed area

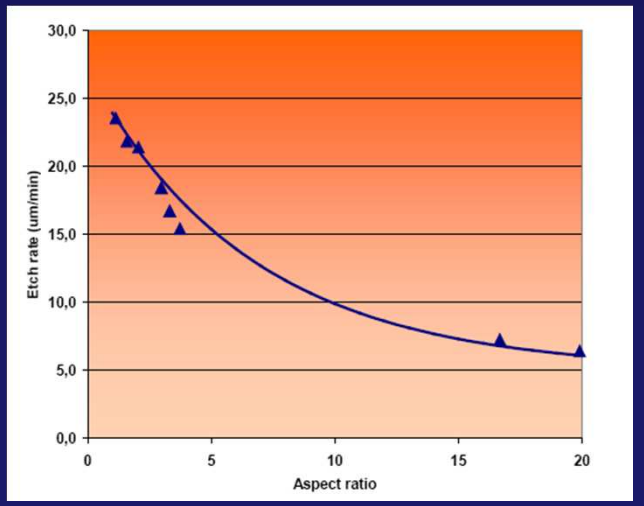

etching rate depends on aspect ratio

Active edge and electrode response of 3D sensors

Fabricated at Stanford, J. Hasi (Manchester PhD thesis)

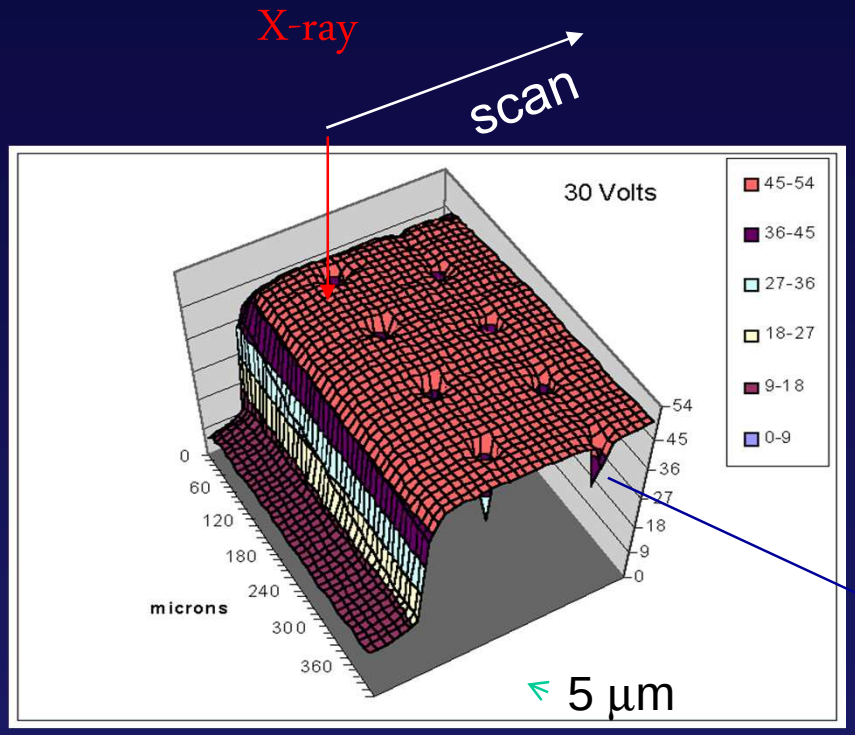

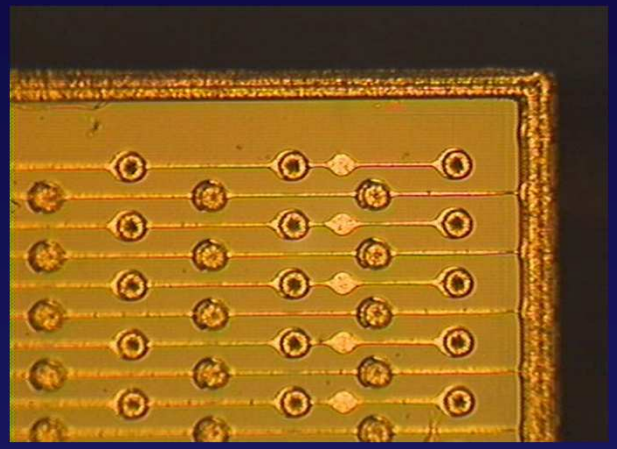

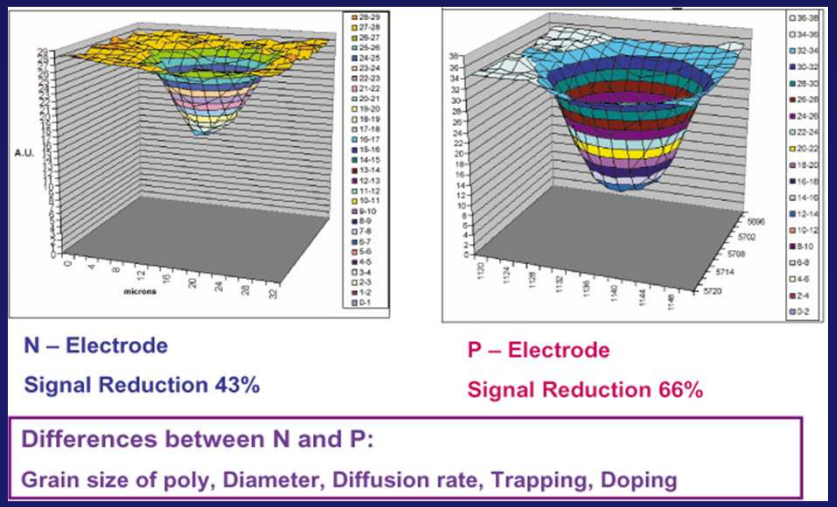

12 KeV X-ray scan at ALS, Berkeley, in 2 µm steps, of a 3D, n bulk and edges,
181 µm thick sensor.

Electrodes ~ 1.8% of total area

Tracking efficiency

P. Hansson et al. Nuclear Instruments and Methods in Physics Research A 628 (2011) 216–220

Test beam setup
SPS, 2009

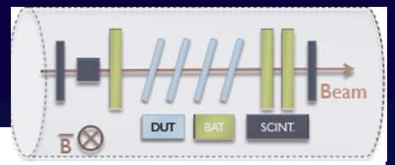

MANCHESTER 1824

- Electrodes are parallel to track at normal incidence
- Striking feature of 3D design

STA-3D mask detail

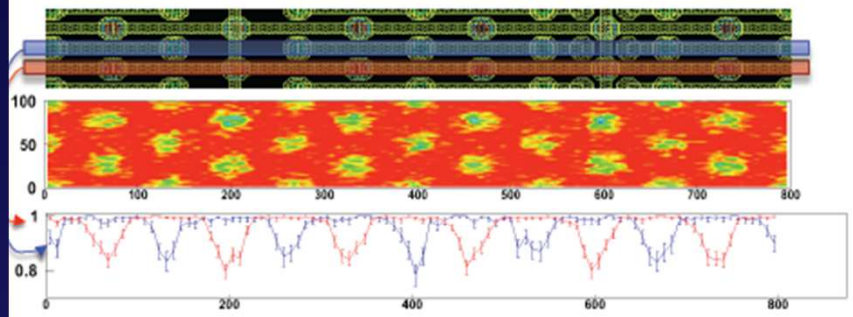

signal

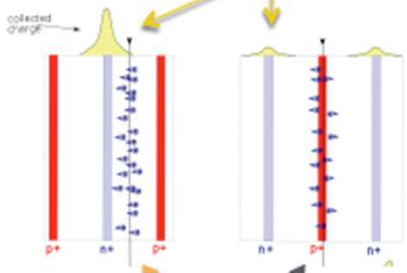

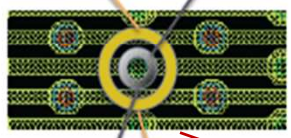

- Holes etched and filled (DRIE)
  - Doped polysilicon or passivation only
- Study charge collection in electrode region
  - Measure 40-60% signal loss J. Hasi, PhD Thesis
- Novel electrode fillings produced; analysis ongoing

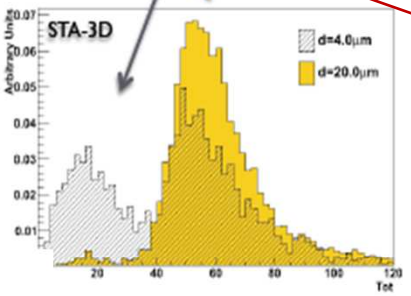

STA-3D mask detail

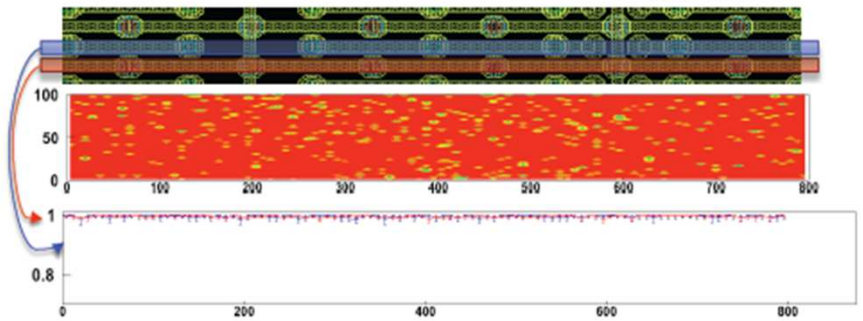

9/10

At 15°

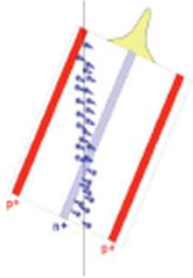

NEW ELECTRODE TREATMENT SHOWS ENCOURAGING EVIDENCES
TEST BEAM DATA AND X-RAY DATA BEING ANALYSED

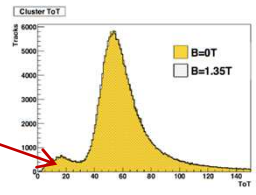

Old Stanford 3E

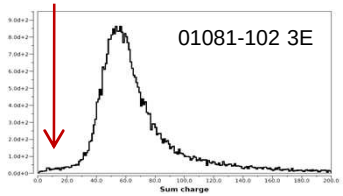

Magnetic field ON

	0°	15°
STA-3D	96.3	99.6
FBK-3E7	98.9	99.8
Planar	99.8	99.8

Active edge processing

A TRENCH IS ETCHED AND DOPED TO TERMINATE THE E-FIELD LINES

AFTER THE FULL PROCESS IS COMPLETED THE MATERIAL SURROUNDING THE DETECTORS IS ETCHED AWAY AND THE SUPPORT WAFER REMOVED : NO SAWING NEEDED!!! (NO CHIPS, NO CRACKS)

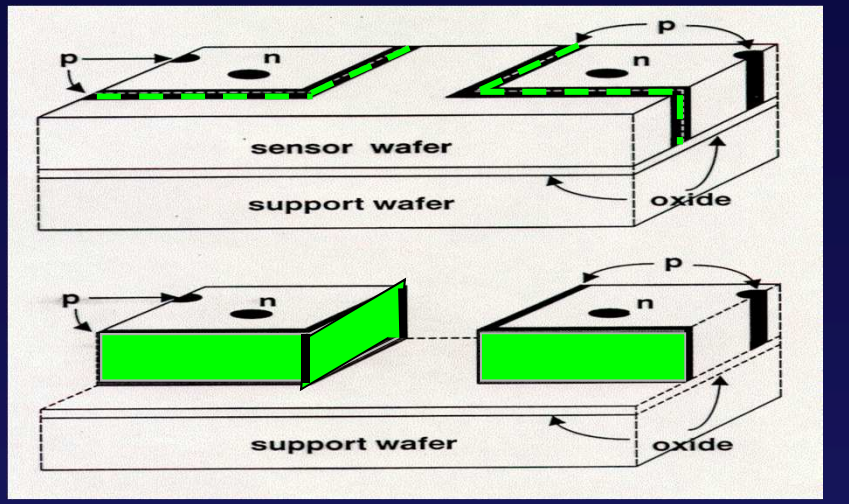

Natural developement → PLANAR+3D = planar/3D
(C. Kenney 1997)

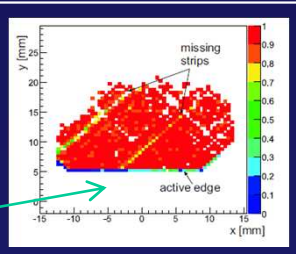

Active edge response

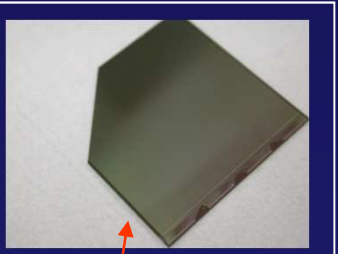

TOTEM detectors
3x4cm^2 512 µstrips

H. Niewiadomski
PhD thesis
Manchester 2009

3D active edge

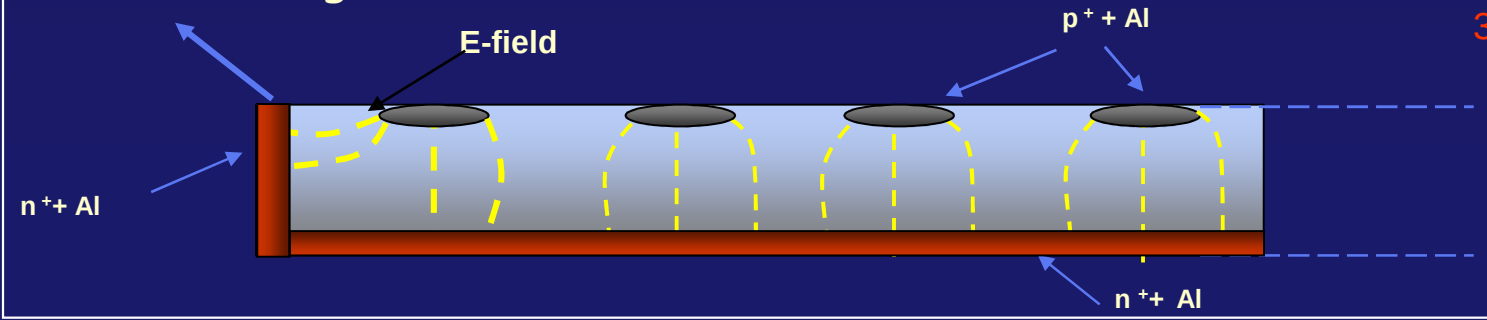

Full 3D with active edges FE-I3 ATLAS

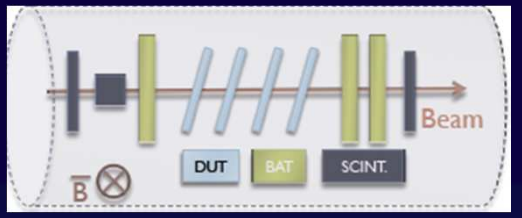

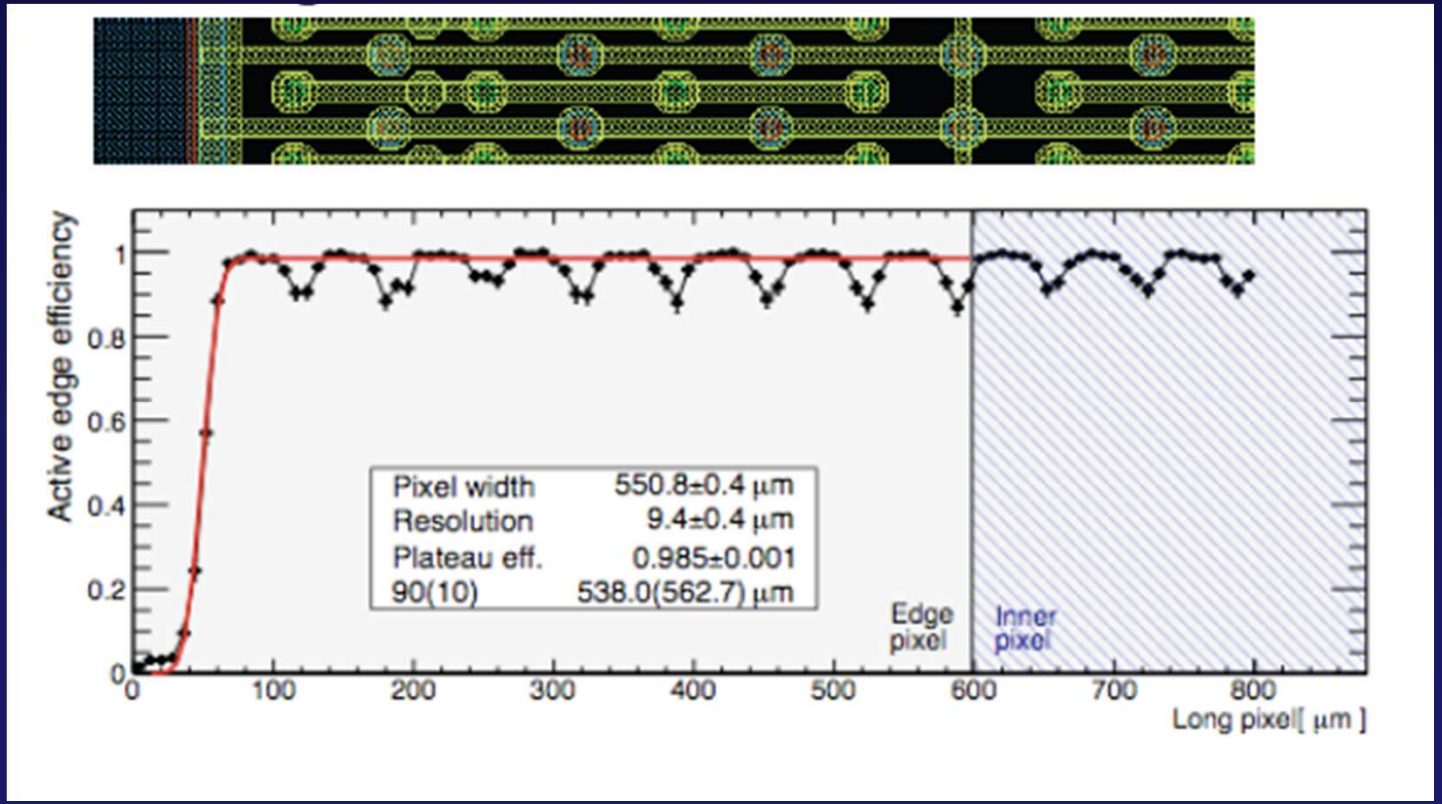

Active Edge = 543-537= 6±9.8 µm

P. Hansson et al. Nuclear Instruments and Methods in Physics Research A 628 (2011) 216–220

3D designs

3D ATLAS R&D Collaboration

3D C ONSORTIUM

The Stanford Nanofabrication Facility

SINTEF

ITC irst FONDAZIONE BRUNO KESSLER

Centre Nacional de Microelectrònica

Full 3D with active edges

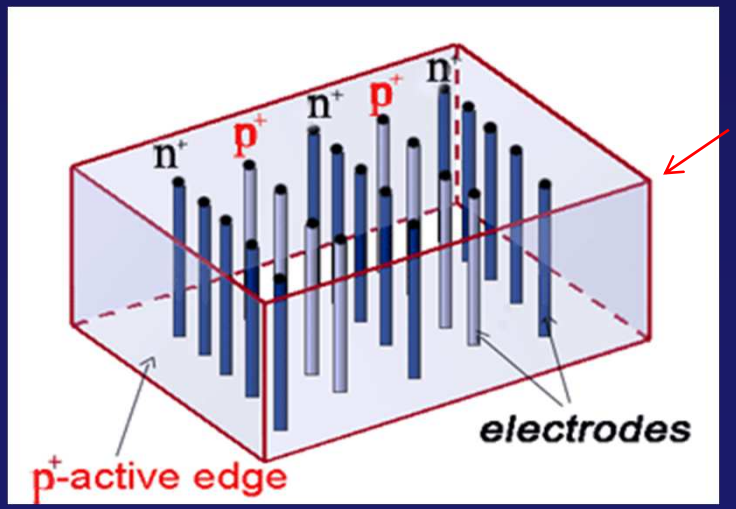

Double Column Design

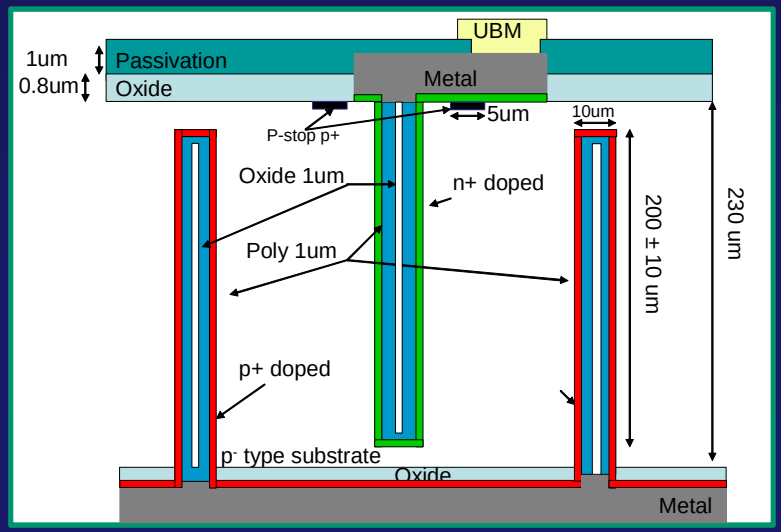

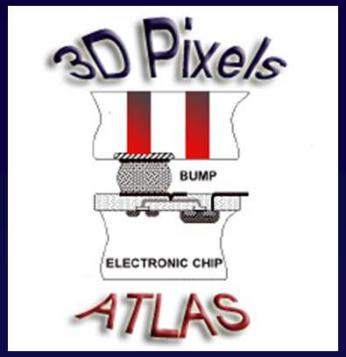

ATLAS 3D Silicon Sensors R&D Collaboration

B. Stugu, H. Sandaker, K. Helle, (Bergen University), M. Barbero, F. Hügging, M. Karagounis, V. Kostyukhin, H. Krüger, J-W Tsung, N. Wermes (Bonn University), M. Capua; S. Fazio, A. Mastroberardino; G. Susinno (Calabria University), C. Gallrapp, B. Di Girolamo; D. Dobos, A. La Rosa, H. Pernegger, S. Roe (CERN), T. Slavicek, S. Pospisil (Czech Technical University), K. Jakobs, M. Köhler, U. Parzefall (Freiburg University), N. Darbo, G. Gariano, C. Gemme, A. Rovani, E. Ruscino (University and INFN of Genova), C. Butter, R. Bates, V. Oshea (Glasgow University), S. Parker (The University of Hawaii), M. Cavalli-Sforza, S. Grinstein, I. Korokolov, C. Padilla (IFAE Barcelona), K. Einsweiler, M. Garcia-Sciveres (Lawrence Berkeley National Laboratory), M. Borri, C. Da Via, J. Freestone, S. Kolya, C. Li, C. Nellist, J. Pater, R. Thompson, S.J. Watts (The University of Manchester), M. Hoeferkamp, S. Seidel (The University of New Mexico), E. Bolle, H. Gjersdal, K-N Sjoebaek, S. Stapnes, O. Rohne, (Oslo University) D. Su, C. Young, P. Hansson, P. Grenier, J. Hasi, C. Kenney, M. Kocian, P. Jackson, D. Silverstein (SLAC), H. Davetak, B. DeWilde, D. Tsybychev (Stony Brook University). G-F Dalla Betta, P. Gabos, M. Povoli (University and INFN of Trento) , M. Cobal, M-P Giordani, Luca Selmi, Andrea Cristofoli, David Esseni, Andrea Micelli, Pierpaolo Palestri (University of Udine)

Processing Facilities: C. Fleta, M. Lozano G. Pellegrini, (CNM Barcelona, Spain); (M. Boscardin, A. Bagolini, P. Conci, G. Giacomini, C. Piemonte, S. Ronchin, E. Vianello, N. Zorzi (FBK-Trento, Italy) , T-E. Hansen, T. Hansen, A. Kok, N. Lietaer (SINTEF Norway), J. Hasi, C. Kenney (Stanford). J. Kalliopuska, A. Oja (VTT , Finland)*

18 institutions and 5 processing facilities

Consistent performance of the considered 3D designs

Simulations and data shows that
The response of full 3D and
3D-DDTC is very close if the
electrode penetration
stops 25 μm from the surface
Before and after irradiation

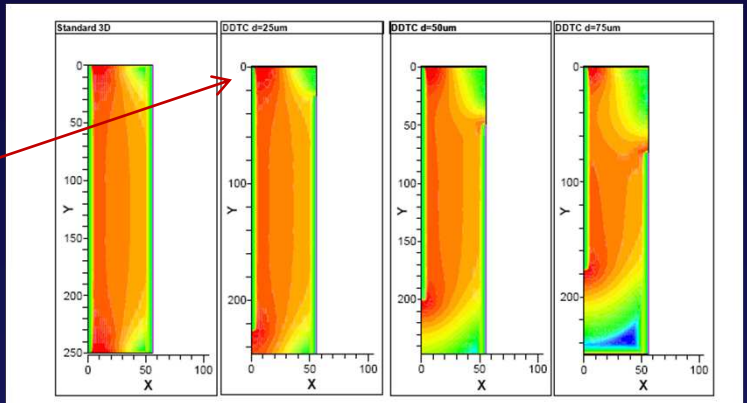

Figure 6.2: Electric field distribution taken from a 2-D cross section of the 3-D structure along the diagonal that connects two columns of opposite doping types. Four cases are here represented: one standard 3D detector and three 3D-DDTC detectors with d spacing of 25, 50 and 75 μm.

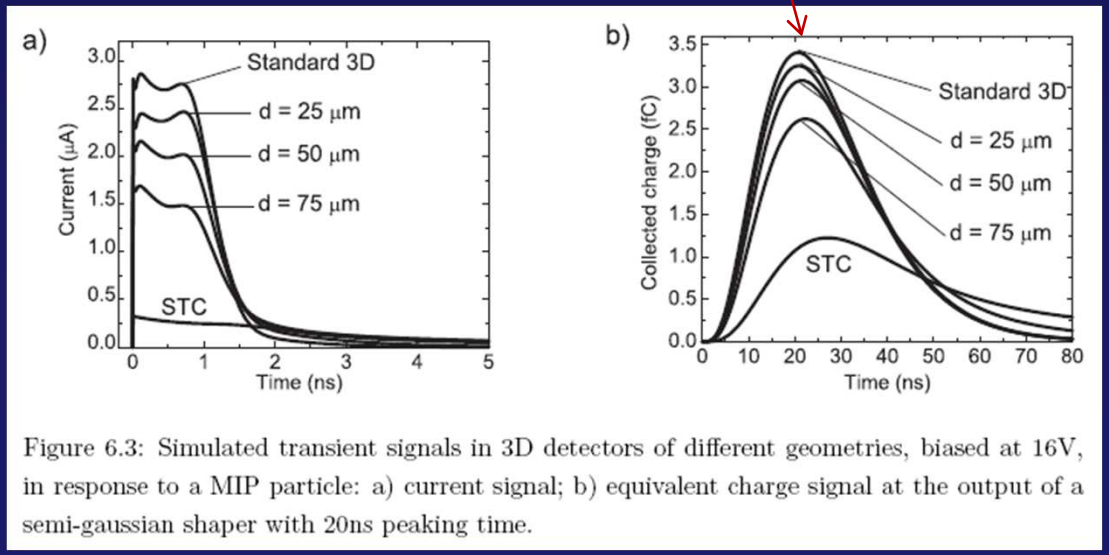

Figure 6.3: Simulated transient signals in 3D detectors of different geometries, biased at 16V, in response to a MIP particle: a) current signal; b) equivalent charge signal at the output of a semi-gaussian shaper with 20ns peaking time.

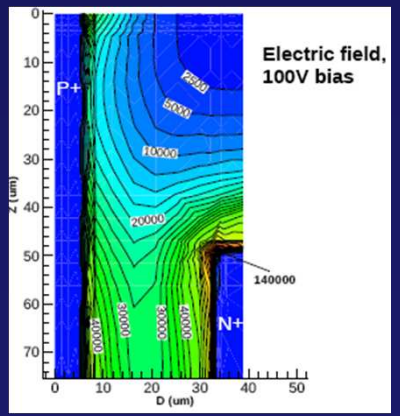

Simulations (from A. Zoboli
PhD thesis, Trento, March 2009)
D. Pennicard, Glasgow IEEE/NSS 08

MANCHESTER 1824

3D silicon has just started to explore its potential: Where could it be applied?

3D features:

Active edges
Low voltage
High speed
Shape flexibility
Radiation hardness

HEP

IBL, PH1-PH2 Vertex
ATLAS Forward Physics

Medical

- Micro structures: endoscopy, dosimetry
- Large area imagers (mammography, synchrotron)
- Focal planes (diffracted x-rays)
- Spectroscopy
- Edge-on scanned imaging (synchrotron mammography)

- PET (embedded converters)
  - photo-multiplication

- TOF-PET (above + speed)

LHC timeline

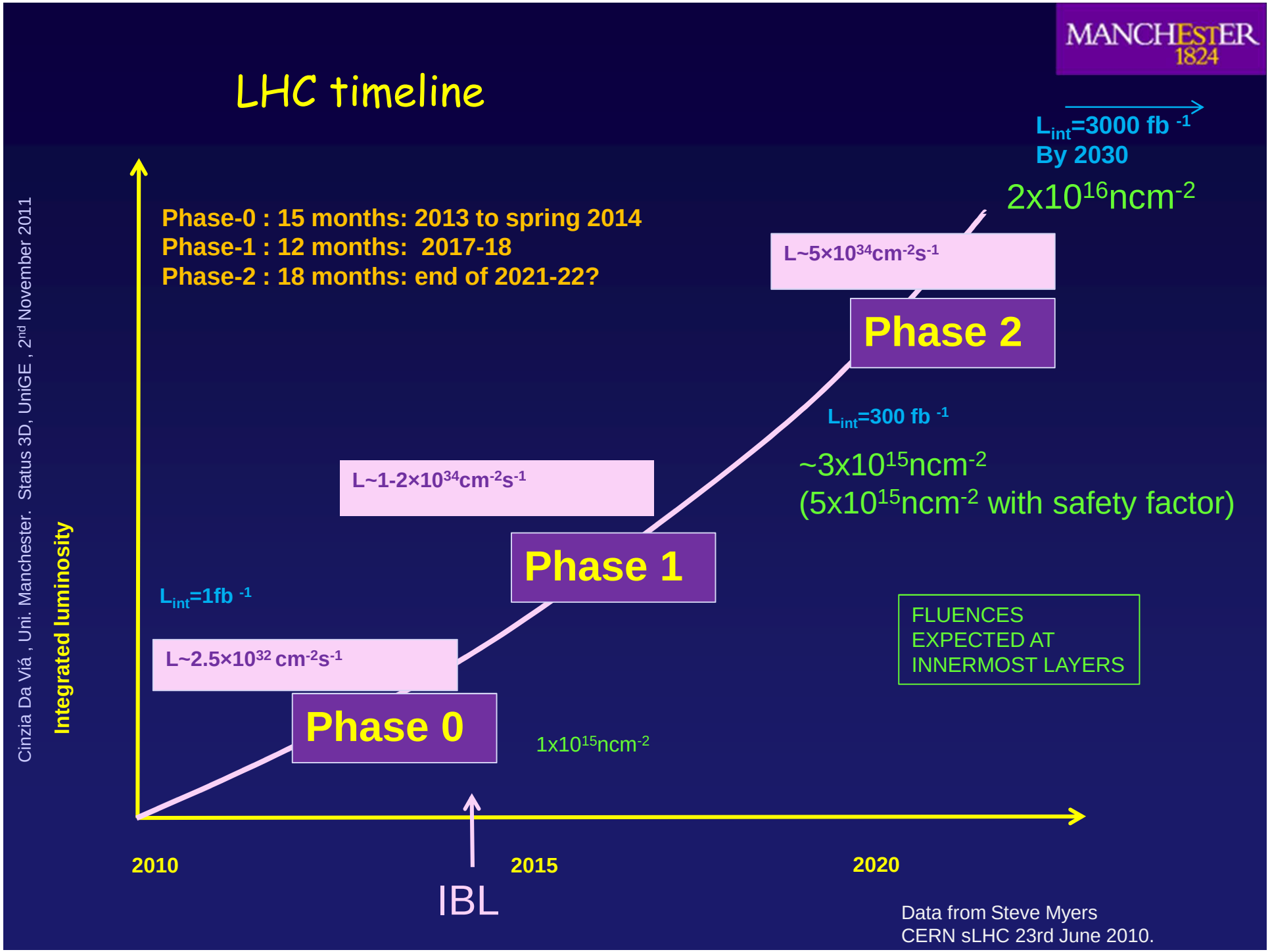

Radiation Induced Bulk Damage in Silicon

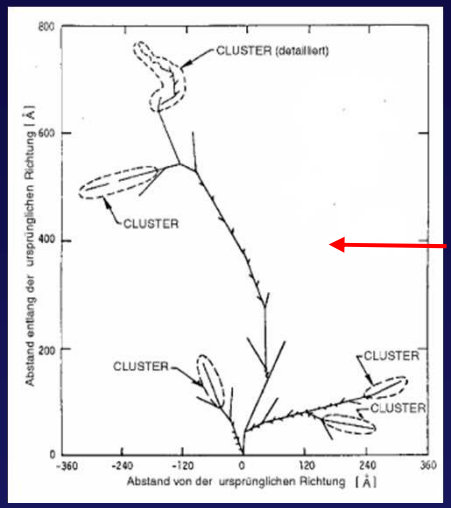

Van Lint 1980

Primary Knock on Atom

Displacement threshold in Si:
Frenkel pair E~25eV
Defect cluster E~5keV

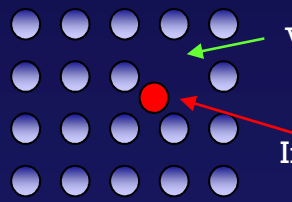

From RD48/ROSE Moll

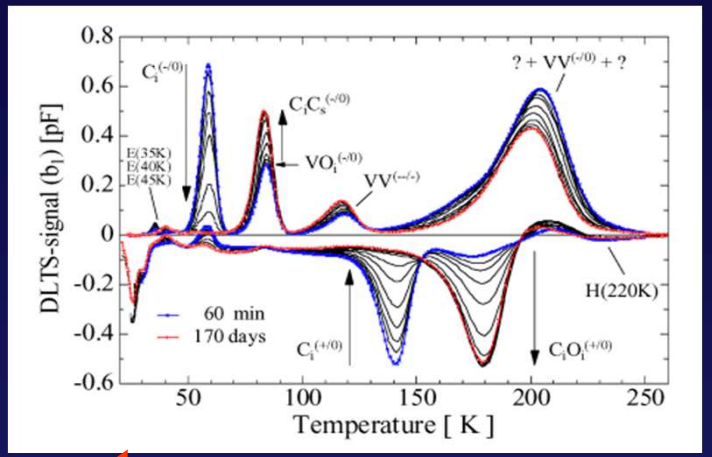

V,I MIGRATE UNTIL THEY MEET IMPURITIES AND DOPANTS TO FORM STABLE DEFECTS

Effect on sensors

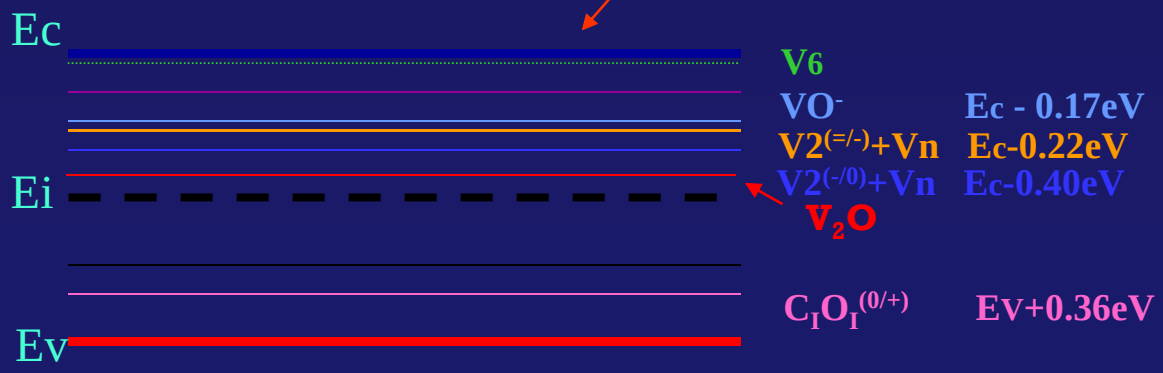

CHARGED DEFECTS==>N_{EFF}, V_{BIAS}

DEEP TRAPS, RECOMBINATION CENTERS ==> CHARGE/SIGNAL LOSS

DEEP TRAPS, GENERATION CENTERS==>LEAKAGE CURRENT

TRAPPING in Si :

The carriers move less → less signal since the signal is formed when charges move – characterized by carrier trapping time τ

=> COLLECT ELECTRONS, INCREASE E-field and USE SHORT 'IES' (THIN SUBSTRATES FOR PLANAR)

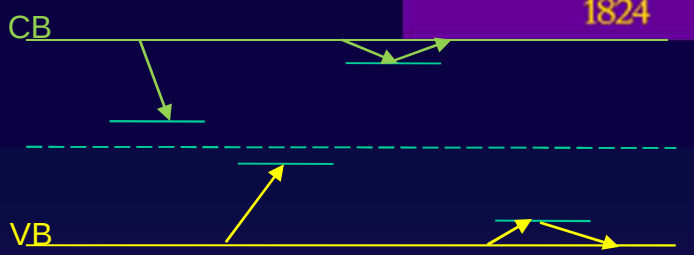

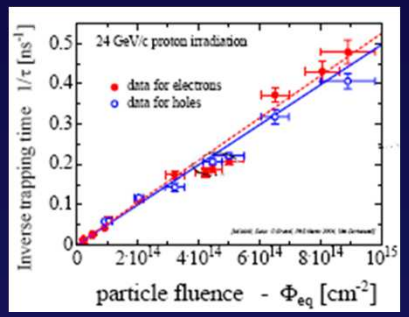

×

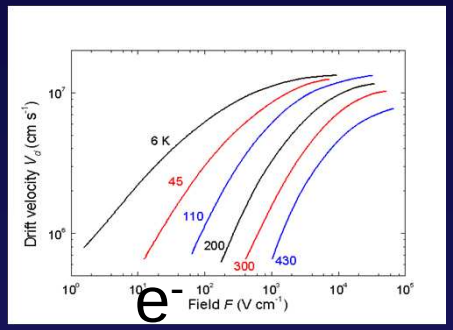

e⁻

=

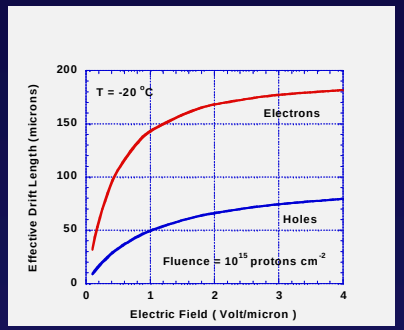

τ_{tr} v_{drift} λ Effective drift length

$$\frac{dS}{dt} = q\frac{dV_W}{dx}\frac{dx}{dt}\exp(-\frac{x}{\lambda})$$

$$S = \frac{\lambda}{L}\left[1-\exp(-\frac{L}{\lambda})\right]$$

Trapping times from Kramberger et al. NIMA 481 (2002) 100

These data: DaVia et al. Nuclear Instruments and Methods in Physics Research A 603 (2009) 319–324

Expected signal yield
After irradiation
Without multiplication
Depends on l/L
This is also true for Diamond sensors

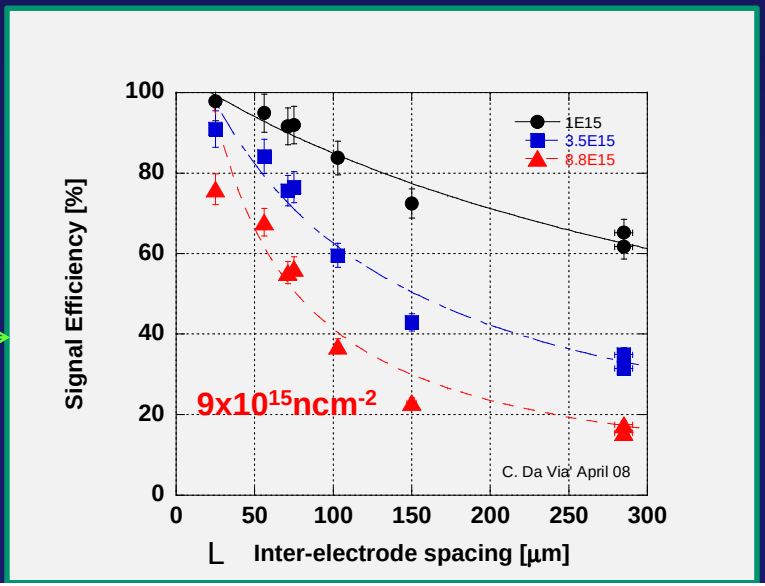

3D Radiation Hardness

Irradiation and measurements performed in Prague
C. Da Viá, T. Slaviceck, V. Linhart, P. Bem, S. Parker,
S. Pospisil, S. Watts (process J. Hasi, C. Kenney)

$8.81 \times 10^{15} n/cm^2$
$1.73 \times 10^{16} p/cm^2$

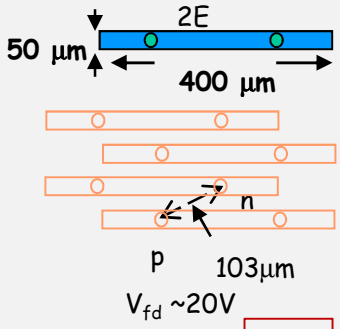

2E
9000e⁻
V_b~130V

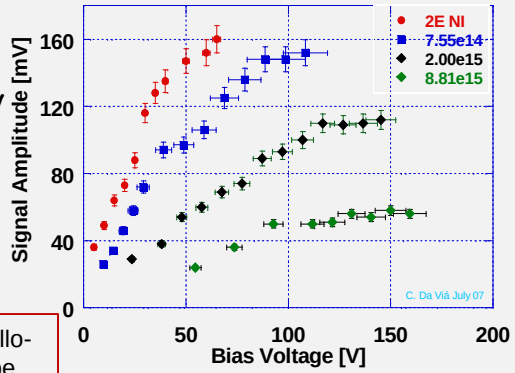

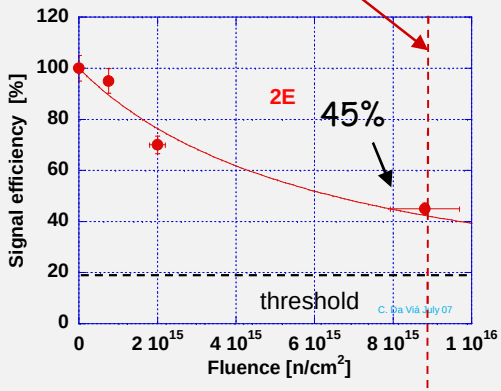

IR Laser

Oscillo-scope

bias

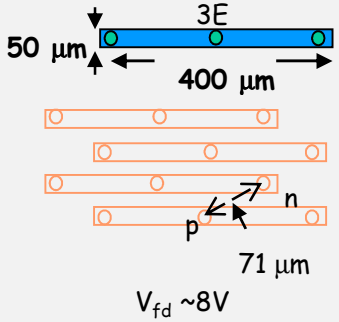

3E
10200e⁻
V_b~112V

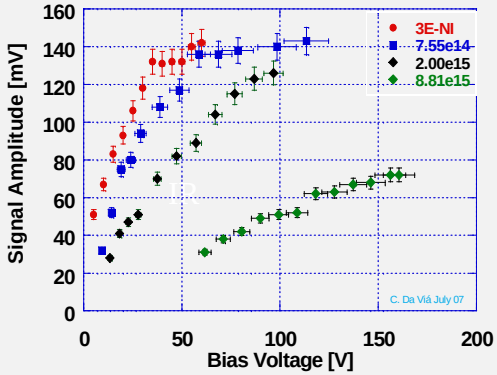

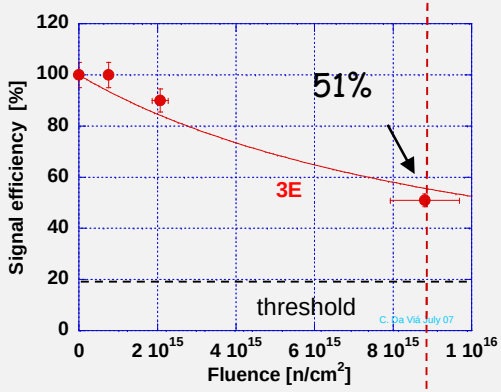

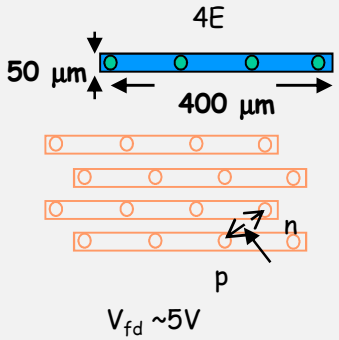

4E
13200e⁻
V_b~94V

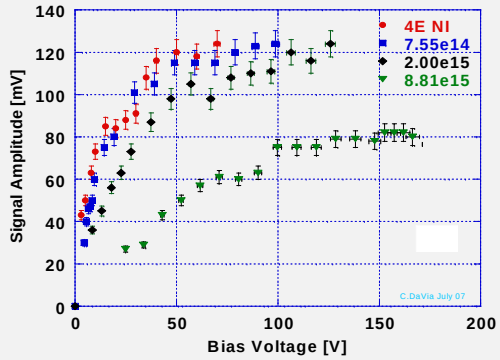

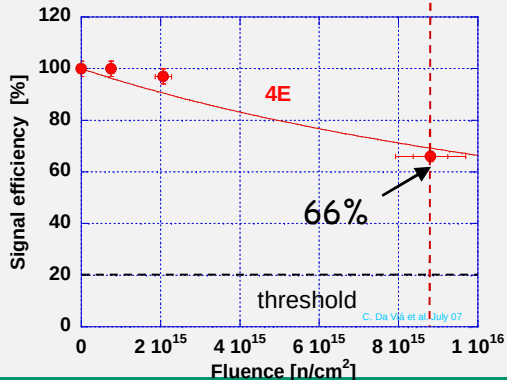

Signal efficiency and signal charge In Si Sensors

[9] C. Da Via et al.", (NIMA-D-08-00587)
[10] G. Kramberger at al., Nucl. Instr. Meths. A 554 (2005) 212-219
[11] G. Kramberger, Workshop on Defect Analysis in Silicon Det, Hamburg, August 2006. http://wwwiexp.desy.de/seminare/defect.analysis.workshop.august.2006.html
[12] G. Casse et al., Nucl. Instr. Meths. A (2004) 362-365
[14] T. Rohe et al. Nucl. Instr. Meths. A 552 (2005) 232-238
[16] F. Lemeilleur et al., Nucl. Instr. Meths. A 360 (1995) 438-444

Cinzia Da Viá , Uni. Manchester. Status 3D, UniGE , 2nd November 2011

Signal Efficiency (prop 1/L IES)

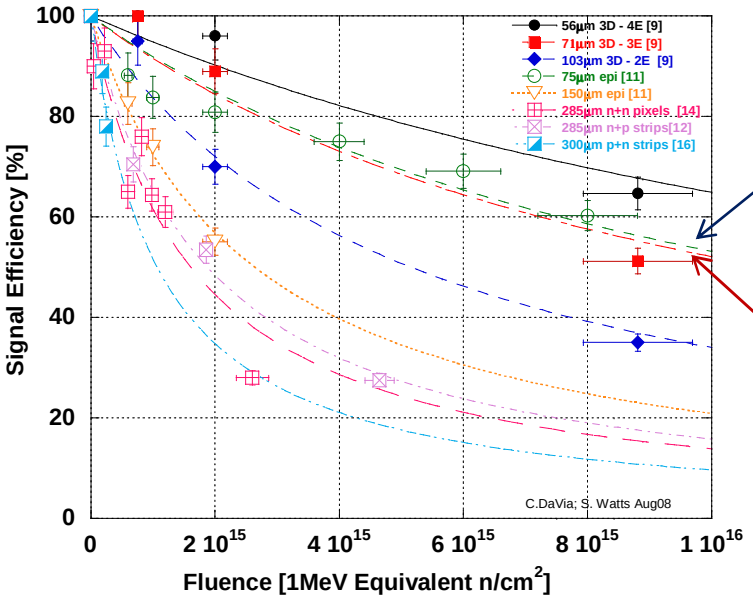

71µm 3D

75µm epi

Signal charge (substrate thick. Δ)

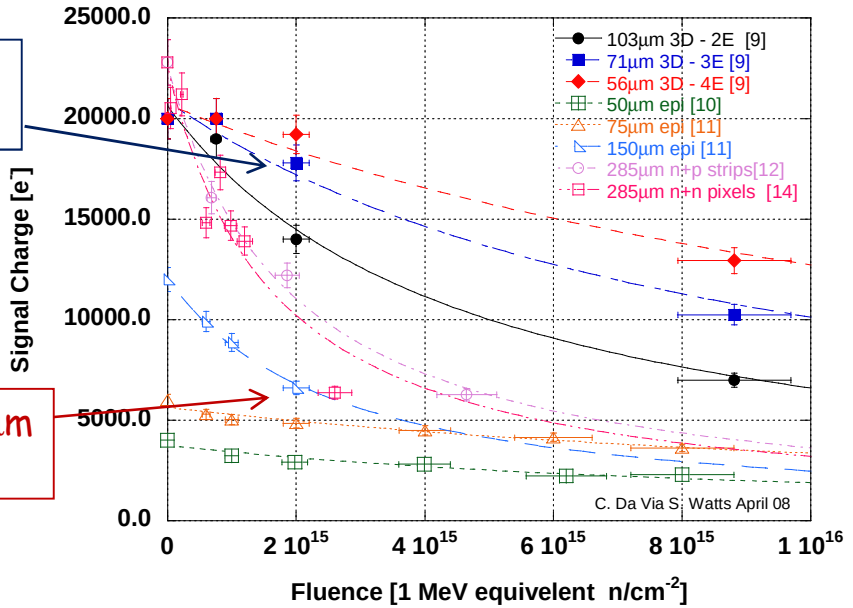

Atlas IBL – timescale 2013-14

- **Baseline layout decided**
  - **14 Staves,**
  - **14 FE chips/stave**
  - **For 3D single chips**
  - **(224 to build 25%)**
  - **For planar double chips (448 to build 75%)**

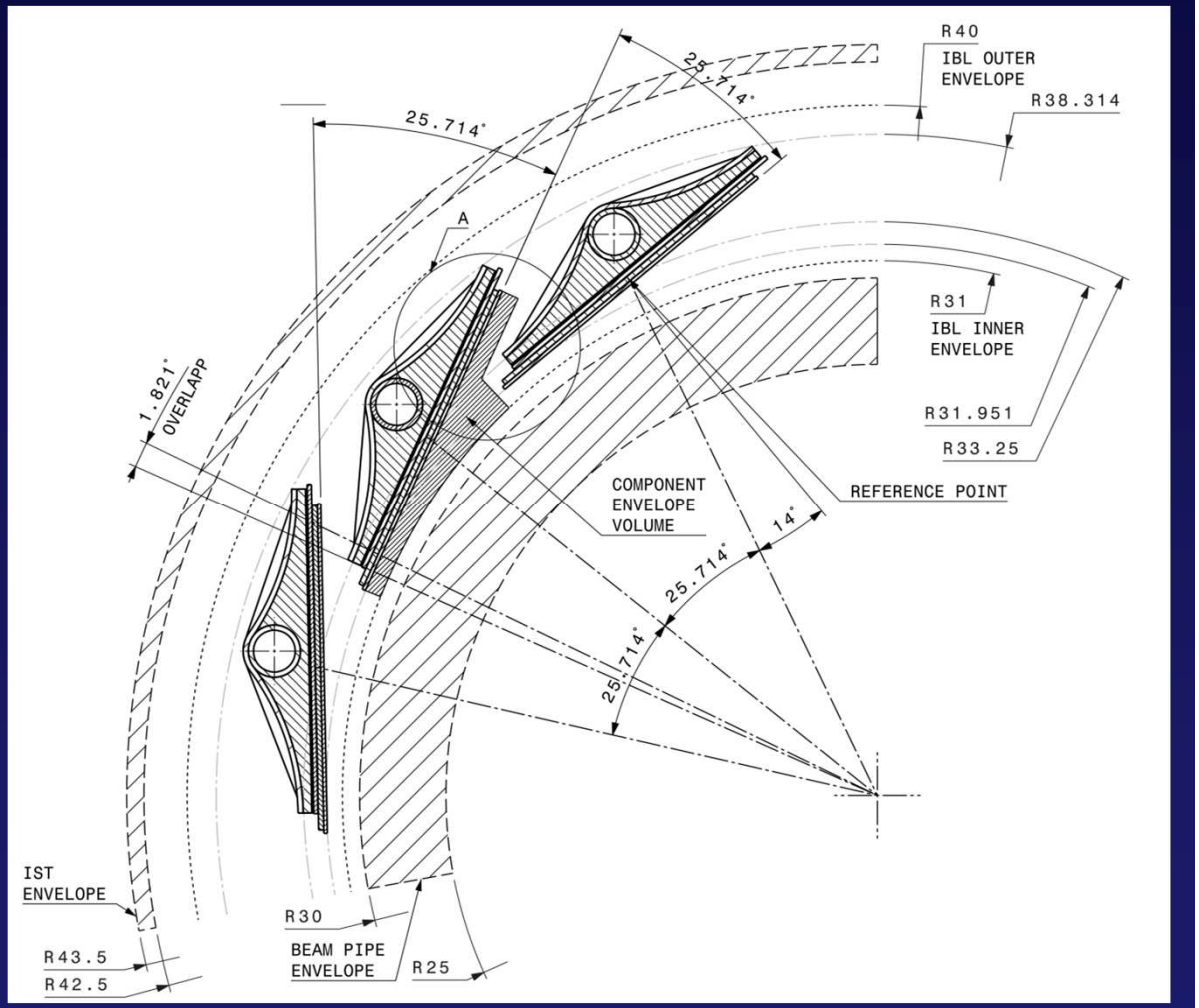

Very tight clearance:

- "Hermetic" to straight tracks in Φ (1.8º overlap)
- No overlap in Z: minimize gap between sensor active area.

Layout parameters:

- IBL envelope: 9 mm in R
- <R> = 33 mm.
- Z = 60 cm (active length).
- η = 2.5 coverage.

IBL Detectors Specifications

MANCHESTER 1824

Sensor specifications for IBL:

- Qualify to 5x10^{15} n_{eq}
- max. power dissipation: 200 mW/cm^2 at -15 C
- tracking efficiency > 98%.

	3D n-in-p sensor	planar n-in-n sensor
active size W x L [mm^2]	16.8 x 20.0	16.8 x 40.9
total size W x L [mm^2]	18.8 x 20.5	18.54 x 41.27 (?)
thickness [mm]	0.23	0.20
Typical depletion voltage [V]	≤ 15	≤ 35
Typical inital operation voltage [V]	25	60 (V_{dep}+30V)
at of at end of lifetime [V]	180	1000

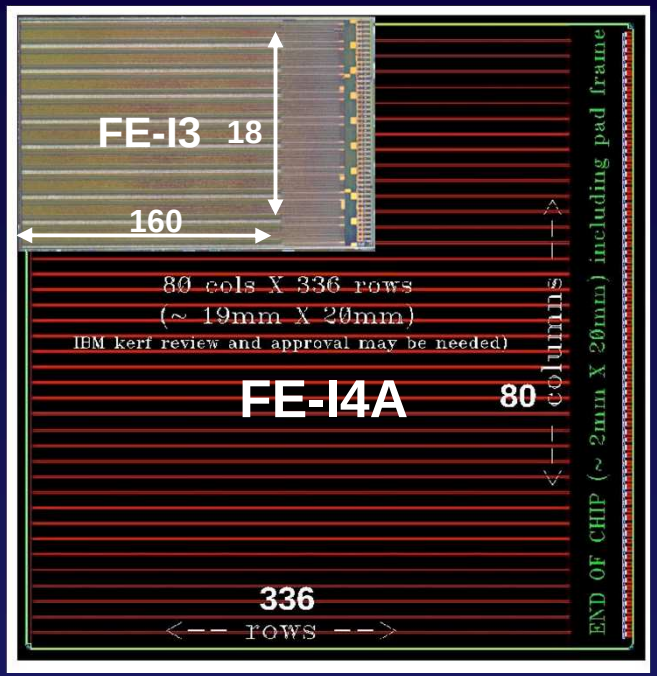

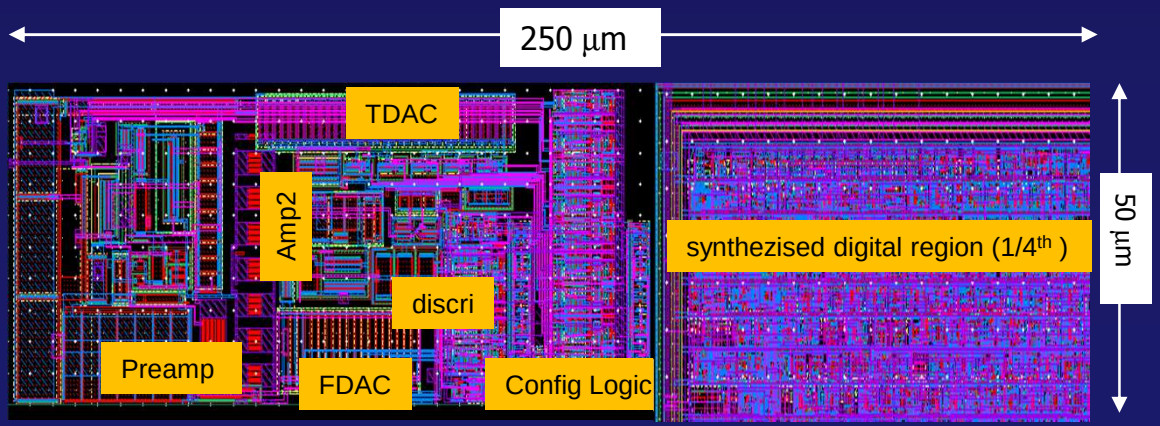

	FE-I3	FE-I4
Pixel Size [µm^2]	50×400	50×250
Pixel Array	18×160	80×336
Chip Size [mm^2]	7.6×10.8	20.2×19.0
Active Fraction	74 %	89 %
Analog Current [µA/pix]	26	10
Digital Current [µA/pix]	17	10
Analog Voltage [V]	1.6	1.4
Digital Voltage [V]	2	1.2
pseudo-LVDS out [Mb/s]	40	160

Strategy: qualify both full3D and DSDC with Common Floor-Plan Design

MANCHESTER 1824

Design by GF Dalla Betta, C. Kenney, A. Kok, G Pellegrini

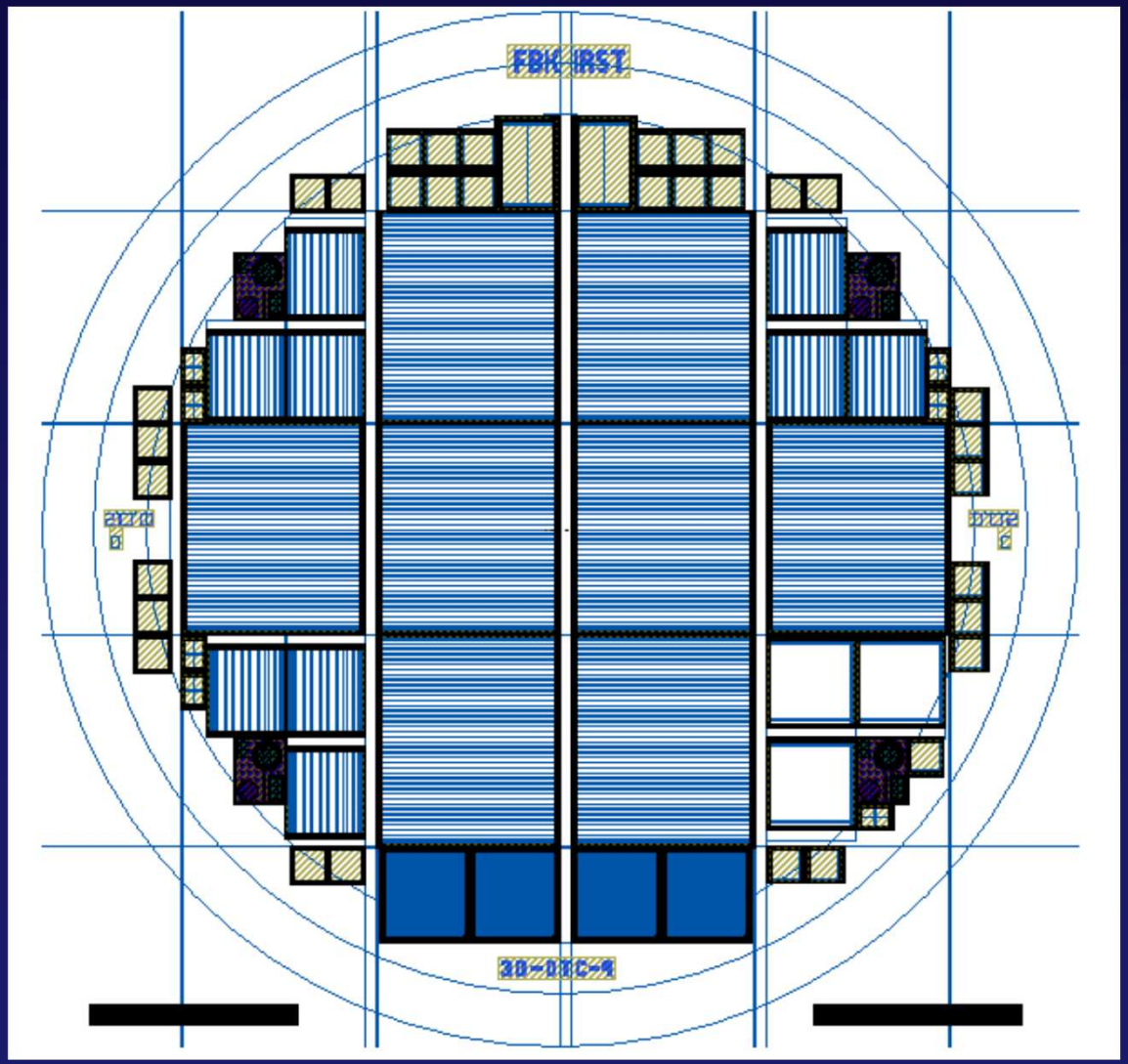

The Stanford Nanofabrication Facility
SINTEF
ITC irst
FONDAZIONE BRUNO KESSLER
cnm
Centre Nacional de Microelectrònica

- 8 x FE-I4
- 9 x FE-I3
- Other test structures

- 120 wafers x 8 = 960 FE-I4

Of which:
- 480 full 3D with active Edges
- 320 double sides with slim fences

And :
1080 x FE-I3

Qualification run for full3D with active edges – at Sintef/Stanford

MANCHESTER 1824

3DC

Manchester, Oslo, SLAC, Prague, Purdue

A. Kok, T-E Hansen

Test structures

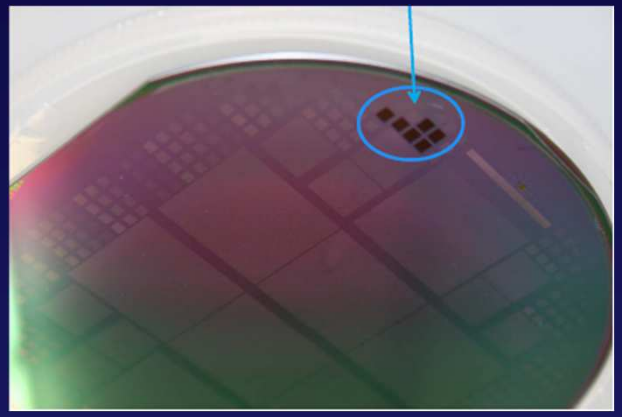

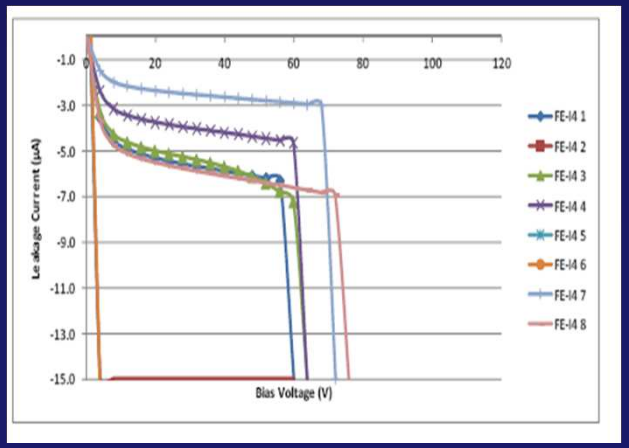

230 um thick with support wafer and Active edges with new doping gases
Run completed

STANFORD completed an independent run With identical layout

18 wafers of the FE-I3 run were completed at the end of 2009.

IVs on FE-I4 wafer

3D sensors for Fast track - IBL
Double sided slim edges

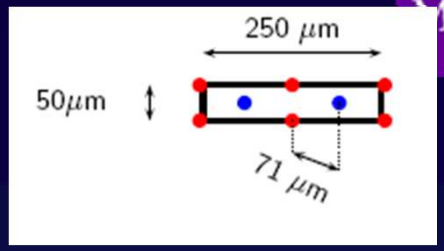

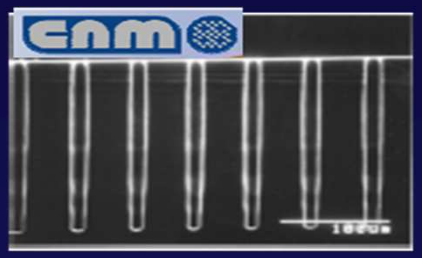

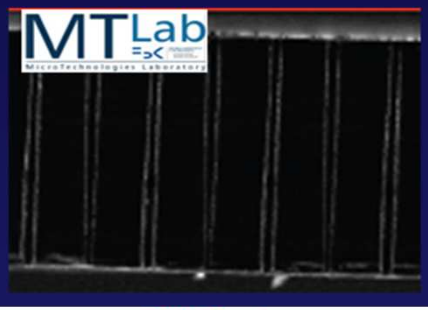

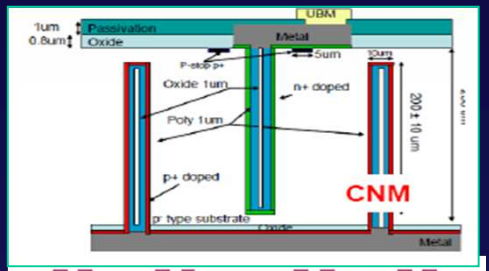

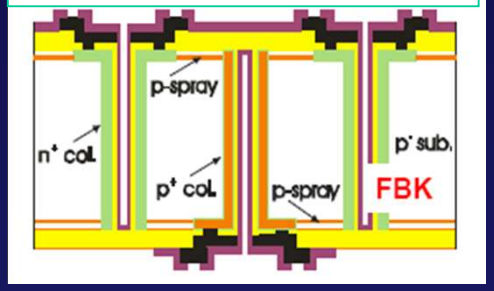

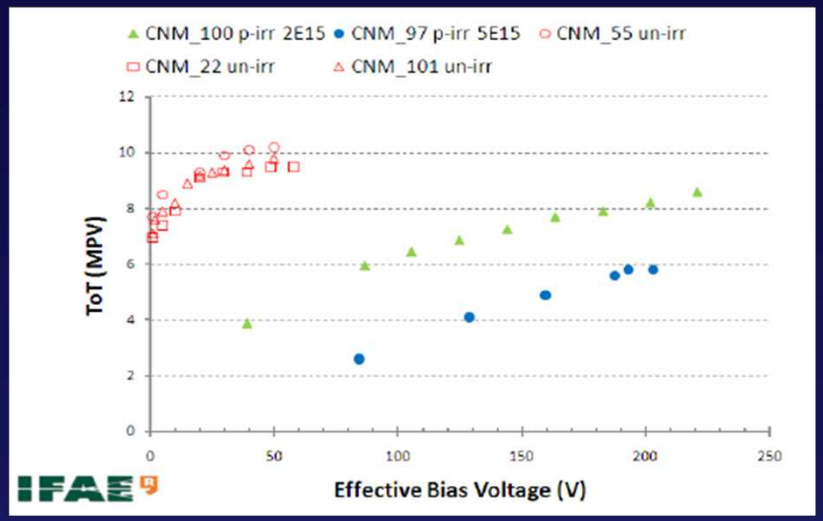

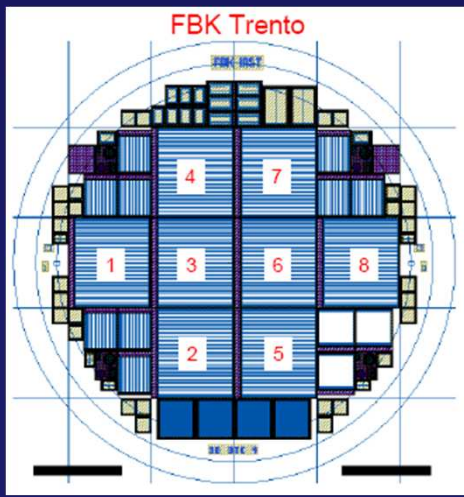

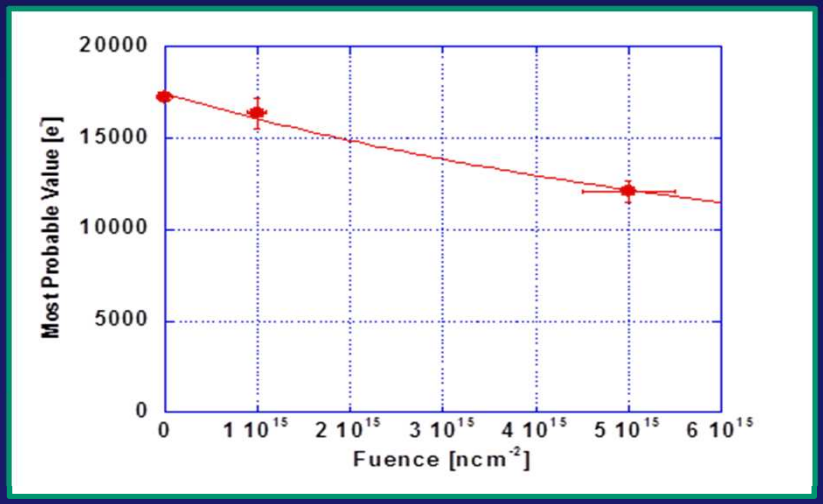

COMMON FLOOR-PLAN WAFER LAYOUT

200 µm guard fences

MANCHESTER 1824

Design and simulation
GF Dalla Betta, Trento

Cinzia Da Viá , Uni. Manchester. Status 3D, UniGE , 2nd November 2011

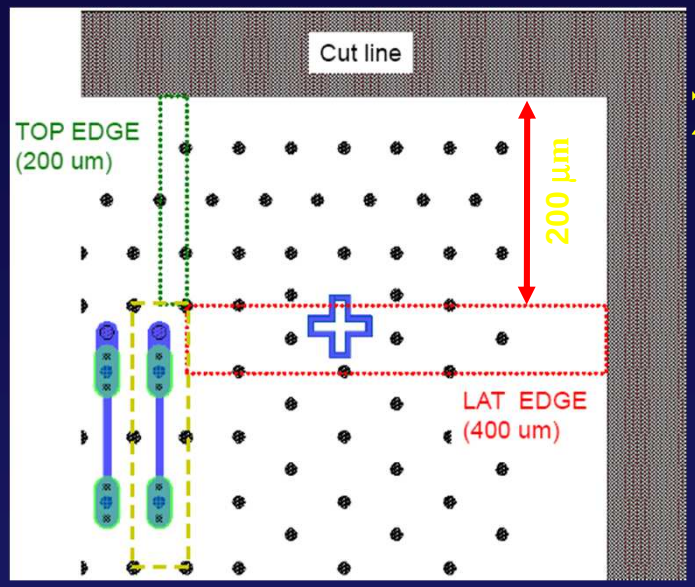

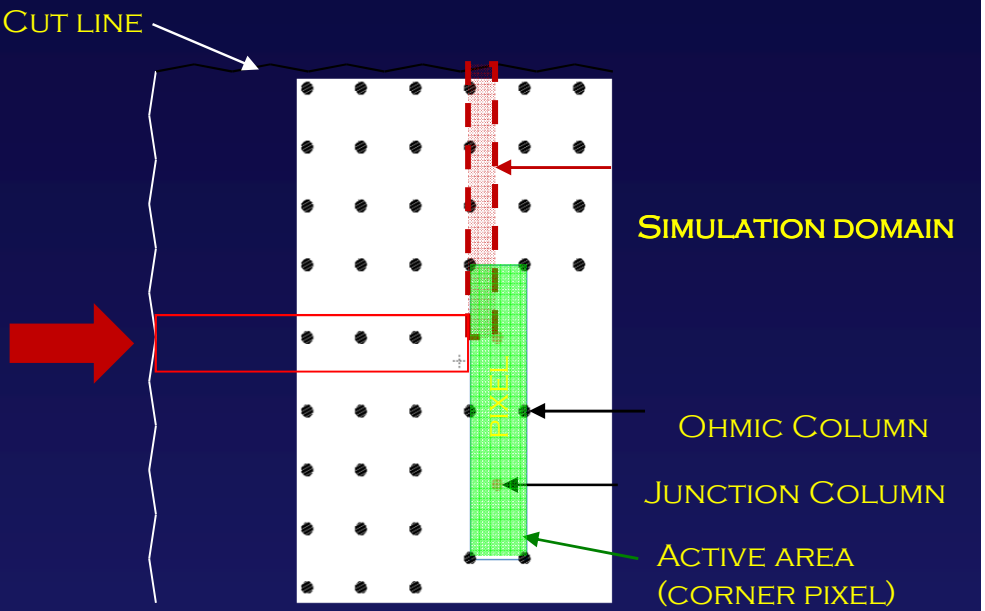

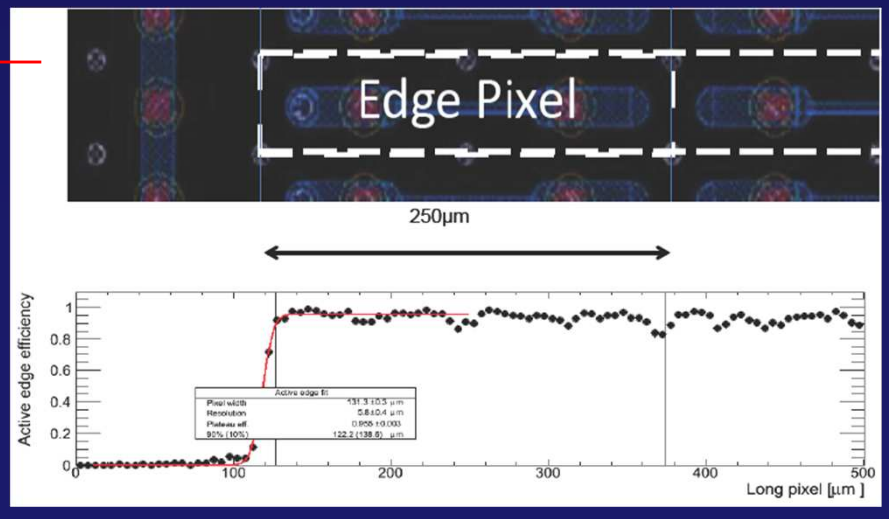

3D-CNM34, irradiated with protons at 5E15neq/cm2: 1D hit efficiency in the long pixel direction for edge pixels. All edge pixels have added together. Operation conditions are: FE-I4 threshold = 1300e, bias voltage = -140V, magnetic field = 1.6T, tilt angle = 0 degrees.

Edge pixel: regular length 250 µm
- Inactive area: 200µm
- Actual efficiency extends:
- 50%: 20-30µm
- Effective inactive area from dicing: ~200µm.
- Same for all 3D samples.

3D IBL production: we need to make 224 FE-I4 modules with 75 wafers

Batch: 5737
Wafer: 7

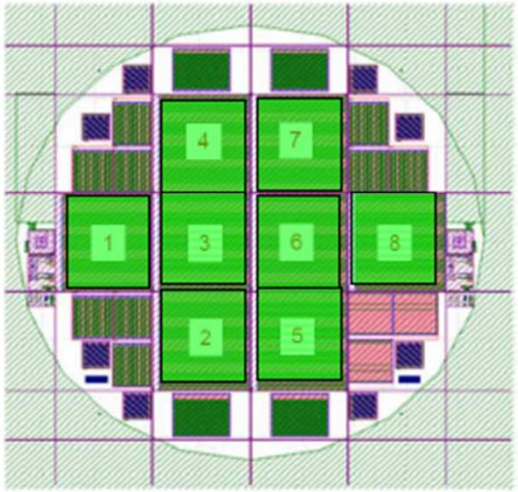

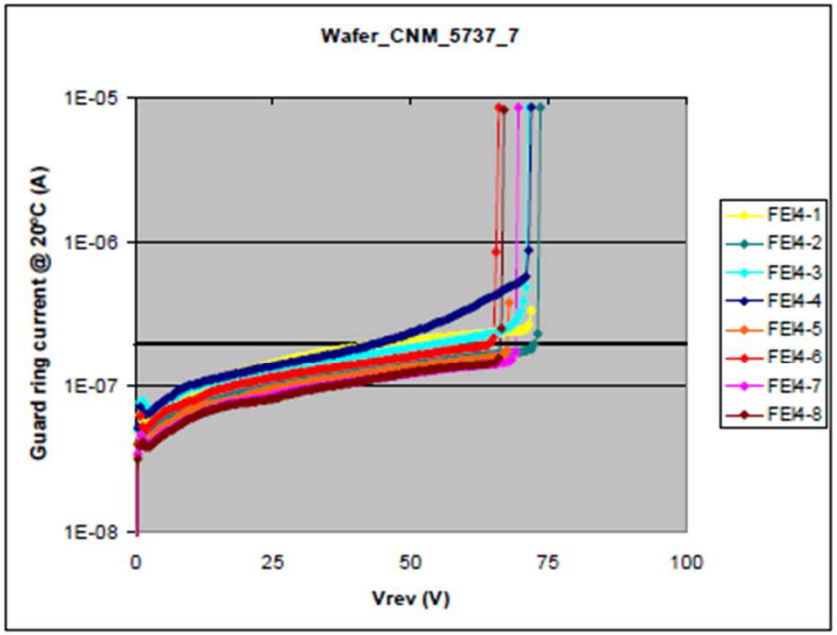

bowing

	Class	GR current @ 25 V (nA)	I(25V) / I(20V)	Breakdown V (V)
S1	A	145.18	1.13	71
S2	A	102.12	1.10	72
S3	A	132.70	1.09	69
S4	A	139.88	1.10	71
S5	A	96.12	1.14	67
S6	A	116.11	1.09	65
S7	A	86.76	1.09	69
S8	A	82.57	1.07	66

Wafer curvature: 60.8µm

class A detectors: 8
class B detectors: 0
class C detectors: 0

Selection Criteria and QA - CNM

3D ATLAS, Review Meeting CERN 07-06--11

CNM I-V tests on guard ring

Measurements from C. Fleta, CNM,
S. Grinstein, IFAE

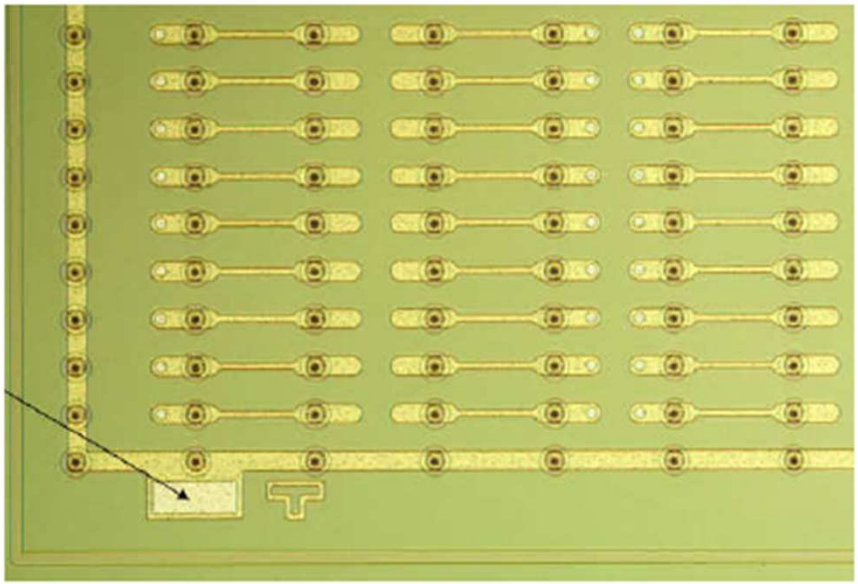

Before bump-bonding:

V_{BD}>25V

I(V_{op})<200 nA per tile

[I (V_{op}) / I(V_{op} – 5V)] < 2

This measurement is not representative of the total current of the sensor but gives a good indication of the presence of defects

CNM IBL Qualification wafers before and after bump-bonding

C. Fleta. S. Grinstein, G. Pellegrini

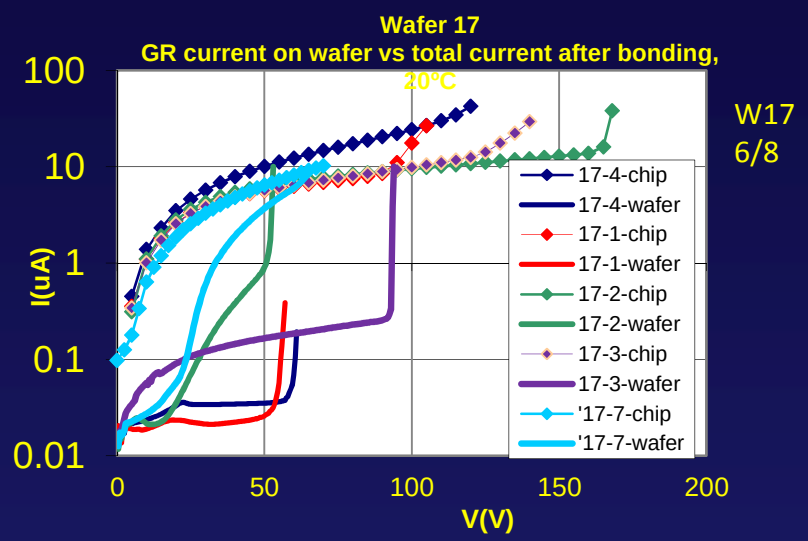

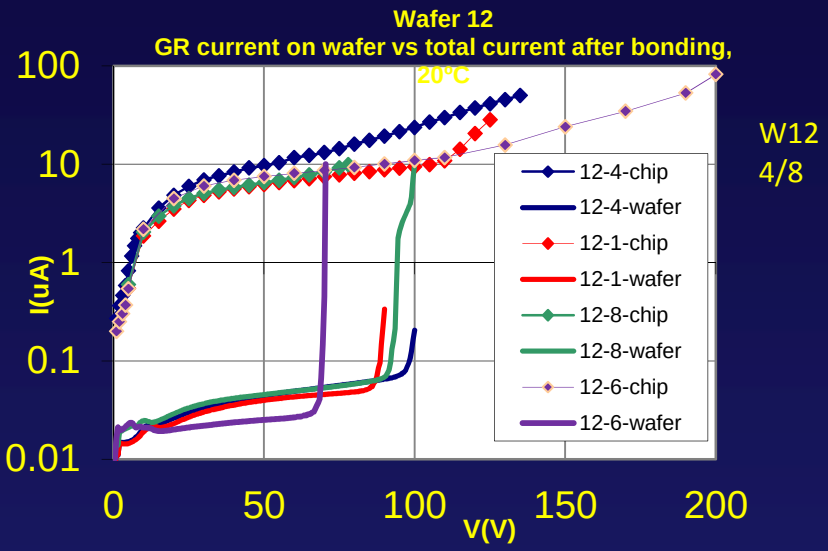

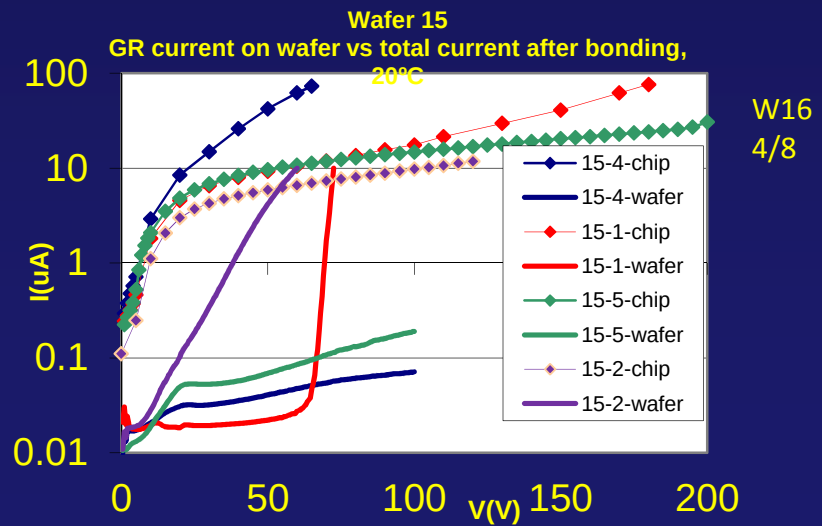

GR current identifies potential defects

Also could be enhanced by stress and neighbour sensors

100% Reproduced behaviour before and after BB

Compilation CNM assemblies after BB 100% supports selection method

I< 2μA
VOP ≥ VDEPL + 10V (20V)
VBD > 25V
SLOPE: [I(VOP)/I(VOP-5V)] < 2

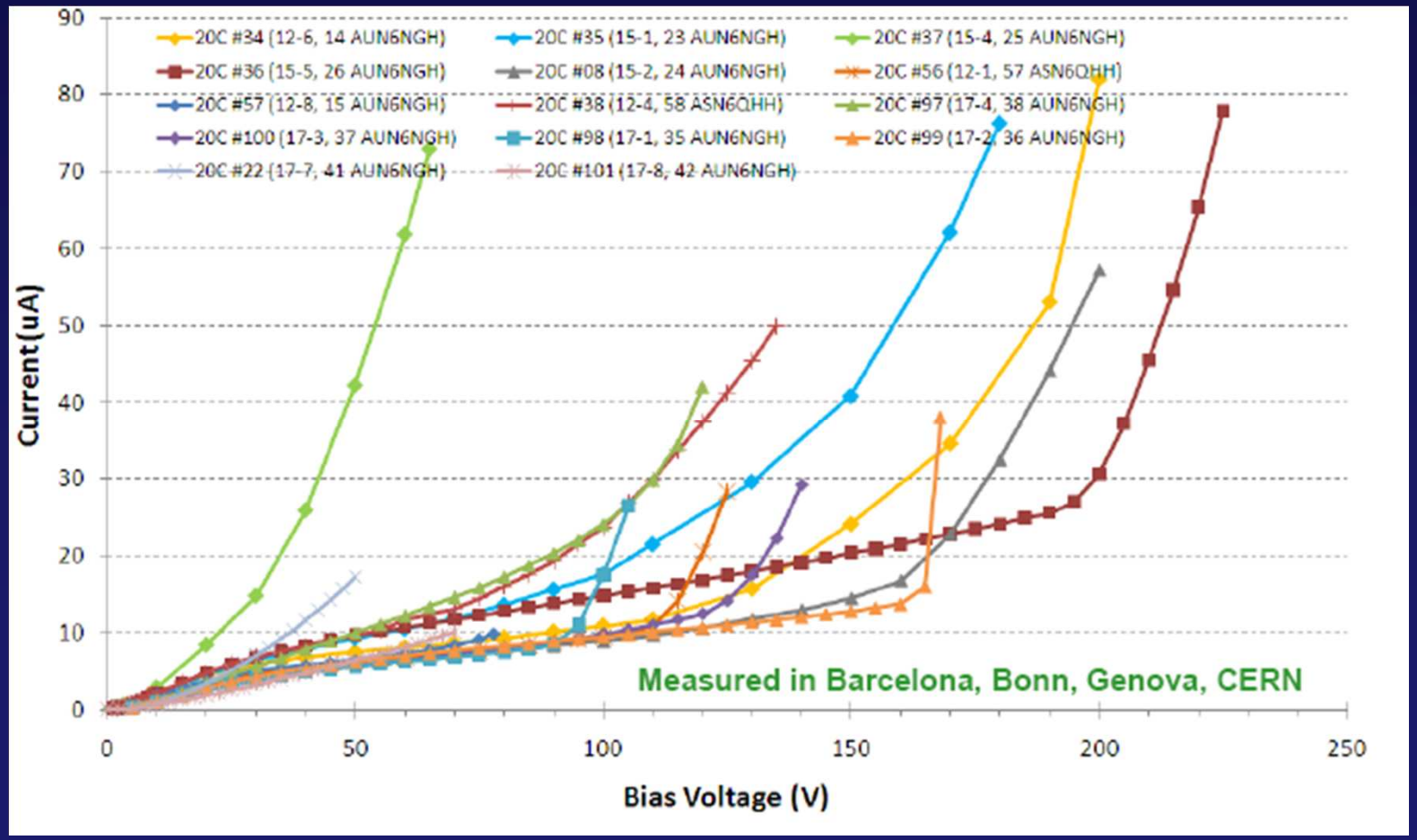

Yield production run : CNM 1

G Pellegrini, C. Fleta

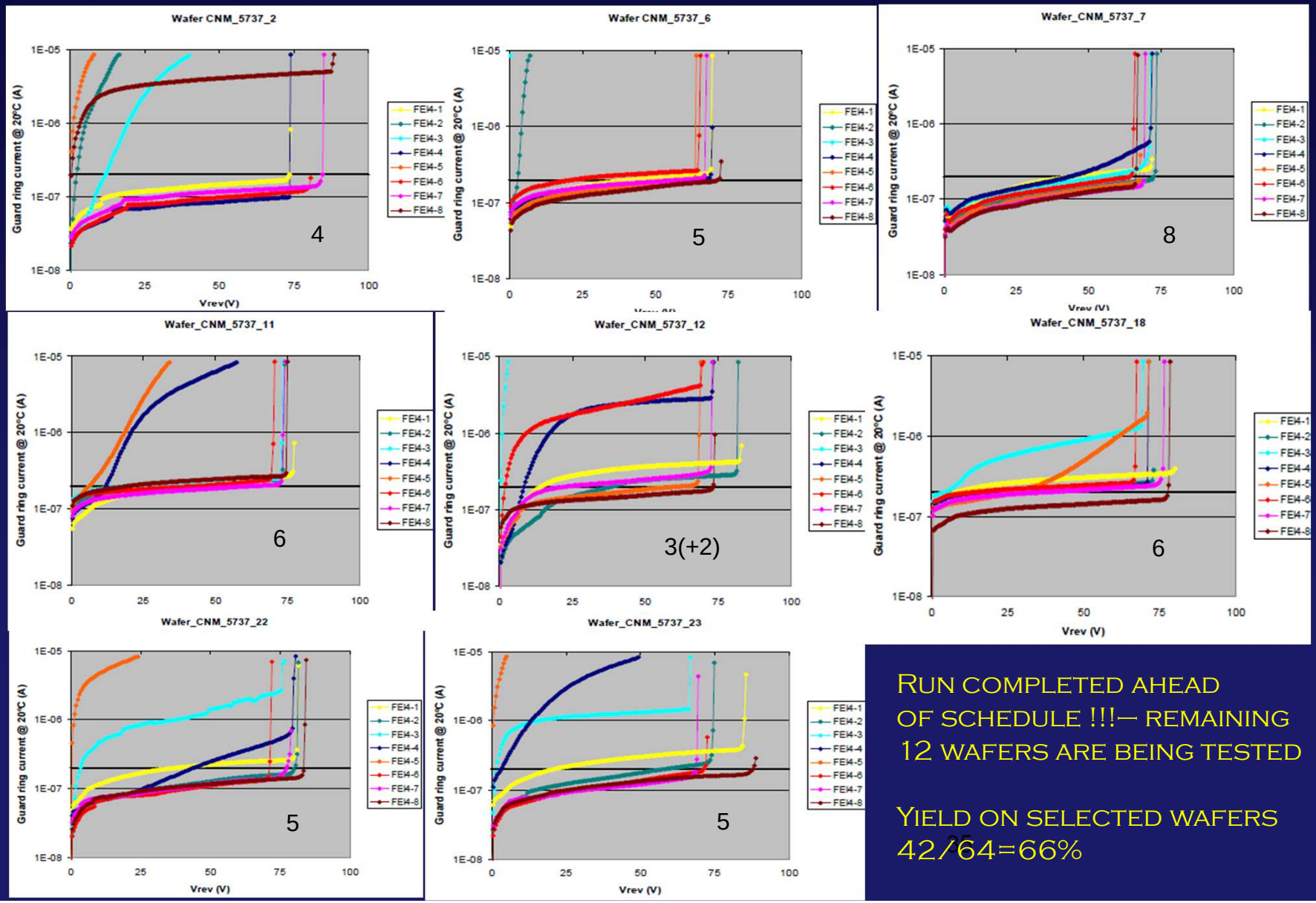

Run completed ahead of schedule !!!– remaining 12 wafers are being tested

Yield on selected wafers 42/64=66%

Selection Criteria and QA - FBK

FBK temporary metal for I-V tests

Measurements from N. Zorzi, G. Giacomini, FBK

- Allows to perform electrical tests on the FE-I4 pixel sensors before bump-bonding
- The temporary metal shorts 336 pixels together in a strip
- 80 strips form a FE-I4 pixel sensor
- Implemented from ATLAS09 batch on

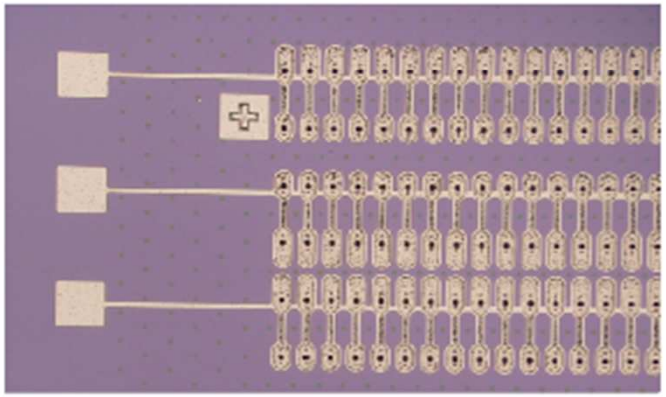

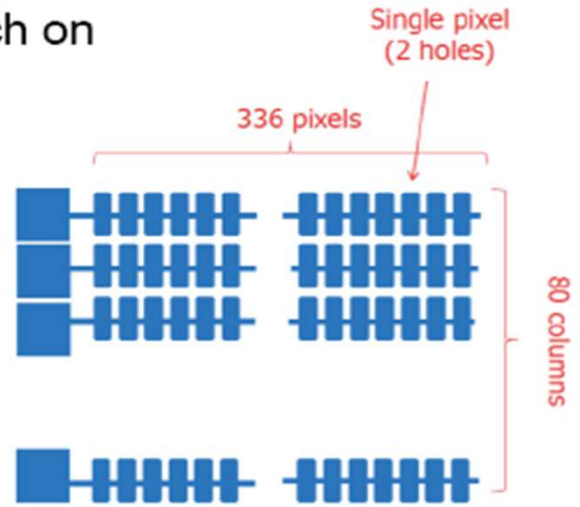

Compilation FBK assemblies after BB

A. Micelli , C. Gemme

I < 2μA
VOP ≥ VDEPL + 10V (20V)
VBD > 25V
SLOPE: [I(VOP)/I(VOP-5V)] < 2

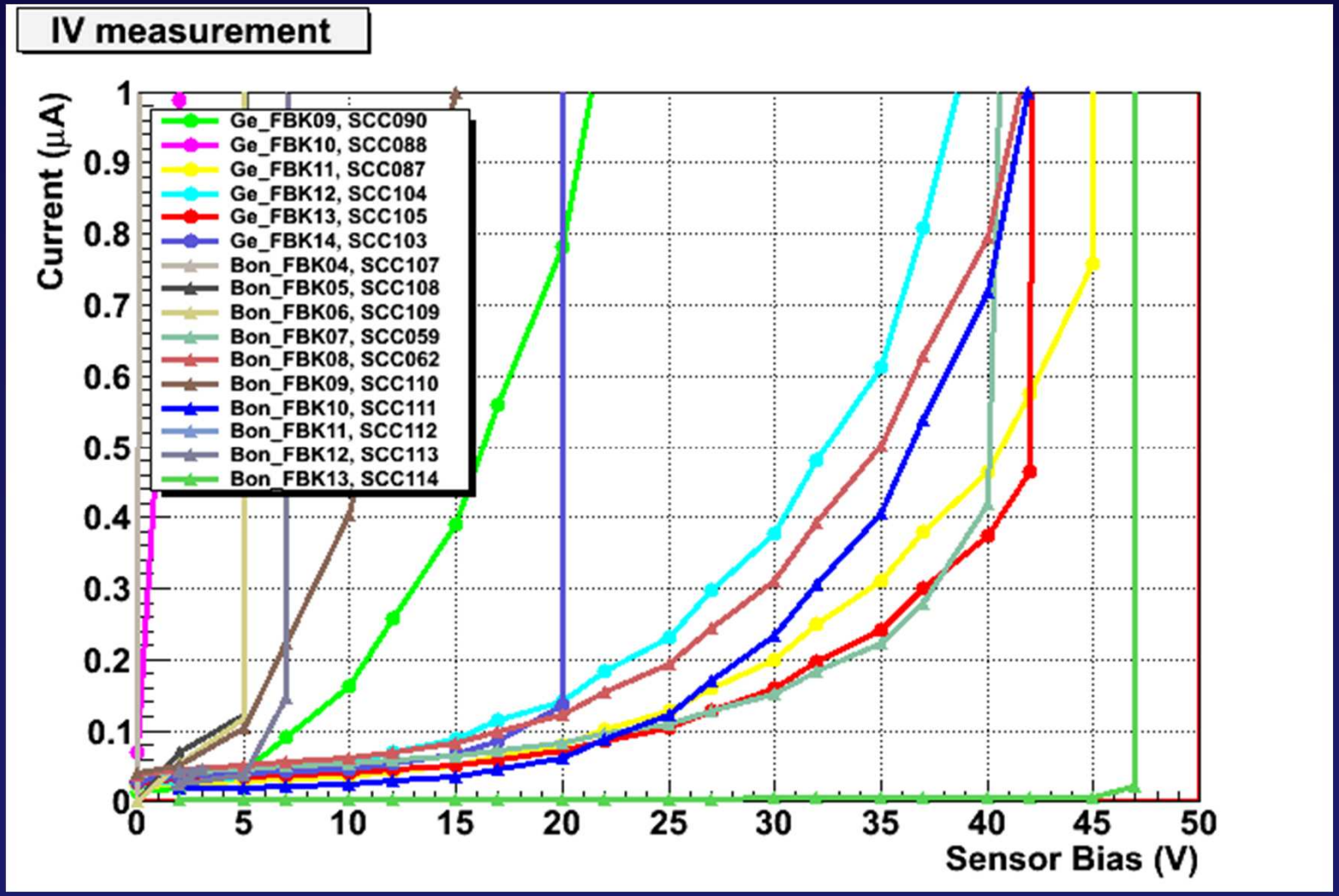

Yield production run : FBK ATLAS10

N. Zorzi, G. Giacomini

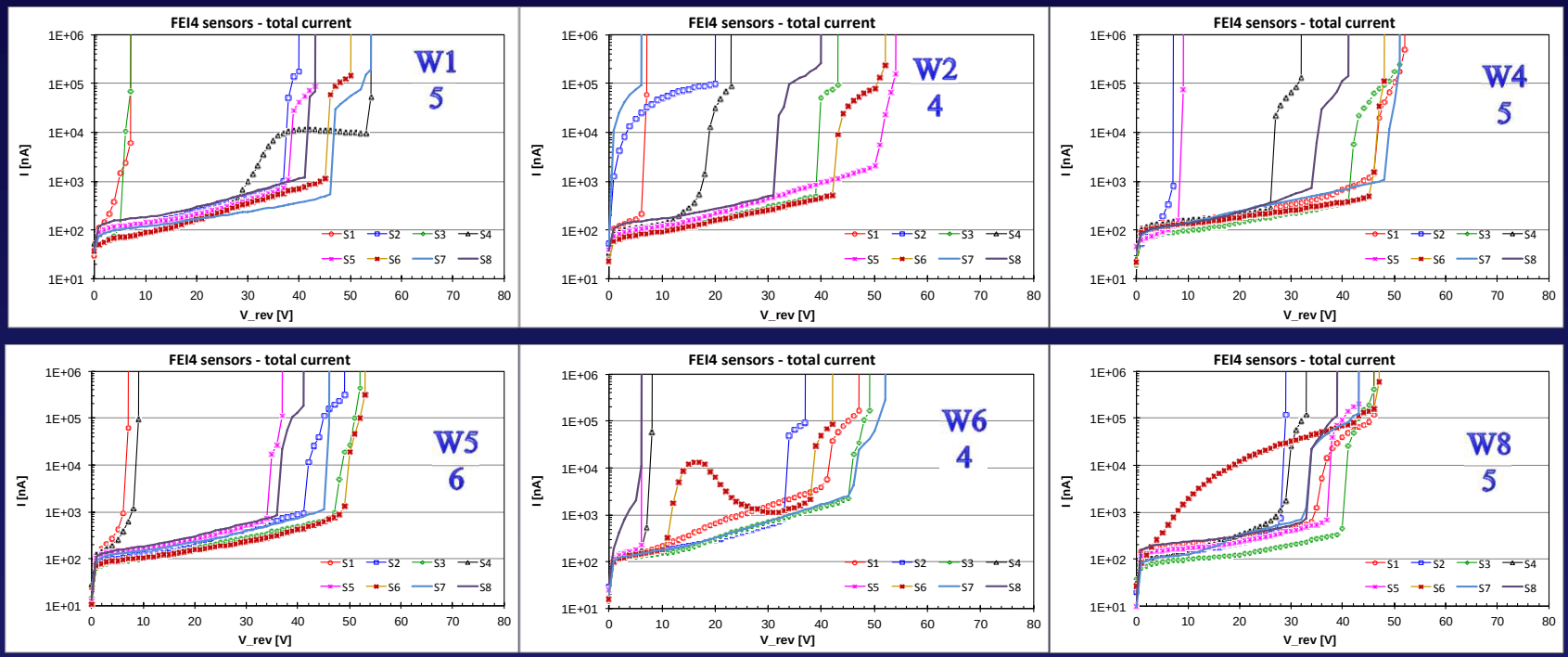

Run Completed in July 2011
Yield on selected wafers: 29/48 = 60%

Yield production run : FBK ATLAS10

N. Zorzi, G. Giacomini

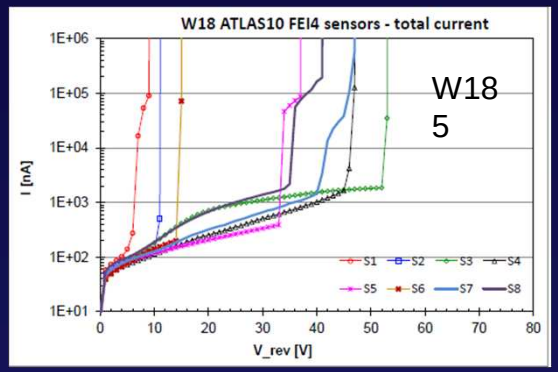

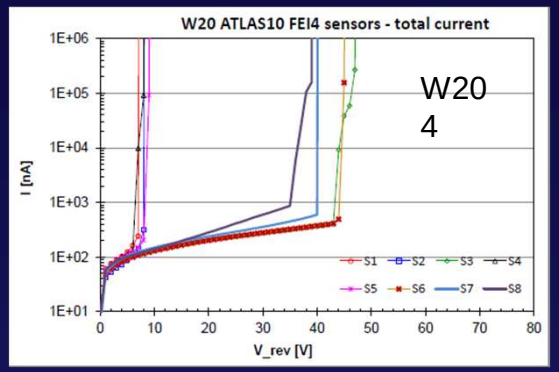

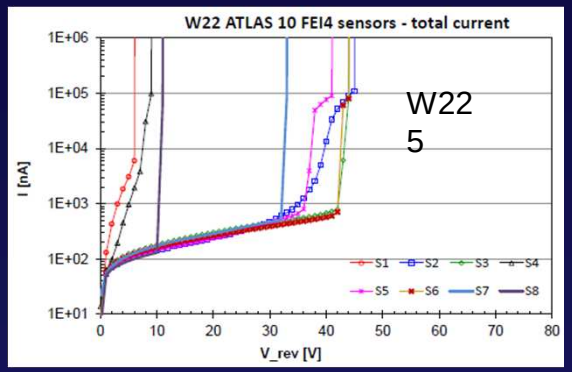

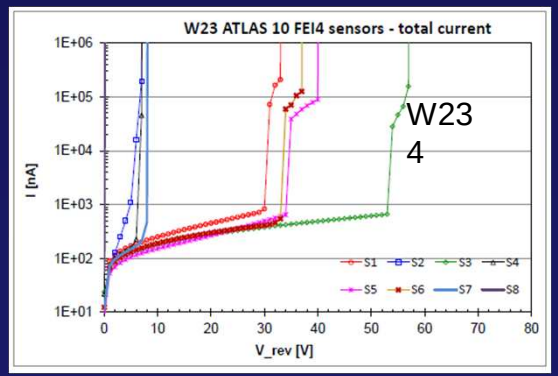

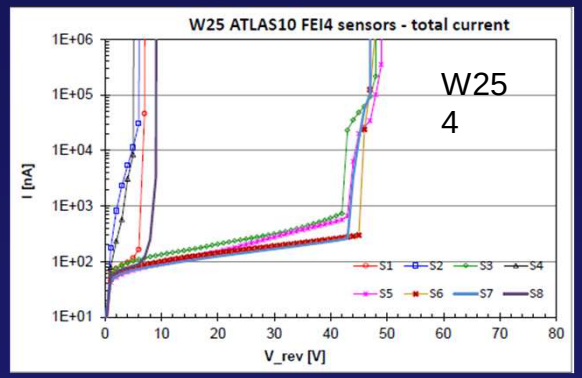

Completed in September 2011
Yield on selected wafers: 22/40 = 55%

Total Yield selected A10 FBK = 57.5% total good sensors =51

Processing status Summary

- A10 completed and tested. 22 wafers measured 11 selected for bump-bonding
- CNM1 completed ahead of schedule. 9 wafers measured 8 Selected for BB, the remaining 12 wafers will be measured by 31-10

batch	Status	Completion date	Tested	Selected wafers	Yield on selected	Number of good sensors
A10	Completed	July/sept11	yes	11	57.5%	51
A11	Completed	18-31Oct	On-going on 13W	-	-	-
A12	Started	30 Jan12	-	-	-	-
CNM1	Completed	10-31Oct	9	8	66%	42
CNM2	On-going	30Nov	-	-	-	-
CNM3	Started	30Jan	-	-	-	-
TOTAL= today				19	62%	93
TO IZM		**7-11-11**		**25**	**62%**	**124**

ATLASFP –
Forward Detectors = use LHC beam-line as a spectrometer
Proton energy loss results in proton trajectory horizontal departure

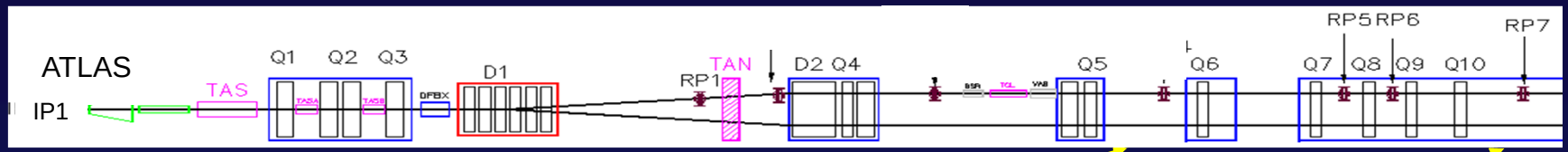

Requires active edge Radhard Devices 3D-FEI4

220m

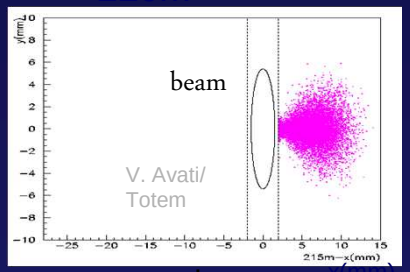

420m

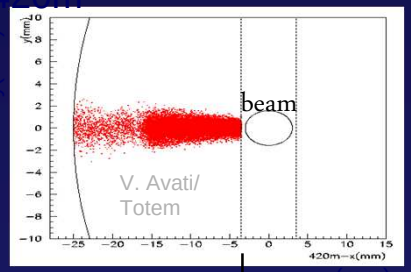

Horizontal detectors in a movable beam-pipe and two vertical pots at 216 and 224 m on each arm.
Detectors as close as possible to the beam: 10σ = 1mm

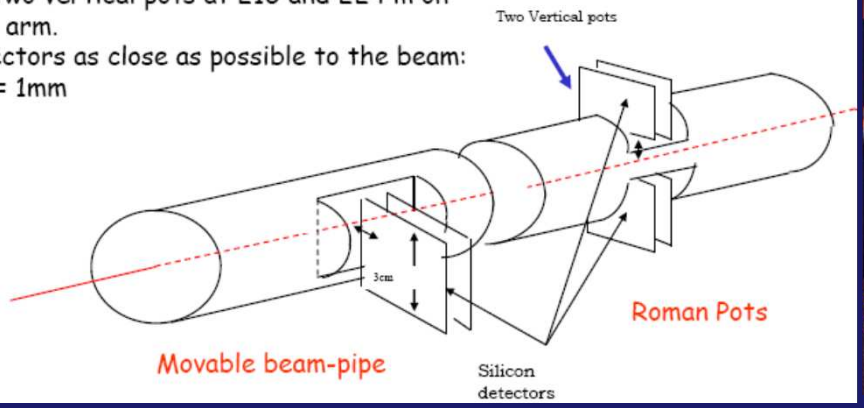

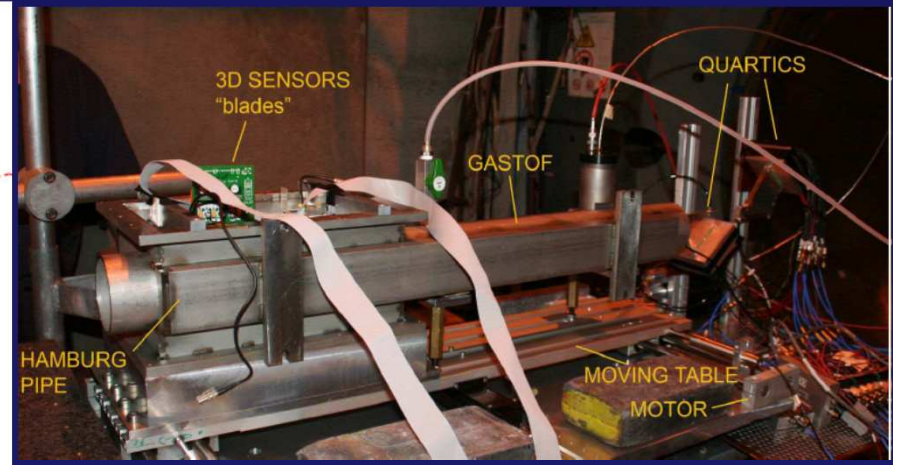

3D in Medicine and Biology?

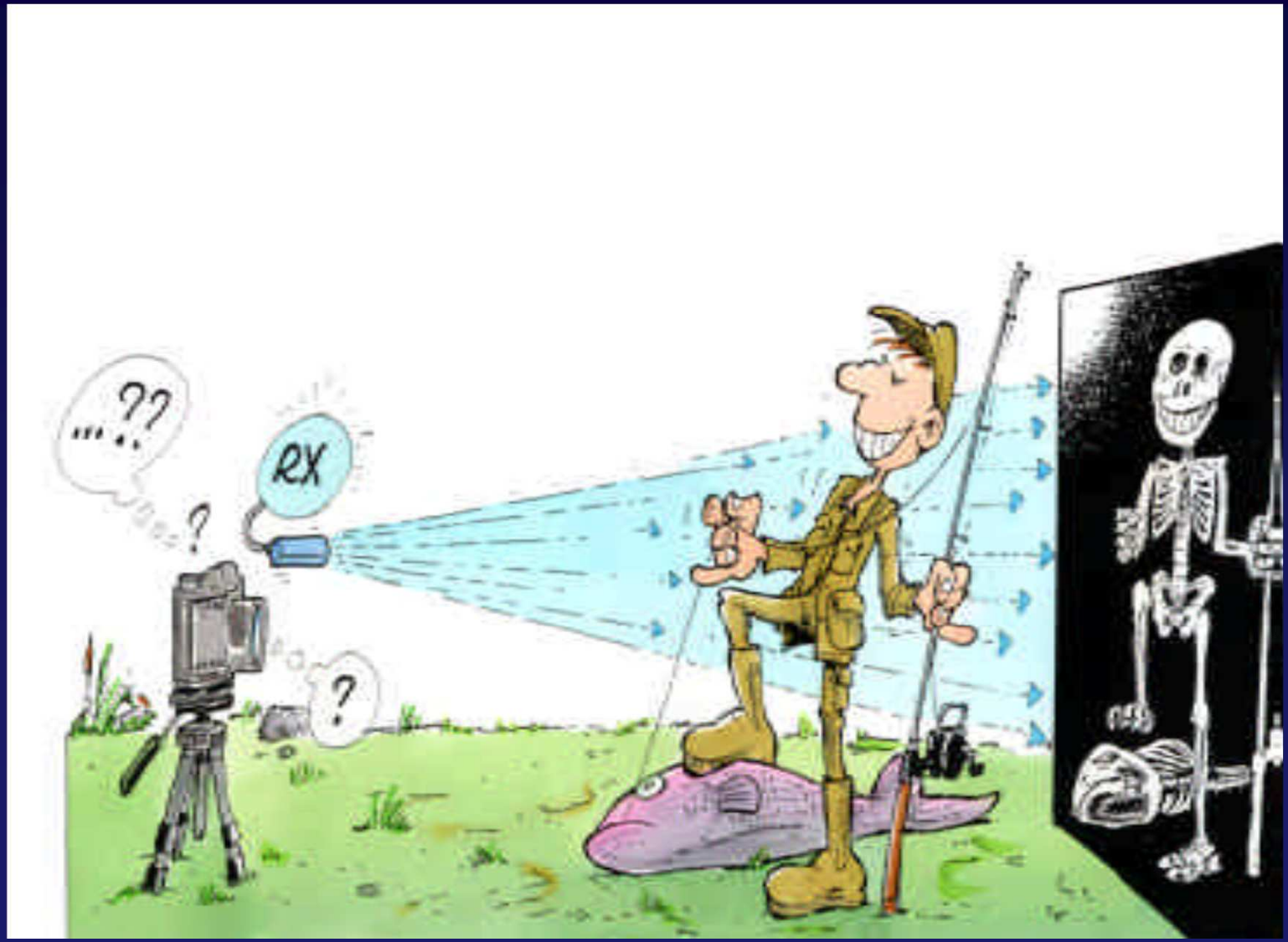

X-ray energy of the most common medical and biological applications

MANCHESTER 1824

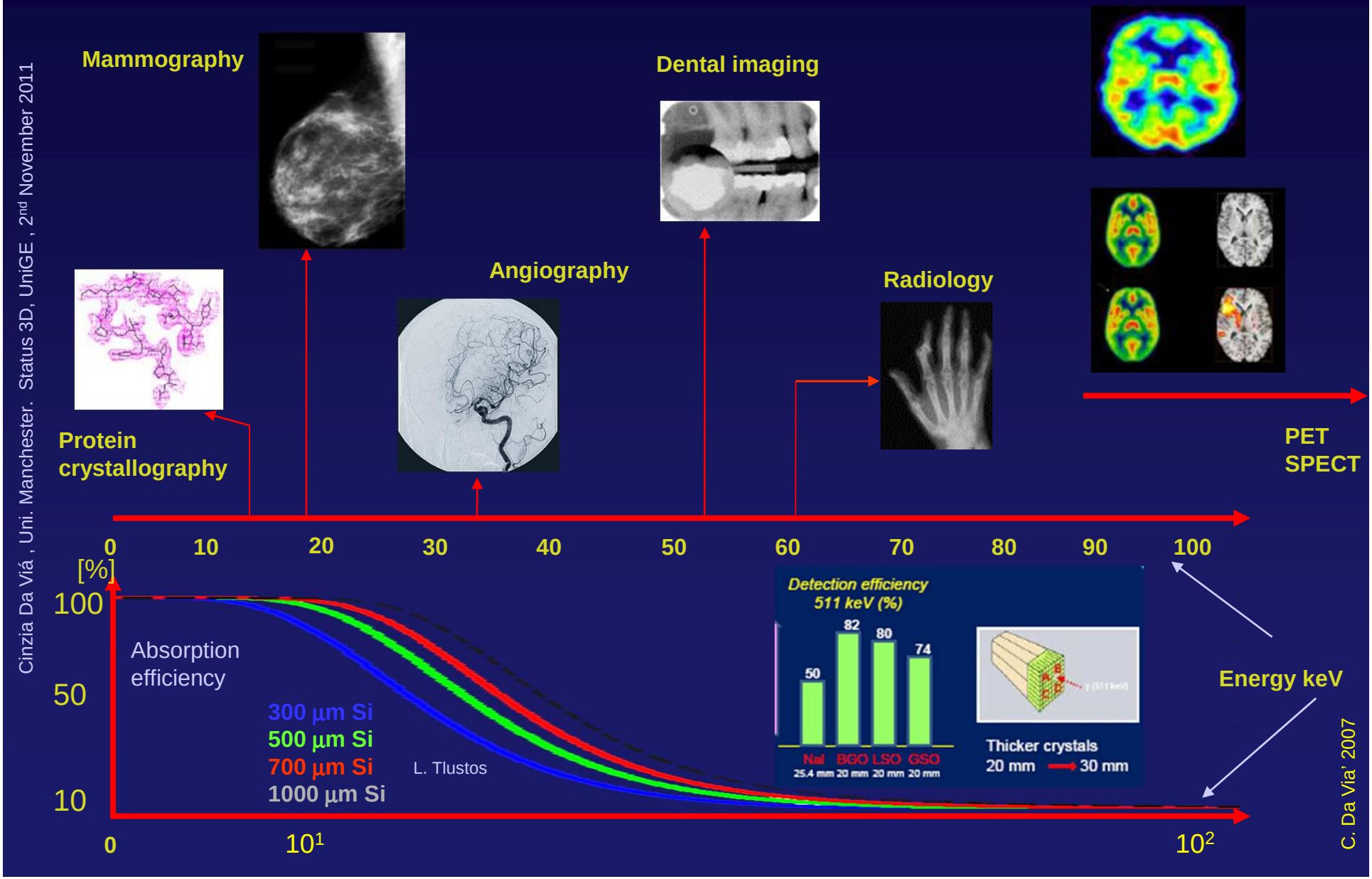

Cinzia Da Viá , Uni. Manchester. Status 3D, UniGE , 2nd November 2011

C. Da Via' 2007

Neutron and x-ray detector array using low aspect ratio 3D pores

C. Da Via et al. submitted to IEEE-NSS 2011

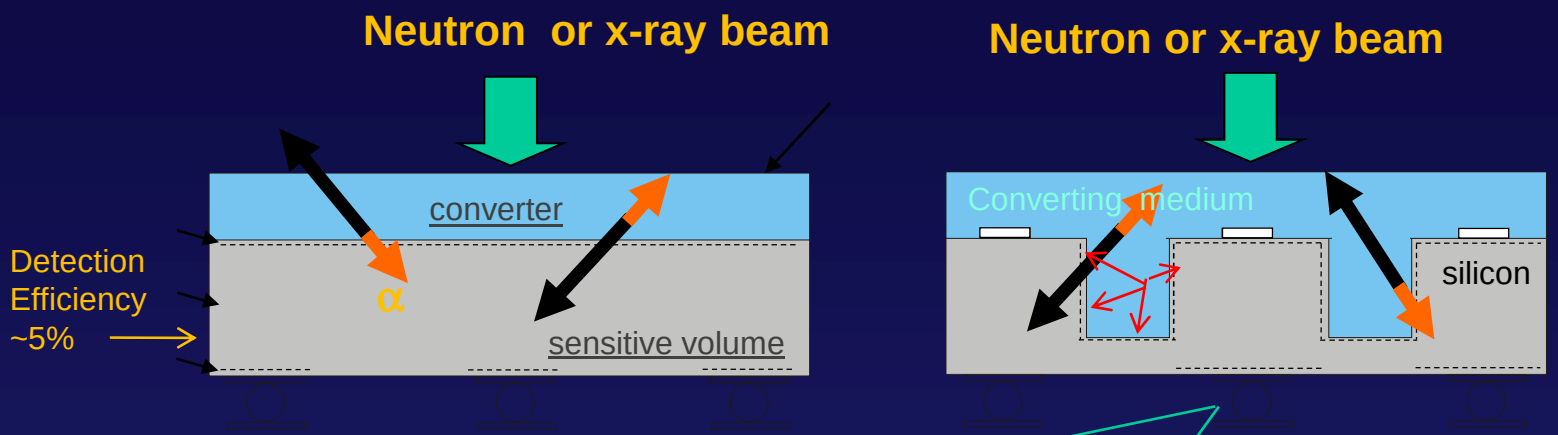

Simulation for neutrons from J. Uher et al. NIM. A 576 (2007) 32–37

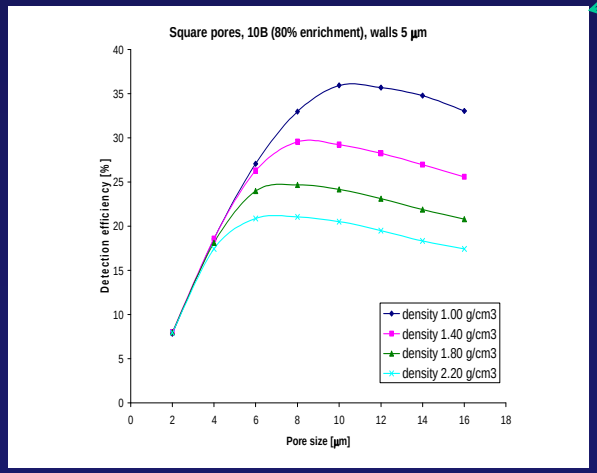

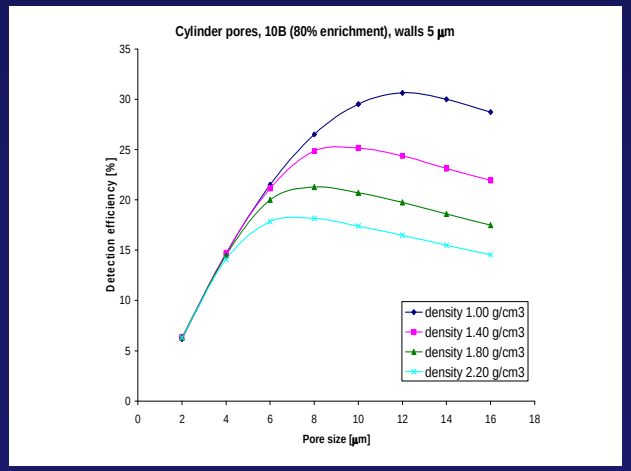

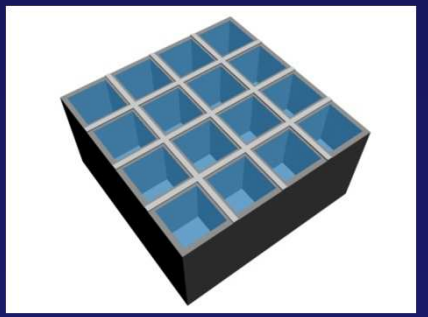

"Channel" 2D type (maximized filling)

Square section
Maximal efficiency: ~36%

Cylindrical section
Maximal efficiency: ~31%

Protein folding 3DX project (MBC)

The Diffraction Pattern of Discrete Bragg Spots
is Captured by the Detector (normally large area CCDs)

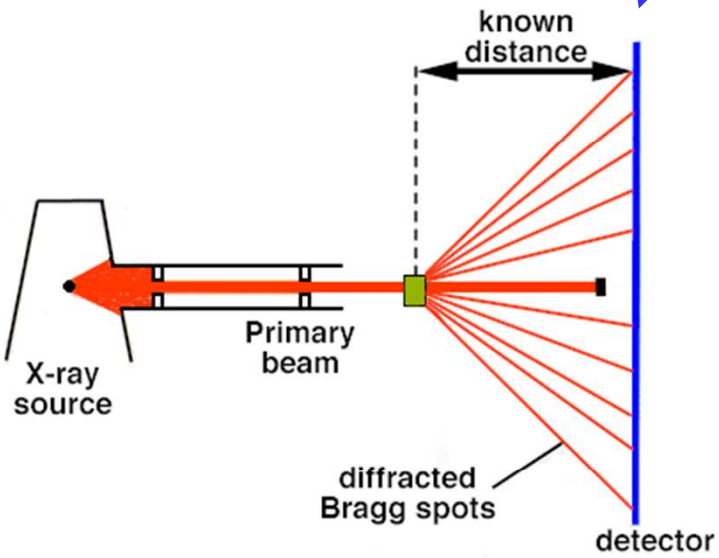

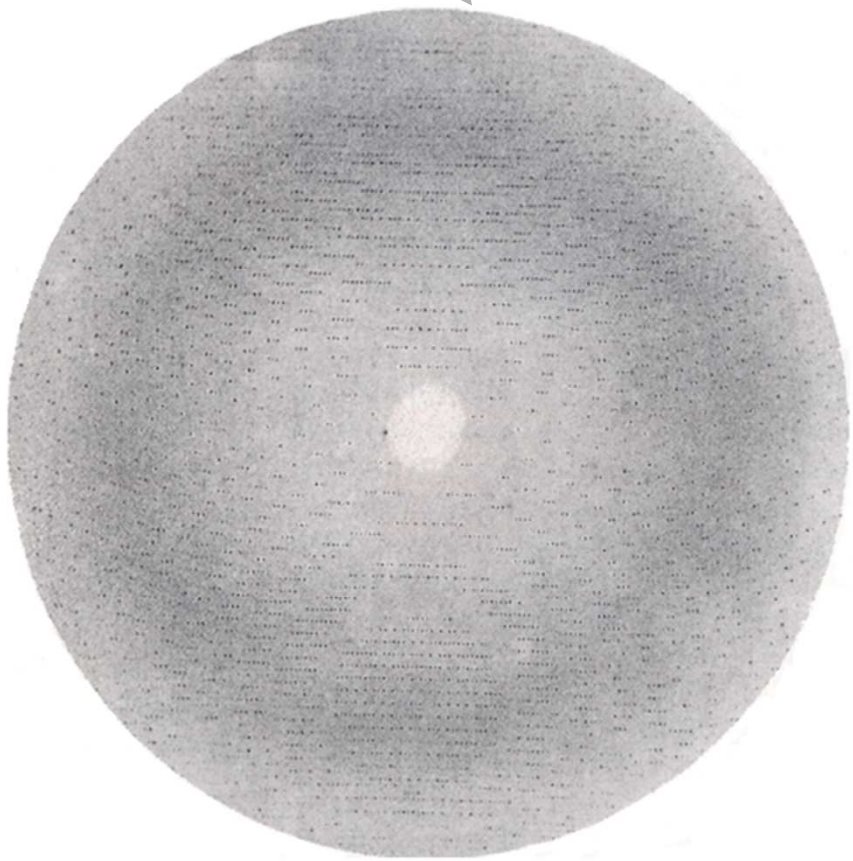

Example of reconstructed structure: Enzyme Active Site (from E. Westbrook)

***Pseudomonas diminuta* phosphotriesterase**: This enzyme catalyzes the hydrolysis of organophosphorus pesticides and nerve agents. Its crystal structure is being studied by Hazel Holden's research group at the University of Wisconsin, Madison (see PDB file 1DPM).
Purple atoms: zinc
Red: bound water
Yellow: side chains
1.8 Å resolution map,

Present detectors:
CCDs. Time resolution ms

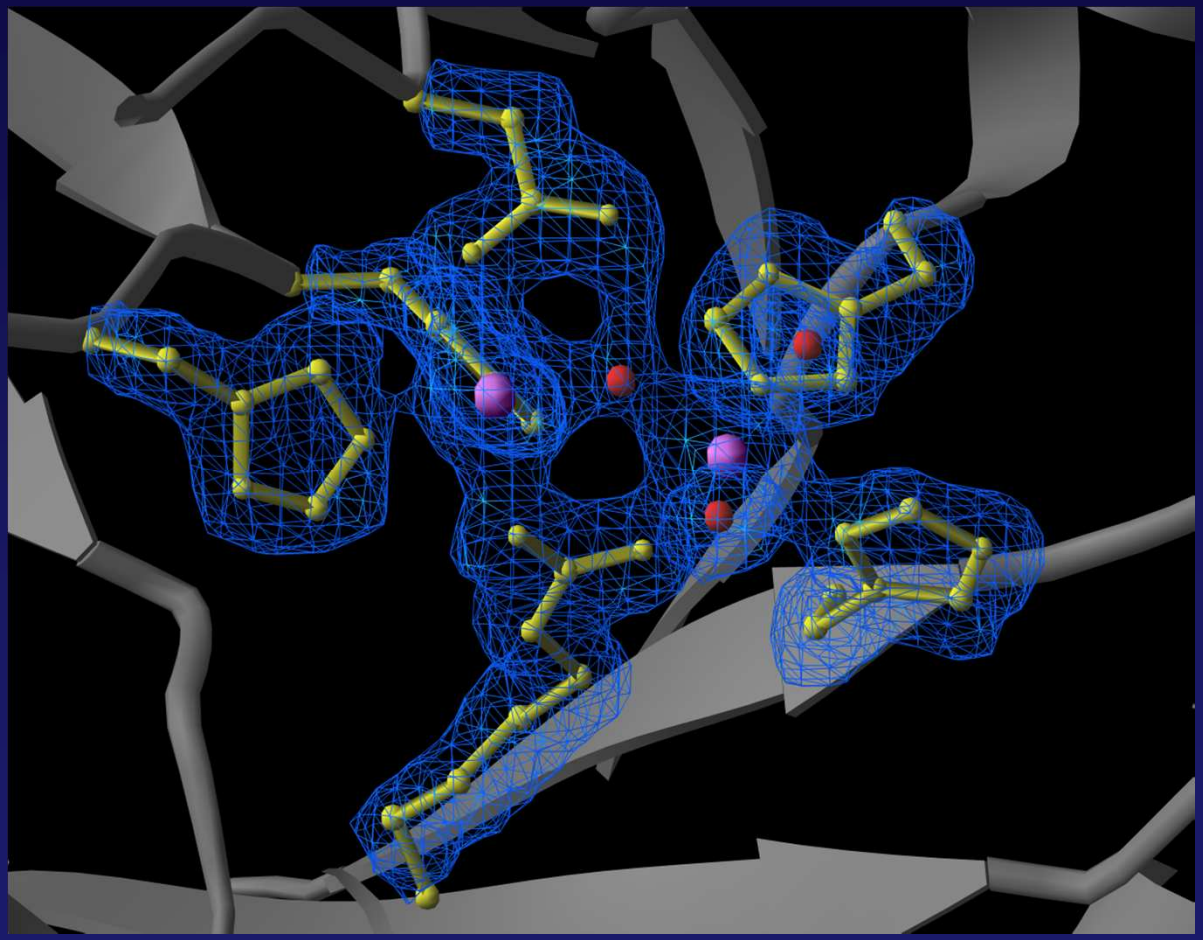

- **Needs faster detection for protein folding**

3D pixel detectors x-ray setup (3DX project)

E. Westbrook et al. (molecular biology consortium) USA

- High signals
- Low noise
- Moderate cost
- High speed – microsecond

GOOD for Protein folding

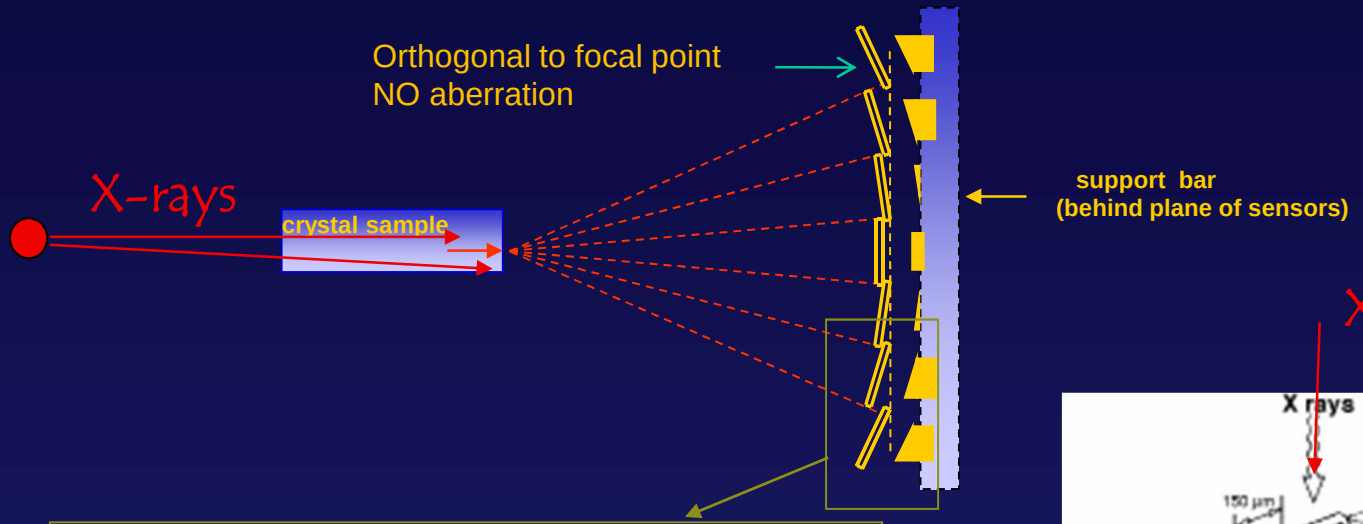

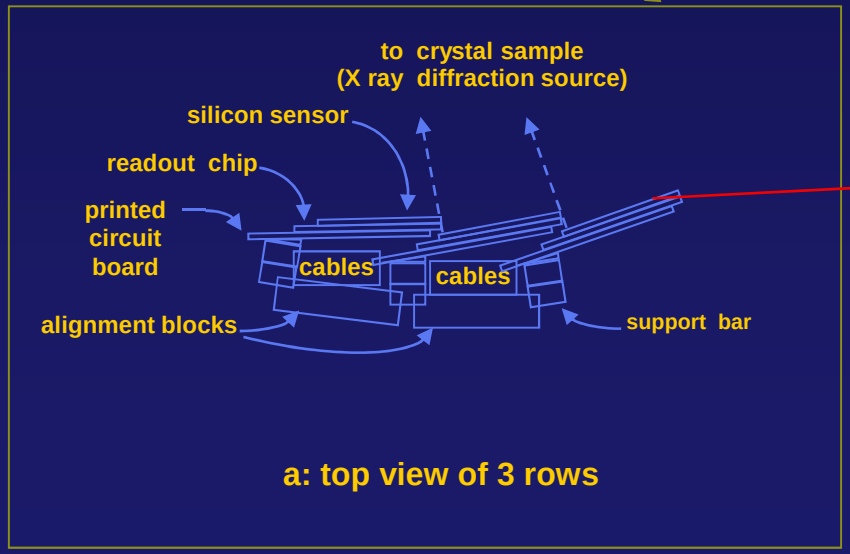

X-rays

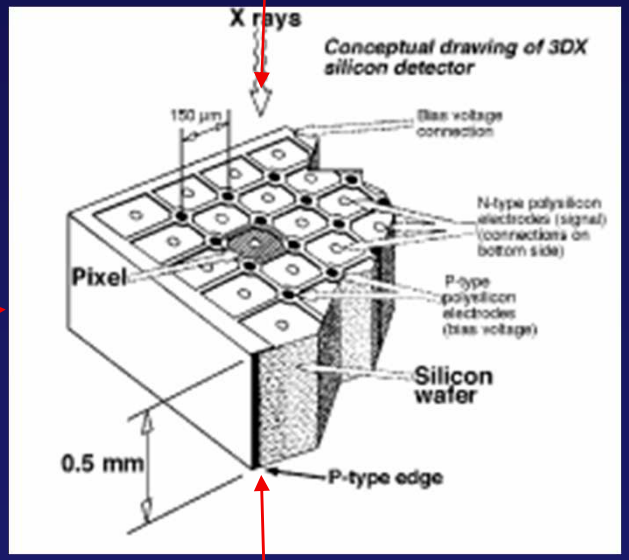

Bump bond to pixel readout electronics

Si Microdosimetry for cancer tretment

Microdosimetry measures the stochastic energy deposition events at cellular level

❖Radio-Biological Effectiveness (RBE) depends on linear energy transfer (LET or Lineal Energy) which is different for different radiation type. **Average chord length <l>** independent on radiation direction

❖**Mixed Field** detection in a small sized array of cell-like elements of well defined Sensitive volume **SV** is required to precisely determine RBE

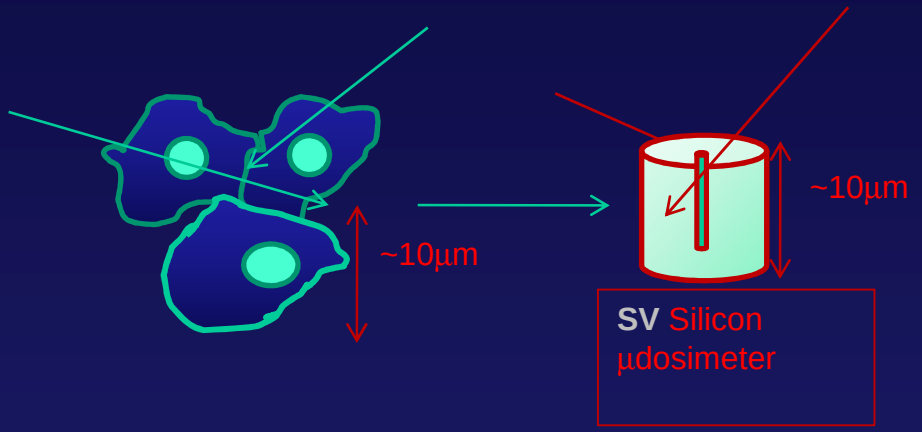

❖Silicon Dose Equivalent can be determined From the lineal Energy Spectra and the tissue equivalent dose $D_{TE.}$. Quality factors **Q** determined Experimentally.

$D_{si} = D_{TE}\ S_{Si}/S_{TE}$

Dose equivalent $H = Q\ D_{si}$

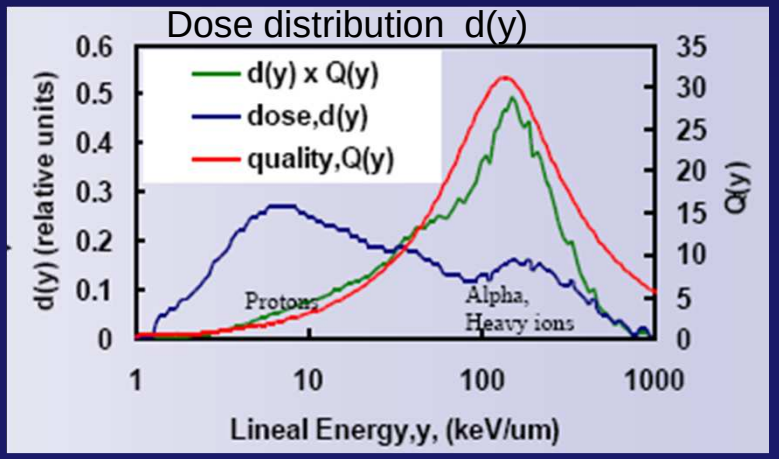

Plot from Rosenfeld et al

Proposal for microdosimetry using 3D sensor technology (C. Da Via et. al. STFC CLASP scheme 2010)

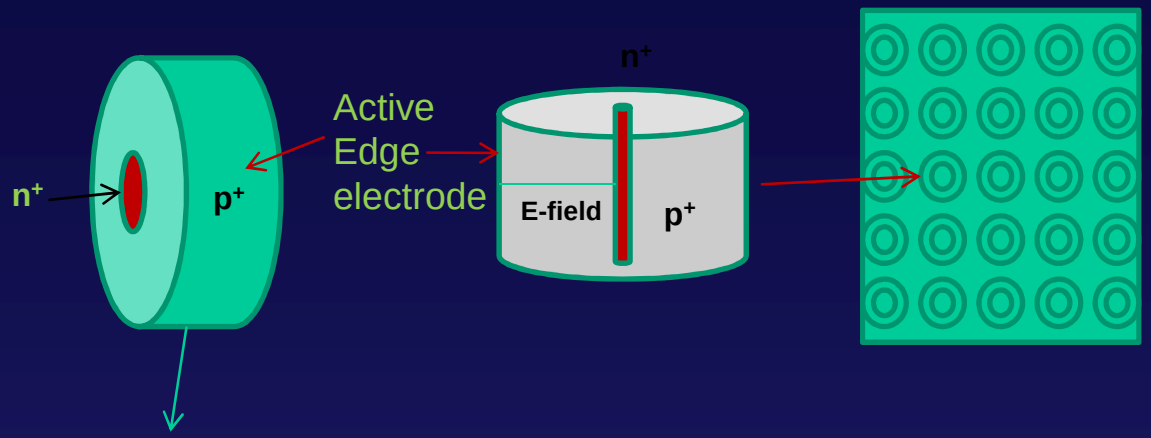

array would enhance performance

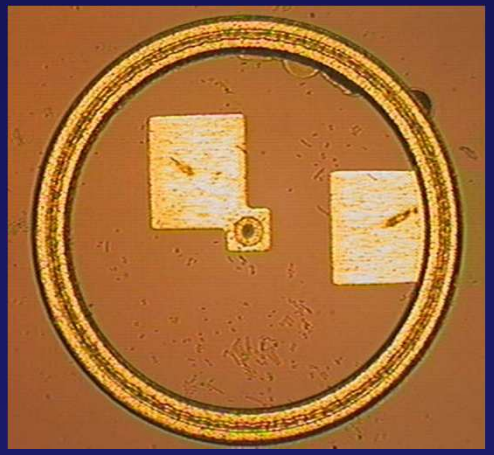

Fabricated at Stanford
J. Hasi, C. Kenney

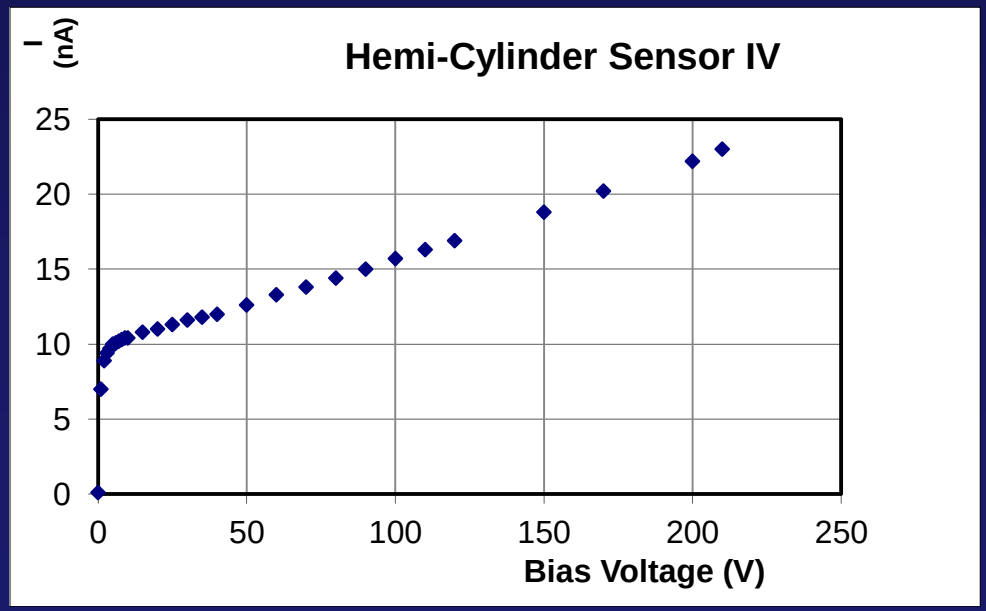

Curved semiconductor detectors

Bernard F. Phlips, *Member, IEEE, and Marc Christophersen*
Presented at IEEE-NSS 2008, Dresden Germany

- Done on Si , GaN and SiC already tried
- Uses Deep reaction Ion Etching
- Key to technology:
- Photo Lithography works: pixels and strips made using 'GrayTone Lithography' (selects photoresists differently at different depths)
- Wafer thinning uses standard processing
- Indium bump-bonding still works on curved structure
- Can be used on all material that allow DRIE
- Resist spray coating
- Alternatives to CMP to improve flatness

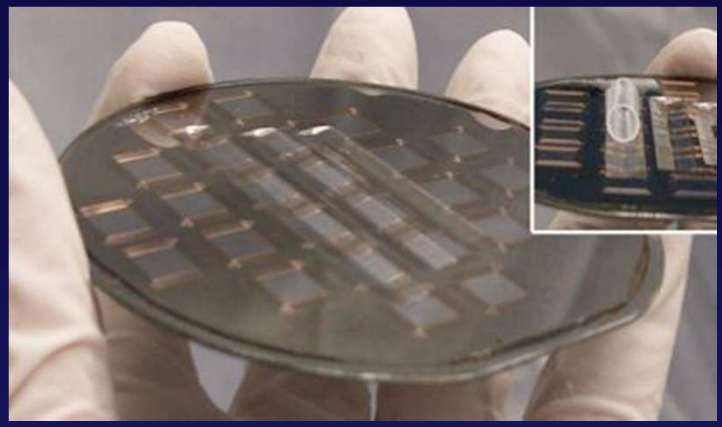

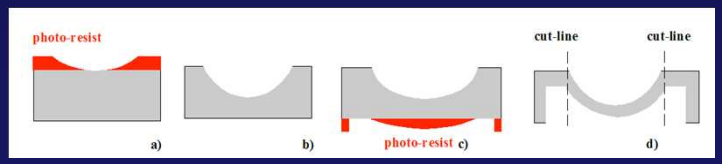

Principle of gray-tone technology: The 3-D resist profile, a) and c), is directly transferred into silicon topography, b) and d).

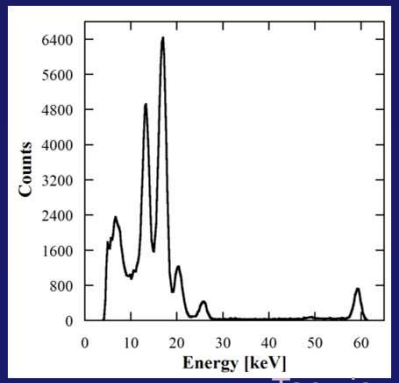

Am-241 photon spectrum taken with a fully depleted curved pixel detector, half-pipe (1.73 keV FWHM at 59.54 eV).

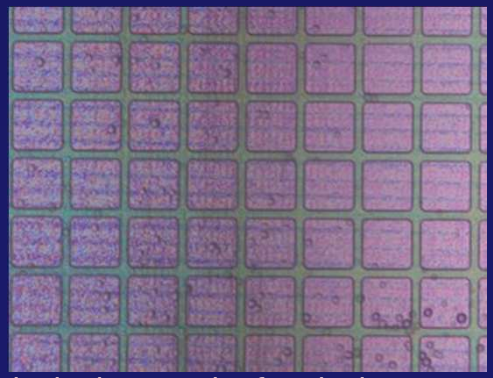

Top-view optical micrograph of a pixel array on a curved detector(pixel dimensions 150 x 150 µm).

Summary and outlook

A long journey and many battles were made after 3D was proposed in 1995:

It was proven that several interesting options as radiation detectors in particle physics and medical applications could be achieved with this Technology:

Low bias voltage,
high radiation tolerance,
active edges
High speed

They can now be manufactured in several facilities working together

Yield is promising and will get better

They should be used soon in experiments and synchrotron beam lines

Therefore….

…… do not be afraid of new technologies!!!!!!

borrowed from P. Le Compte at the Liverpool Atlas Tracker Upgrade Workshop Dec 2006

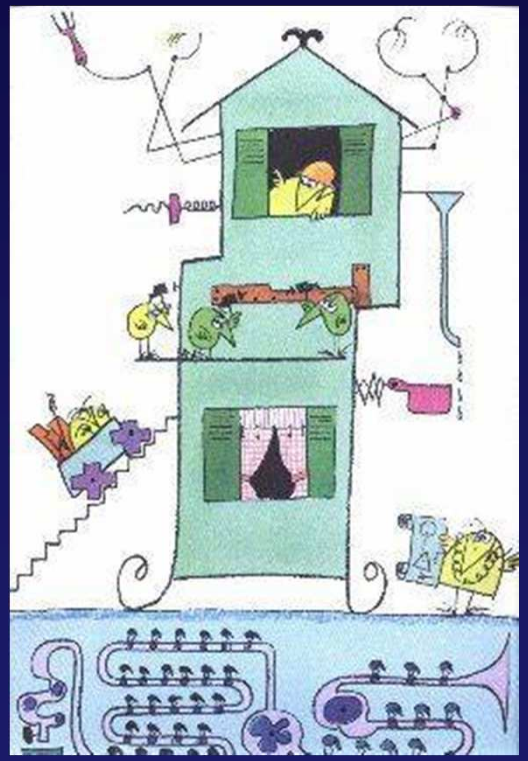

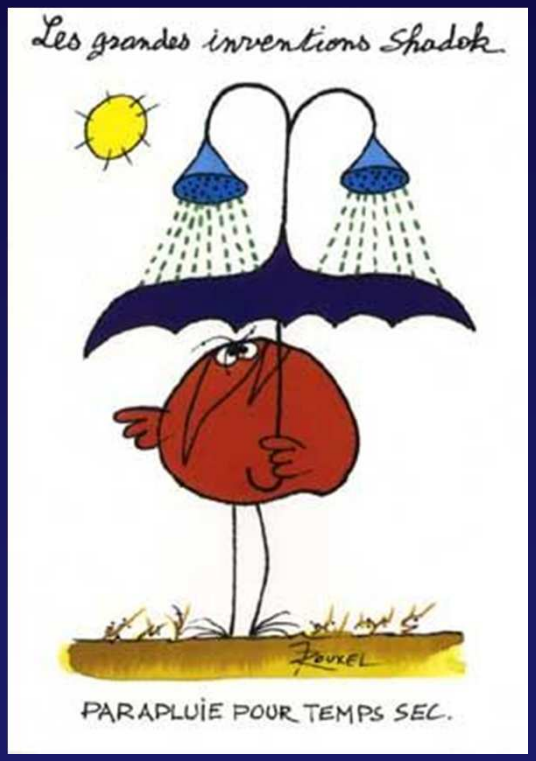

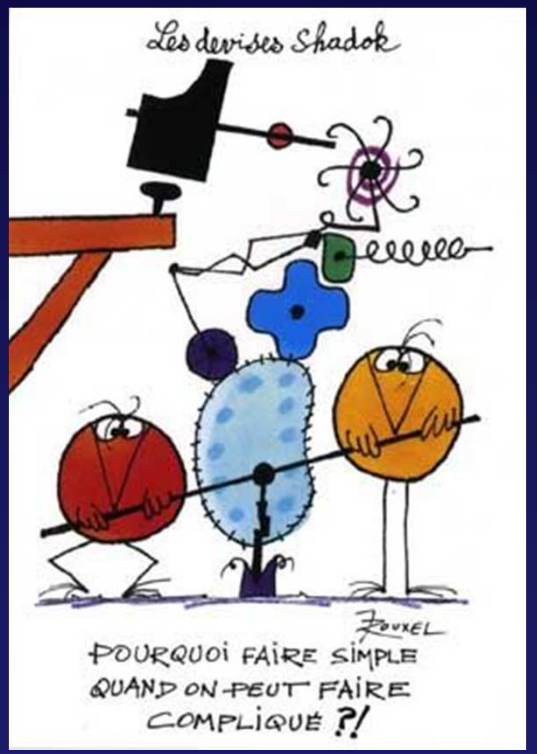

spares

QA for wafer bowing is < 60 microns with an alignment <5 microns This is valid for both FBK (this slide) and CNM

from E. Vianello, FBK,
3D processing meeting 19-5-11

Wafer bowing

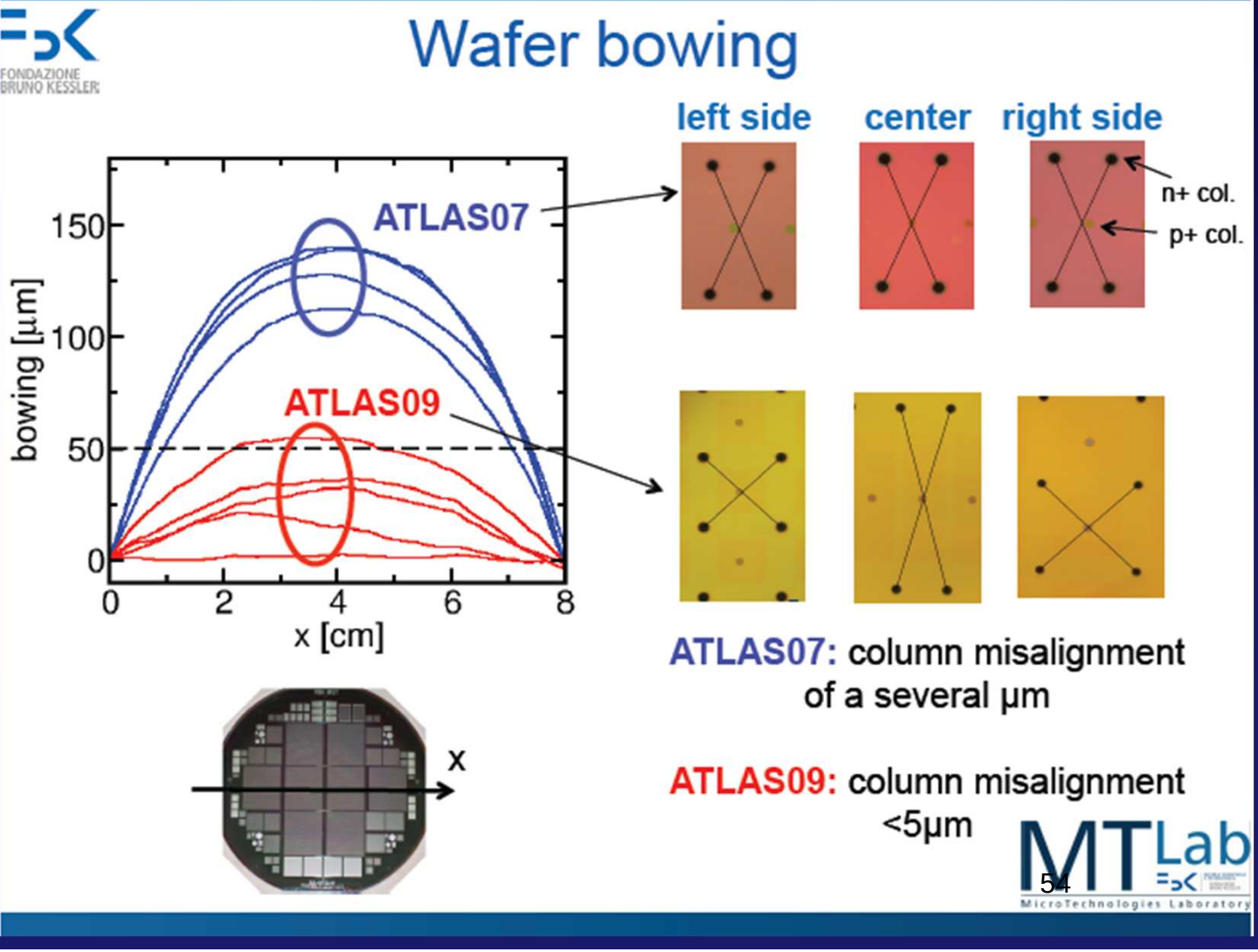

Leakage currents and operational voltages After irradiation

A. Micelli, C. Gemme, S. Grinstein

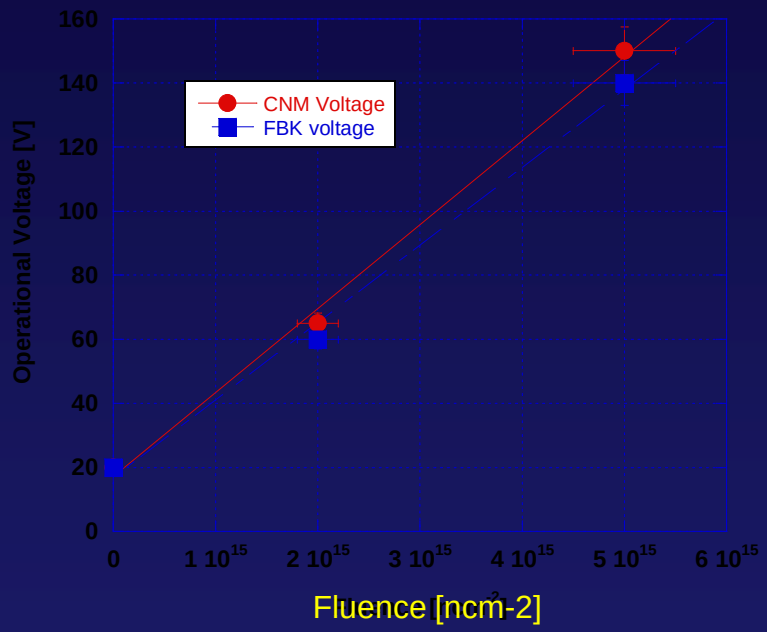

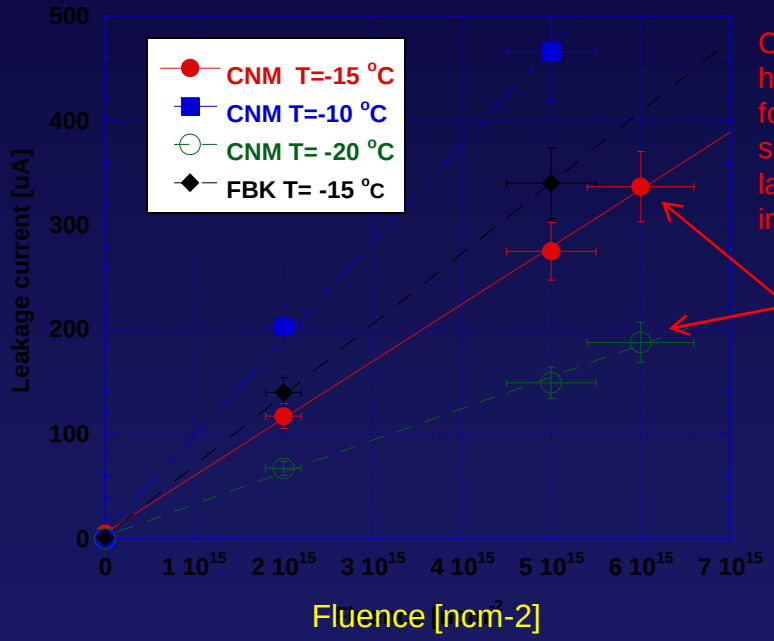

Confirms higher damage for second raw samples during last KA proton irradiation

CNM SSC97

T [°C] FEC-off	Fluence x 10 ^{15} [ncm^{-2}]			Vop [V]			Current [uA] Per chip		
-20 CNM	2	5	6	63	151	151	67	149	188
-15 CNM	2	5	6	63	152		117	275	326
-15 FBK	2	5		60	140		137	340	
-10 CNM	2	5		64	158		203	466	
-5 CNM	2	5		63	145		569	795	

Power dissipation at different Temperatures after irradiation

C. Gemme, A. Micelli, S. Grinstein

IBL requirement on sensor Power dissipation
< 200 mW/cm^2 at 5 x 10^{15} n_{eq}/cm^2 and -15 ^{o}C (after annealing)

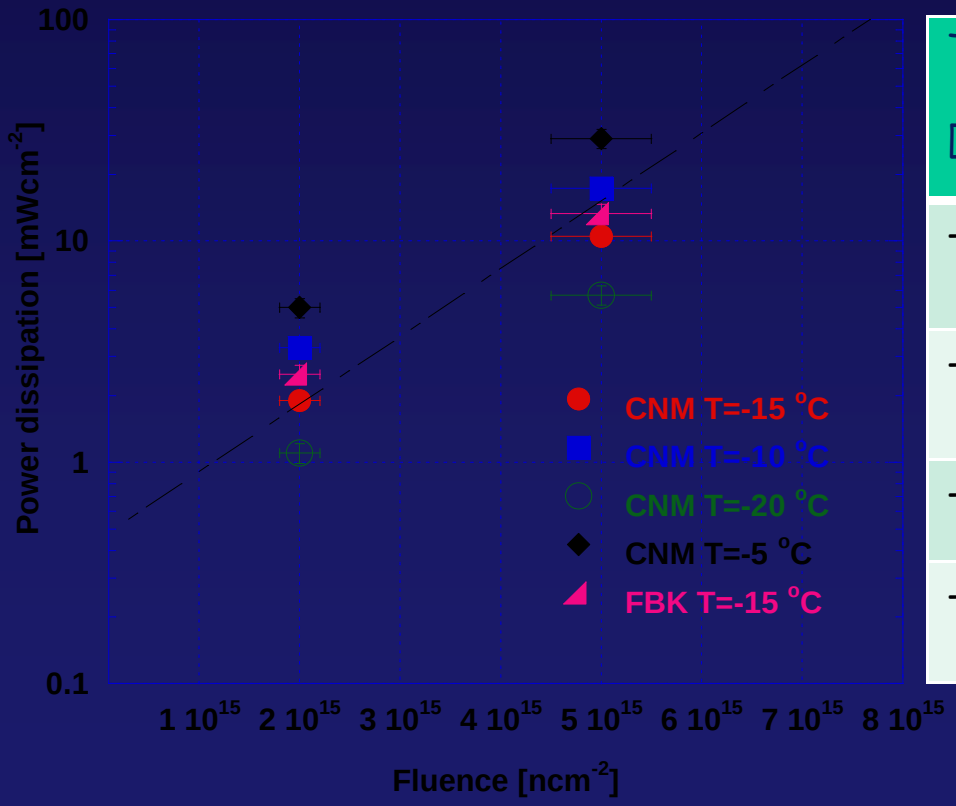

Temp. [^{o}C]	Fluence x10^{15} [ncm^{-2}]		W CNM [mWcm^{-2}]		W FBK mWcm^{-2}]	
-20	2	5 6	1.1	5.7 7.1		
-15	2	5 6	1.9	10.5 12.7	2.5	13
-10	2	5	3.3	17.3		
-5	2	5	5	29		

Most probable signal after IBL fluence

Compilation of Stanford, CNM,FBK

MPS predicted=230μm x 75e$^-$ = 17 250 e$^-$

Fluence [ncm^{-2}]	MPS [e$^-$]
0	17250
1x10^{15}	16380
5x10^{15}	12075

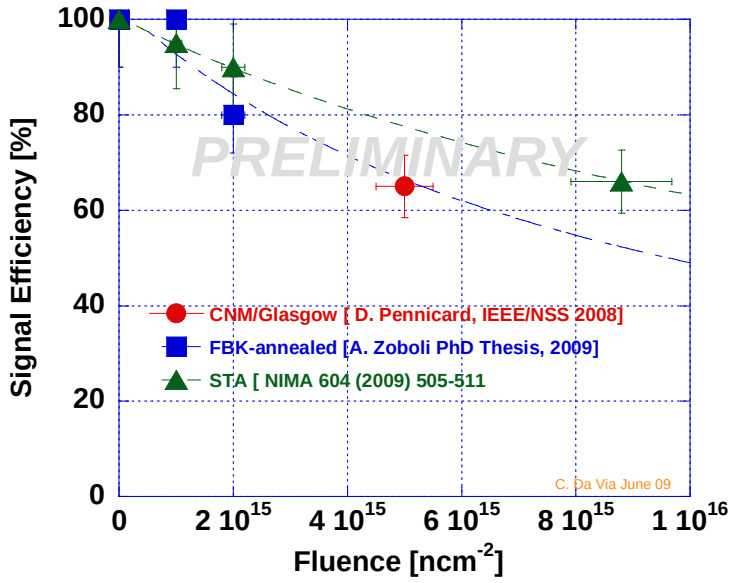

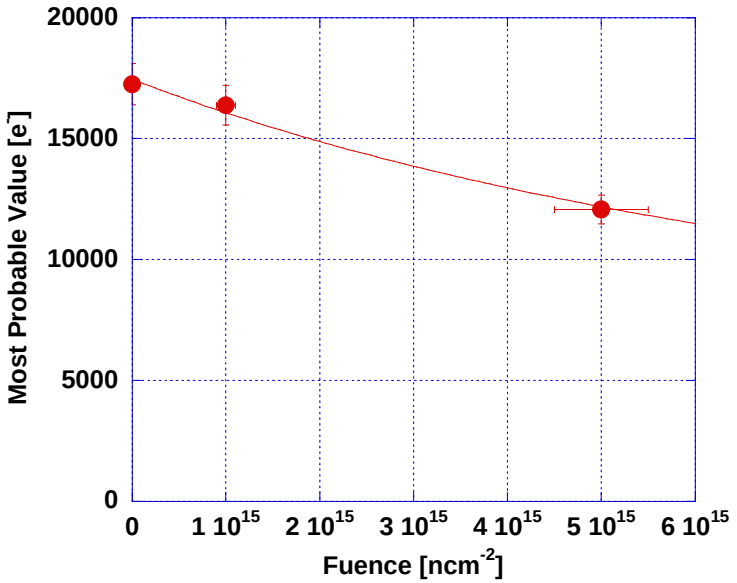

The Insertable B-Layer

Stave and module arrangement

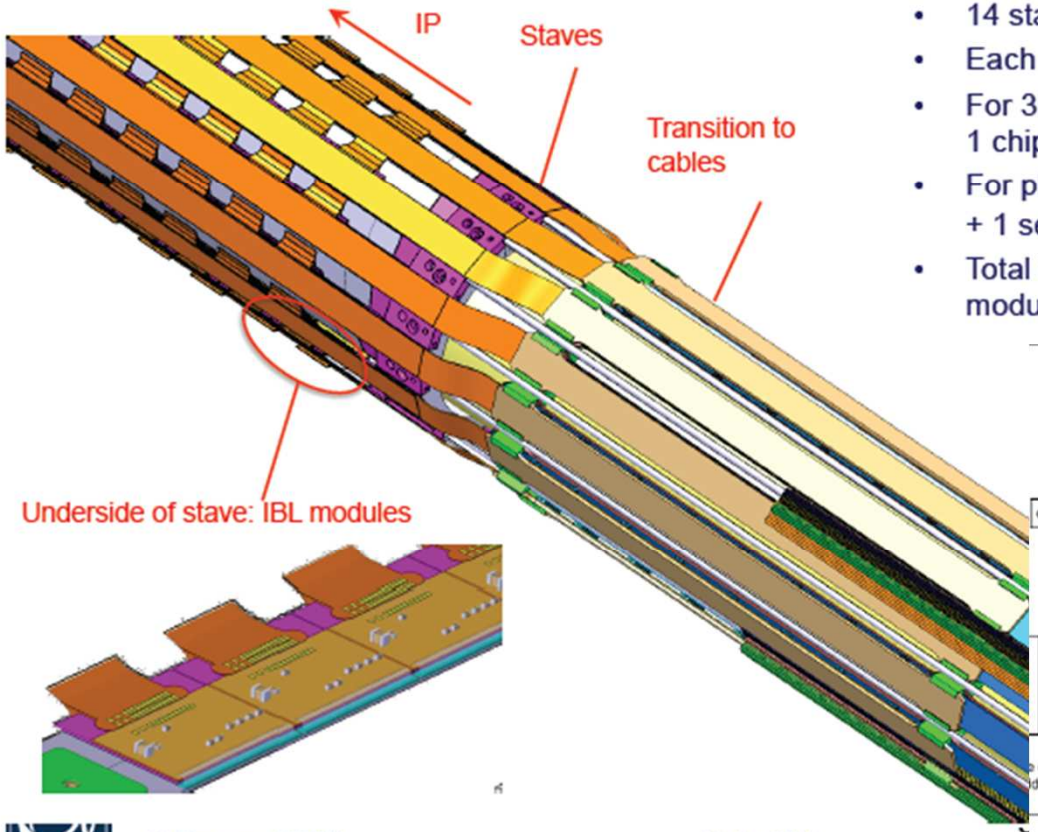

- 14 staves
- Each stave: 32 FEI4 chips
- For 3D sensors: 1 sensors + 1 chip = 1 module
- For planar sensors: 2 chips + 1 sensor = 1 module
- Total installed 224 planar modules or 448 3D modules

FE-I4

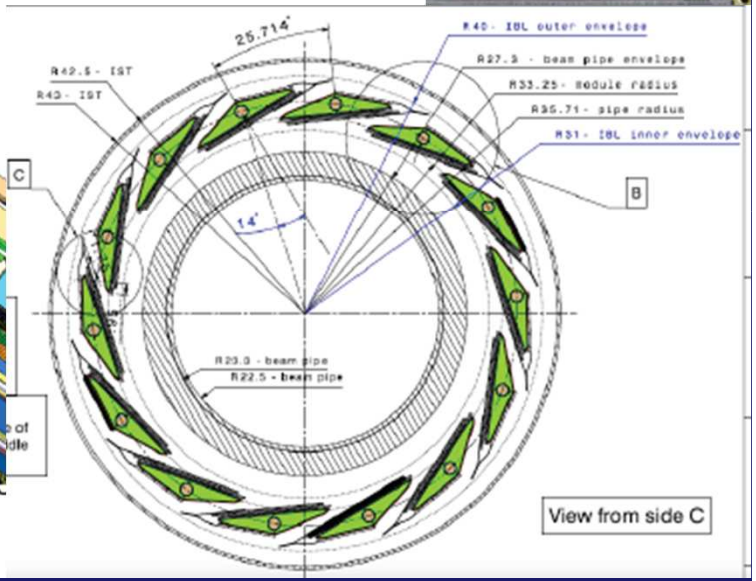

H. Pernegger/CERN

Vertex 2011

IBL Sensors

	3D n-in-p sensor	planar n-in-n sensor
active size W x L [mm²]	16.8 x 20.0	16.8 x 40.9
total size W x L [mm²]	18.8 x 20.5	18.54 x 41.27 (?)
thickness [mm]	0.23	0.20
Typical depletion voltage [V]	≤ 15	≤ 35
Typical inital operation voltage [V]	25	60 (V_{dep}+30V)
at of at end of lifetime [V]	180	1000

From Pernegger, Vertex 2011

Sensor specifications for IBL:

- Qualify to 5x10¹⁵ n_{eq}
- max. power dissipation: 200 mW/cm² at -15 C
- tracking efficiency > 98%.

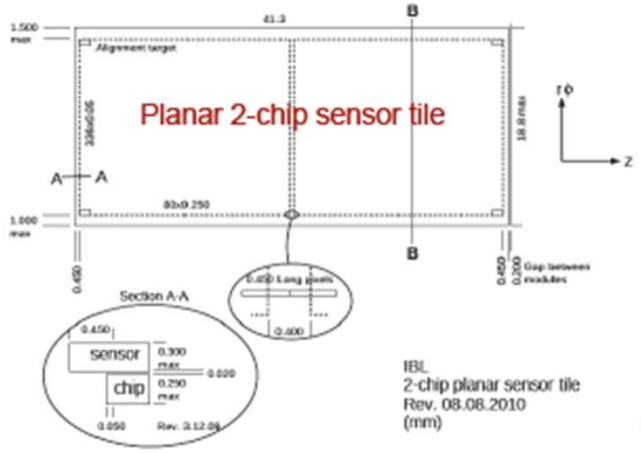

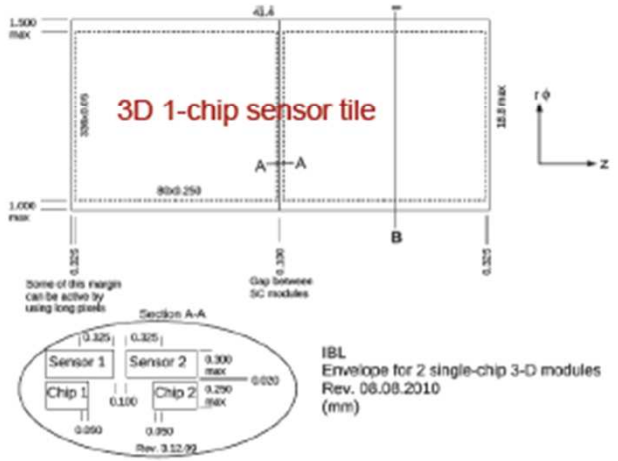

5

FLIP-CHIP QUANTITIES (ASSEMBLIES) Agreed scenarios:	PLANAR	3D
Modules as installed target (75%, 25%)	336 (168 mod.)	112
Modules to be prepared for 100% planar	448 (224 mod.)	112
Modules to build (2x as installed)	896 (448 mod.)	224

3D and planar in magnetic field

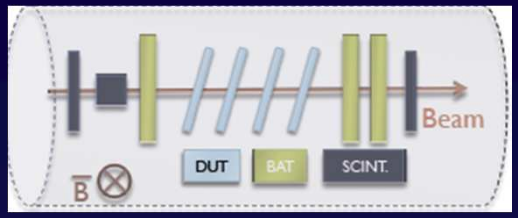

Atlas barrel solenoid configuration

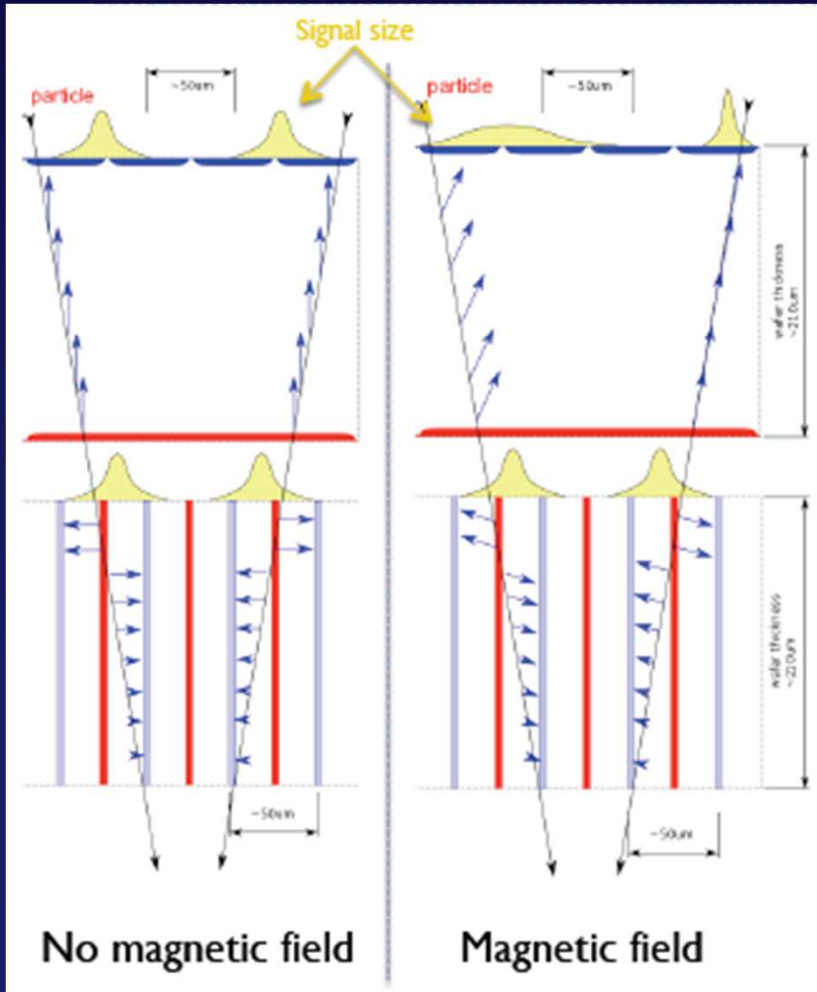

Planar sensors

- Orthogonal electric- and magnetic field
- Focusing or de-focusing drifting charges
- Minimum cluster size at Lorentz angle incidence

3D sensors

- Coplanar electric- and magnetic field
- Lorentz angle out of coplanar
- Depends on hit position
- Possibly small surface effects

Expect very small effect from magnetic field in 3D sensors!

P. Hansson et al. Nuclear Instruments and Methods in Physics Research A 628 (2011) 216–220

Charge sharing, tracking resolution and Lorentz effect

P. Hansson et al. Nuclear Instruments and Methods in Physics Research A 628 (2011) 216–220

- Charge sharing between pixels is important
  - Cluster size ~ tracking resolution
  - Signal size ~ operational characteristics after irradiation

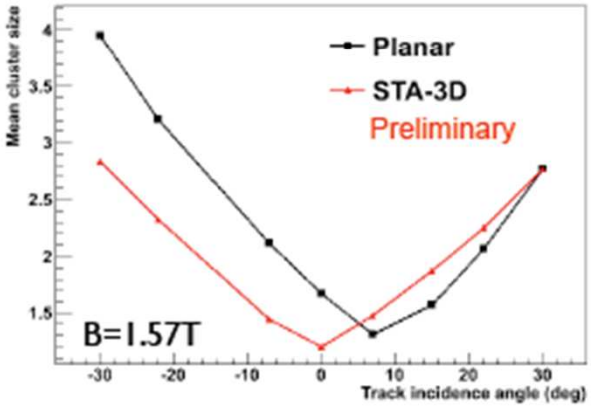

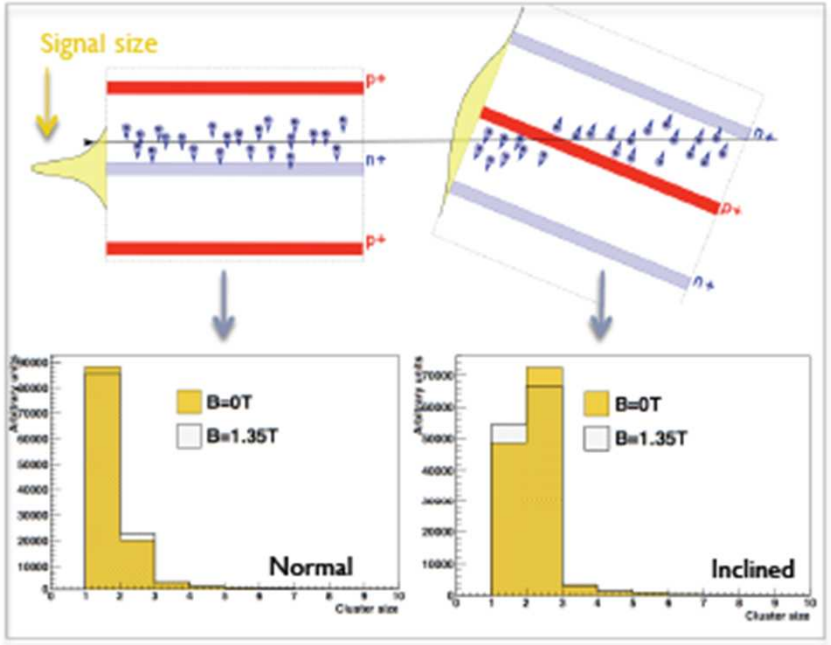

- Tilt angle important for resolution
- Measured resolution similar to planar sensor
- 3D sensors insensitive to magnetic field

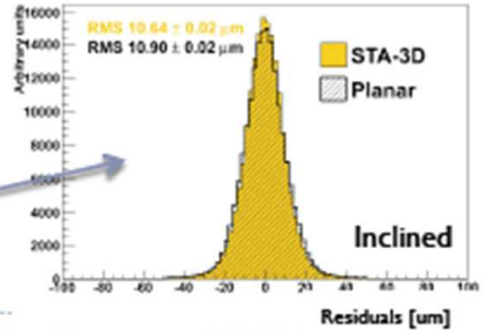

σ= 10.9 µm

Track resolution not de-convoluted

Per Hansson 2/10/10

MANCHESTER 1824

Other structures already fabricated at STANFORD (C. Kenney, J. Hasi) to improve speed and detection properties

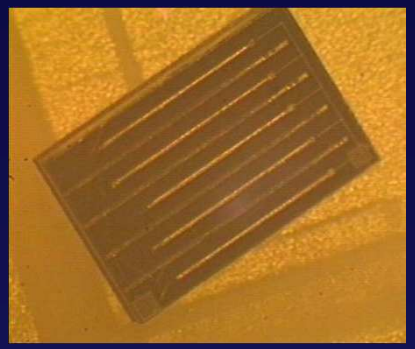

3D Parallel trenches

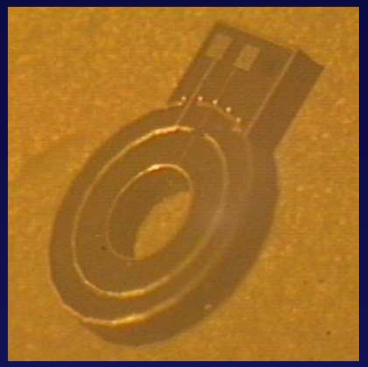

3D coaxial layout

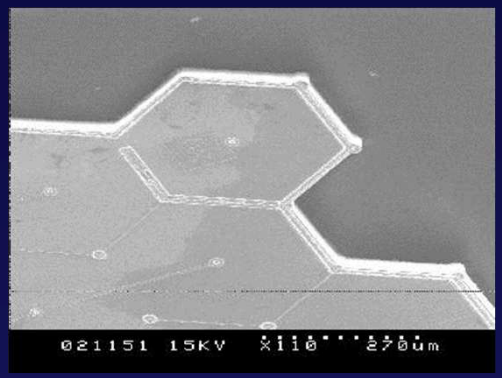

3D hexagonal

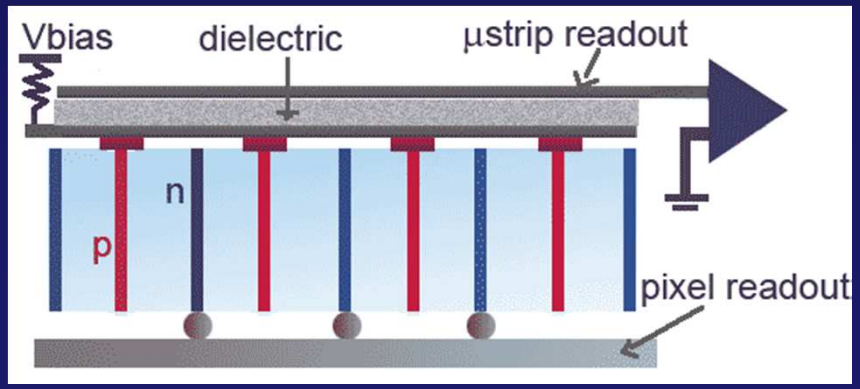

Dual readout:

Improved spatial resolution
With the same material budget

C. Da Via et al., "Dual readout – strip/pixel systems", NIM A594, pp. 7-12 (2008).

Also started to fabricate 3D on diamond substrates (with A. Oh, Manchester, H Kagan Ohio)

Medical Imaging strategies

1- 10keV<E<20KeV

Thick silicon (Si) ; a-Si; a-Se (thickness is a problem)
Direct detection:

high detection efficiency for Si
high spatial resolution for Si
large area for flat panels

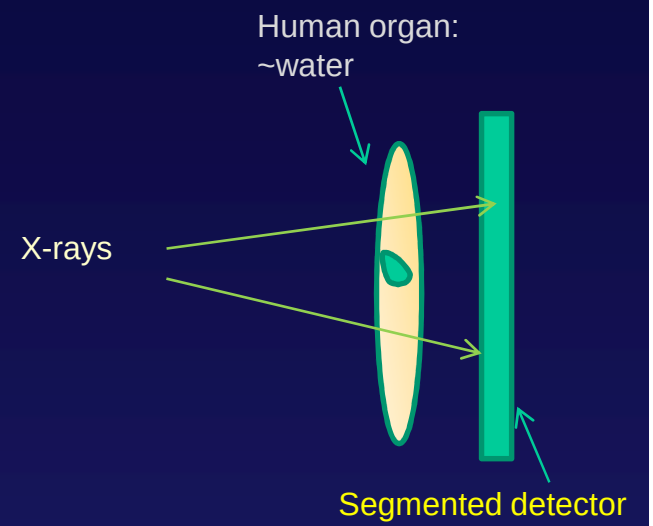

2- 20KeV<E
high Z semiconductors

high detection efficiency
high spatial resolution
large area? homogeneity

Indirect detection :
Converter + photo detector

low spatial resolution
high detection efficiency

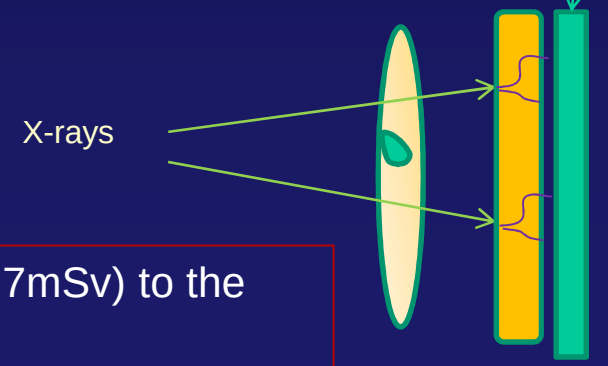

Example breast cancer screening: lowering the dose (~0.7mSv) to the patient is the goal!

*-Micro-calcification has high contrast and small size→ High spatial resolution detector
**-Fibro adenoma has low contrast and big size → high detection efficiency detector